Selective Removal of Non-Basic Nitrogen Compounds from Heavy Gas Oil Using Functionalized Polymers

A Thesis submitted to the College of Graduate Studies and Research

in Partial Fulfillment of the Requirements for the

Degree of Master of Science

in the Department of Chemical Engineering

University of Saskatchewan

Saskatoon

By

Danish Rizwan

COPYRIGHT

ABSTRACT

The inhibiting and deactivating effects of basic nitrogen species present in gas oils on catalyst active sites has been well recognized over the years; however, recent studies have shown comparable inhibiting and deactivating effects exhibited by non-basic nitrogen species. A novel pre-treatment technique employing the heterogeneously cross-linked macroporous polymer poly(glycidyl methacrylate) (PGMA) as the hydrophilic support coupled with organic compound tetranitrofluorenone has shown promising results for the selective elimination of non-basic nitrogen heterocyclic species from bitumen derived heavy gas oil (HGO). Characterization techniques such as Scanning electron microscopy (SEM), low temperature N_2 adsorption–desorption (BET), CHNOS elemental analysis, fourier transform infrared spectroscopy (FT-IR), epoxy content titration, and thermo gravimetry/differential thermal analyzer (TG/DTA) were employed for determining the optimum parameters during each step of the polymer synthesis.

Step 1 comprised of direct polymerization of the monomers under the determined optimum conditions, with specific surface area of 34.7 m^2/g and epoxy content of 5.8 wt% for the PGMA polymer support. Step 2 comprised of substitution of the epoxy ring with the acetone oxime functionality; FT-IR results indicated characteristics peaks at 1650 cm^{-1} which ascertained the presence of acetone oxime on the polymer, with epoxy content titration indicating a decrease of up to 33% of the epoxy content due to the substitution. Coupling of the organic compound tetranitrofluorenone with the polymer was performed in the final step, with TGA and DTG results indicating highest weight loss of approximately 126.9 μg, which signified that sample T had the greatest amount of organic compound present in comparison to the other samples (sample N to Sample S). The optimized polymer (sample T) was capable of removing nitrogen up to 6.7%, while having little to no influence on the sulphur or aromatic species. These results

were in agreement with step 4 TGA analysis that showed sample T had the highest presence of the organic compound.

Reusability of the polymer multiple times with consistent removal is another known advantage of such a pre-treatment technique; hence reusability studies were performed, and showed that the polymer was indeed capable of multiple uses, with consistent removal of nitrogen compounds at approximately 6.5% from fresh heavy gas oil feedstocks.

Kinetic studies were performed as the final phase in order to evaluate the performance of the treated HGO in comparison to non-treated HGO. The effect of parameters such as temperature and LHSV were determined, with higher temperatures resulting in higher conversion of HDS and HDN. Similarly, as the LHSV was decreased, the conversions were increased for both HDS and HDN due to longer contact time between the feed and the catalyst. The highest obtained conversions were at an LHSV of 0.5 hr^{-1} and temperature of 395°C with treated HGO having HDS of 97.5% and HDN of 90.3%; while non-treated HGO having HDS of 94.9% and HDN of 78.3%. Employing the power law model, the results indicated that for treated HGO the reaction order for both HDS and HDN was 1.50; while for non-treated HGO the reaction order for HDS was 2.25 and for HDN was 2.00. The activation energies were then calculated with 141.4 kJ/mol being obtained for HDS and 113.8 kJ/mol for HDN for treated HGO; while for non-treated HGO the activation energy for HDS was 150.4 kJ/mol and for HDN was 121.4 kJ/mol.

It was observed that the conversion of both HDS and HDN were higher and the activation energies were lower for treated HGO, indicating that the removal of non-basic nitrogen species prior to hydrotreatment had a positive impact on catalyst performance and consequently the level of conversion.

ACKNOWLEDGEMENT

I would first like to acknowledge and give my most sincere thanks to my supervisors Dr. Ajay K. Dalai and Dr. John D. Adjaye for their continuing supervision and guidance throughout the perseverance of this research. I would also like to acknowledge and thank the members of my M.Sc. committee Dr. Jafar Soltan and Dr. Ikechukwuka Oguocha for their time, contribution, and guidance, which was immensely helpful in improving the quality of my work.

Secondly, I would like to acknowledge Mr. Richard Blondin and Ms. Heli Eunike for their continuing assistance in performing several characterization analyses that contributed towards my research. Financial assistance provided by NSERC and Syncrude Canada Ltd in the form of IPS is also gratefully acknowledged.

I would also like to extend my gratitude towards all of the members of Catalysis and Chemical Reaction Engineering Laboratory at the University of Saskatchewan, who made this a very enjoyable journey.

Lastly, I would like to express my heartfelt thanks to my father (Mr. Rizwan Hussain), my mother (Mrs. Shaheen Rizwan) and my brother and sister for their unconditional love and constant encouragements. Above all, I thank god for continuing to bless me with such wonderful opportunities and individuals in my life.

TABLE OF CONTENTS

APPENDICES

LIST OF TABLES

LIST OF FIGURES

NOMENCLATURE

α	proportionality constant relating system pressure to H_2 pressure
β_{HDS}	isothermality ratio for the catalyst pellet in a HDS reaction
β_{HDN}	isothermality ratio for the catalyst pellet in a HDN reaction
γ_P	tortuosity of the catalyst pellets, dimensionless
$\Delta H_{R,HDN}$	heat of the hydrodenitrogenation reaction kJ/mol
$\Delta H_{R,HDS}$	heat of the hydrodesulphurization reaction kJ/mol
ε	catalyst bed porosity, dimensionless
ε_P	porosity of the catalyst pellets, dimensionless
η	effectiveness factor
Φ	thiele modulus
μ_L	viscosity of HGO at the operating temperature, g/(s·cm)
ρ_L	density of HGO at operating condition, g/mL
ρ_T	density of HGO at the operating conditions, g/mL
λ_N	adsorption energy for all nitrogen heteroatoms within gas oil, J/mol
λ_S	adsorption energy for all sulfur heteroatoms within gas oil, J/mol
°API	American Petroleum Institute gravity of petroleum liquids, dimensionless
A	surface area of catalysts and catalyst supports found from BET analysis, m^2/g
A_{HDN}	Arrhenius constant for the hydrodenitrogenation reaction rate, $s^{-1}\cdot(mol/L)^{(1-v)}$
A_{HDS}	Arrhenius constant for the hydrodesulphurization reaction rate, $s^{-1}\cdot(mol/L)^{(1-n)}$
Al	aluminum
Al_2O_3	aluminum oxide
ATM	atmospheric

BET	Brunauer-Emmett-Teller method
BT	benzothiophene
BTU	British thermal unit
C_i	concentration of species i, mol/L
C_N	concentration of all nitrogen heteroatoms within gas oil, mol/L
C_S	concentration of all sulfur heteroatoms within gas oil, mol/L
d	average pore diameter of catalysts and catalyst supports, nm
DBT	dibenzothiophene
DDS	direct desulphurization
DMDBT	dimethyldibenzothiophene
E_A	activation energy for the hydrotreating reaction of species ‘A’, J/mol
EDGMA	ethylene glycol dimethacrylate
E_{HDN}	activation energy for the hydrodenitrogenation reaction, J/mol
E_{HDS}	activation energy for the hydrodesulphurization reaction, J/mol
FCC	fluid catalytic cracking unit
FTIR	Fourier transform infrared spectroscopy
G/O	ratio of volumetric flow rates between hydrogen gas and gas oil
GMA	glycidyl methacrylate
HC	hydrocarbon
HDA	hydrodearomatization
HDM	hydrodemetallization
HDN	hydrodenitrogenation
HDS	hydrodesulphurization

HGO	heavy gas oil
HYD	hydrogenation
IBP	initial boiling point
ICP-MS	inductively coupled plasma mass spectroscopy
k_A	apparent rate constant for species 'A', $(mol/L^{)(1-n)}.s^{-1}$
k_{HDN}	apparent rate constant of hydrodenitrogenation, $(mol/L)^{(1-n)}.s^{-1}$
k_{HDS}	apparent rate constant of hydrodesulphurization, $(mol/L)^{(1-n)}.s^{-1}$
K_A	adsorption equilibrium constant for component A, L/mol
K_{H2S}	adsorption equilibrium constant for hydrogen sulphide, MPa^{-1}
K_i	adsorption equilibrium constant for i species within gas oil, L/mol
K_N	adsorption equilibrium constant for nitrogen heteroatoms within gas oil, L/mol
K_S	adsorption equilibrium constant for sulfur heteroatoms within gas oil, L/mol
LGO	light gas oil
LHSV	liquid hourly space velocity, s^{-1}
M_{AVE}	average molecular weight of HGO, g/mol
Me	methyl
Mo	molybdenum
MoO_3	molybdenum trioxide
n	reaction order constant, dimensionless
NMR	nuclear magnetic resonance
PGMA	poly(glycidyl methacrylate)
PGMA-TENF	poly(glycidyl methacrylate) with tetranitrofluorenone
P_{H2}	partial pressure of hydrogen gas, Pa

P_{H2S}	partial pressure of hydrogen sulphide, Pa
r_A	reaction rate of species A, mol/(L·s)
r_{HDN}	rate of the overall hydrodenitrogenation reaction, mol/(L·s)
r_{HDS}	rate of the overall hydrodesulphurization reaction, mol/(L·s)
R	universal gas constant, J/(mol-K)
R^2	coefficient of regression for the reaction models, dimensionless
S_{BET}	surface area found from BET analysis, m^2/g
SCO	synthetic crude oil
SEM	scanning electron microscopy
SG	specific gravity, dimensionless
T_b	average boiling point of HGO, K
TENF	Tetranitrofluorenone
TGA	thermogravimetric analysis
TS	pellet surface temperature, K
TEM	transmission electron microscopy
υ_C	critical specific molar volume of HGO, mL/mol
υ_{Cm}	critical specific mass volume, mL/g
υ_i	molar volume of sulphur/nitrogen under standard conditions, mL/mol
υ_L	molar volume of HGO under standard conditions, mL/mol
υ_N	hydrogen molar volume at standard conditions, L/mol
V_b	hydrogen molar volume at the normal boiling point, mL/mol
V_C	volume of loaded catalyst, mL
VDU	vacuum distillation unit

VGO	vacuum gas oil
V_P	total pore volume found for catalysts and catalyst supports, cm^3/g
x_{HDN}	stoichiometric ratio of H_2 consumption for nitrogen removal, dimensionless
x_{HDS}	stoichiometric ratio of H_2 consumption for sulphur removal, dimensionless

CHAPTER 1

INTRODUCTION

1.1 Research Background

Crude oil is known as the "feedstock" from which refineries are able to produce a wide range of petroleum products required by consumers in the transportation, residential, commercial, and industrial sectors. Due to increasing demand for gasoline and diesel fuels, the exploitation of heavy oil and bitumen from various deposits is quickly becoming a vital option for meeting the present and future energy requirements (Ferdous, 2003). Continuing depletion of lighter crude oil and advancement of oil sand technology has resulted in tendencies towards conversion of lower grade heavy feedstocks, particularly bitumen-derived heavy gas oil (Ancheyta et al., 2007). The western Canadian sedimentary basin (underlying Alberta, Saskatchewan, and part of Northwest Territories) has been the main source of Canadian oil production for the last 50 years; and is spread across 77,000 sq. km of relatively remote northern Alberta landscape in the western Canada sedimentary basin (Ferdous, 2003). It is estimated that throughout the oil sands, about 20 percent of the oil sand layer is buried at depths of 80 m or less, making surface mining economically feasible. The remaining reserve is buried as deep as 760 m (Energy, 2000). Oil sands are primarily a mixture of bitumen, sand, water, and clay. Each grain of sand is enveloped by a thin film of water that also contains extremely fine particles of clay and other trace materials. Bitumen, which is a very heavy, asphalt-like form of crude oil, surrounds the sand and water; thus, making it difficult to process in most refineries. The situation is further complicated as the dependence on heavier and sour crudes increases due to shortage in the availability of light and sweet crude oils. The bitumen derived gas oil contain high levels of nitrogen (approx. 0.3 wt%) and sulphur (approx. 4 wt%) compounds as compared to those

present in conventional crude oils (approx. nitrogen: 0.13 wt% & approx. sulphur: 2.5 wt%). Therefore, the products such as heavy gas oil obtained from processing of bitumen also contain high level of these contaminants, especially nitrogen (Ferdous, 2003). It is well known that gas oils derived from bitumen are difficult to hydrotreat and that conventional, hydrotreating catalysts are deactivated much more than expected because of poisoning and inhibition by nitrogen bearing components. Nitrogen heterocycles may also affect the quality of the final product through the formation of insoluble sediments and gums (Woods et al., 2004). Therefore, removal of these contaminants is essential in ensuring that regulatory standards are being met.

The susceptibility of catalysts capable of refining petroleum feedstocks, to organic nitrogen bearing compounds has long been recognized and studied (Hong et al., 2004; Koltai et al., 2002). Although several species are capable of inhibiting and deactivating the catalyst active sites during hydrodesulphurization (HDS), the order of inhibition can be classified as follow: nitrogen compounds > organic sulphur compounds > polyaromatics ≈ oxygen compounds ≈ H_2S > monoaromatics (Hong, 2004). It has also been proposed that upon achieving high levels of desulphurization, the concentration of refractory sulphur compounds decrease to a point where polyaromatics and nitrogen compounds naturally occurring in gas oils inhibit the HDS process through competitive adsorption (Koltai, 2002).

Numerous studies have been performed concerning basic nitrogen compounds acting as inhibitors during HDS reactions; however, non-basic moieties, such as carbazole and indole have also been observed to show levels of inhibition comparable to those of the basic species (Georgina et al., 2003). These inhibiting effects are due to either hydrogenation reactions occurring during the process, leading to the formation of basic species (Nagai et al., 1983), or to adsorption of the parent non-basic compounds themselves onto the catalyst active sites (Dong et

al., 1997; Muegge et al., 1991; and Yang et al., 1984). Studies performed by Nagai et al. (1983) and LaVopa et al. (1988) also took into account the inhibiting effect of carbazole on thiophene and dibenzothiophene (DBT) during HDS reactions; their results were comparable to those of the basic nitrogen species such as acridine, pyridine, and piperidine. Furimsky et al., (1999) performed long-term adsorption studies using indole as the non-basic nitrogen compound during HDS reaction of DBT, and showed that catalyst recovery was substantially weak, even after removal of indole from the feedstream.

Over the years, numerous non-catalytic processes have been investigated for the removal of nitrogen bearing compounds, including CuY zeolites, capable of adsorbing sulphur and nitrogen compounds, with high adsorptive capacities at ambient temperatures and pressures (Kwon et al., 2008); activated carbon from numerous sources such as coconut, wood, petroleum coke, coal, and aluminas such as strong acid alumina, weak acid alumina, and basic alumina; from these, activated carbon samples have generally shown higher nitrogen removal than activated alumina samples, and the adsorption capacity and selectivity of the activated carbons toward nitrogen compounds is presumed to be correlated to their textural properties and more so, their oxygen content (Masoud et al., 2009a; Yosuke et al., 2004a; Masoud et al., 2009b; and Yosuke et al., 2004b). Transition metal salts such as $CuCl_2.2H_2O$ have also been utilized due to their ability to extract nitrogen compounds of the basic and those of the heterocyclic nature from synthetic crude oils by complex formation (Janchig et al., 2008). These aforementioned methods tend to be fairly effective in the removal of basic nitrogen compounds as well as sulphur compounds; however, none of them are efficient enough for the selective removal of non-basic or neutral nitrogen compounds, an area which has not been extensively explored.

The primary objectives of this research are to explore the synthesis of a novel polymer, poly(glycidyl methacrylate) incorporated with the organic compound tetranitrofluorenone (PGMA-TENF) for selectively targeting the non-basic nitrogen species present in bitumen-derived heavy gas oil extracted from the Athabasca Oil Sands; without having a significant effect on the presence of basic nitrogen or sulphur species in the gas oil. The removal of non-basic nitrogen species will give an insight into the level of inhibition and deactivation of catalyst active sites due to their presence.

1.2 Knowledge Gaps

A comprehensive review of research articles to date focusing on pre-treatment of gas oil and the inhibitory and deactivating effects of nitrogen bearing species has revealed that the following key areas have not been extensively investigated:

1. Synthesis and optimization of functionalized polymer such as poly(glycidyl methacrylate) (PGMA) incorporated with organic compound tetranitrofluorenone for selective removal of non-basic nitrogen bearing species from bitumen derived heavy gas oil, to the best of our knowledge, has never been investigated.
2. Hydrotreatment studies using bitumen derived heavy gas oil with selective removal of non-basic nitrogen bearing species in order to investigate their effect on catalyst inhibition and deactivation has never been investigated.
3. Kinetic studies evaluating the performance of the catalyst due to the absence of non-basic nitrogen bearing species in bitumen derived heavy gas oil has not been explored.

1.3 Hypotheses

The following hypotheses have been proposed based on extensive literature review which is to follow:

1. Enhanced hydrodesulphurization and hydrodenitrogenation may be achieved through reducing temporary and permanent poisoning of the catalyst active sites by decreasing non-basic nitrogen bearing species such as indoles and carbazoles from bitumen derived heavy gas oil.
2. Pre-treatment of heavy gas oil by means of functionalized polymers will selectively reduce the non-basic nitrogen species content that competitively adsorbs onto the catalyst active sites causing inhibition and deactivation during the hydrotreatment process.
3. Elimination of non-basic nitrogen species can in turn improve catalyst life while simultaneously requiring lower temperatures for achieving the same conversion levels.

1.4 Research Objectives

The main objective of this proposed research was to synthesize an electron deficient polymer capable of selectively removing non-basic nitrogen species from heavy gas oil in order to study the effects of catalyst inhibition and deactivation during the hydrotreatment process. The research objectives have been divided into three phases, each of which is discussed in further detail below.

Phase I: Synthesis and Optimization of PGMA-TENF

Phase I dealt with synthesizing the functionalized polymer in a four step process, with step 1 consisting of developing the poly(glycidyl methacrylate) polymer beads as the polar support for the π-acceptor molecules; the second step consists of substitution of the epoxide

functionalities on the polymer by the use of acetone oxime; the third step is a separate procedure dealing with the synthesis of the organic compound tetranitrofluorenone (TENF); finally, the fourth step consists of coupling of TENF onto the oxime functionality thereby producing a polar polymer with electron deficient sites. Each step of the polymer synthesis was optimized and characterized by varying experimental parameters in order to obtain the highest yield. Once the optimized polymer was produced, a contact study was performed in order to determine the optimum contact time between the polymer and the heavy gas oil, as well as the maximum quantity of the polymer beads that should be used with respect to the amount of heavy gas oil being treated.

Phase II: PGMA-TENF Batch Production and Hydrotreatment Study

Phase II involved studying the effects of inhibition and deactivation caused by non-basic nitrogen species present in heavy gas oil. Selecting and mass producing the most effective synthesized polymer, as determined from phase I, three heavy gas oil feedstocks at varying non-basic nitrogen concentrations were produced – herein referred to as HGO I (as obtained HGO), HGO II (5 % nitrogen removal), and HGO III (3% nitrogen removal). Inhibition and deactivation due to the presence and absence of non-basic nitrogen species was studied by means of alternating feed between specific heavy gas oil (HGO I, HGO II, HGO III) and clean feed – which consisted of hydrotreated gas oil with an addition of 2 wt% sulphur (1wt% thiophene and 1 wt% dibenzothiophene, and measuring the hydrodesulphurization and hydrodenitrogenation conversions. Hydrotreatment tests were performed using a commercial NiMo/γ-Al_2O_3 catalyst.

Phase II: Kinetic Study and Model Development

Final phase of this research involved determining the reaction kinetics in order to understand and promote the effects of non-basic nitrogen species. Hydrotreatment reactions were carried out at varying temperature and LHSV conditions in order to develop kinetics models using power law and Langmuir-Hinshelwood kinetic expressions.

CHAPTER 2

LITERATURE REVIEW

This chapter provides a comprehensive literature review that was performed during the formulation of this research work. Section 2.1 provides a brief overview of world energy consumption and Canada's contribution; section 2.2 describes the characterization of gas oil; sections 2.3, 2.4, and 2.5 relate to the hydrotreating process, hydrotreating reaction mechanisms, and hydrotreating catalysts; and finally sections 2.6 and 2.7 cover the pre-treatment technique using functionalized polymers and the kinetic study.

2.1 Global Energy Consumption and Canada's Contribution

Significant portion of the world's raw energy requirements are presently met through the use of fossil fuels formed by natural processes. Statistics based on the international energy outlook from 2011, as shown in Figure 2.1 illustrate an approximate increase in the world energy consumption by 53 percent, from 505 quadrillion Btu in 2008 to 770 quadrillion by 2035 (U.S. Energy Information Administration, 2011a).

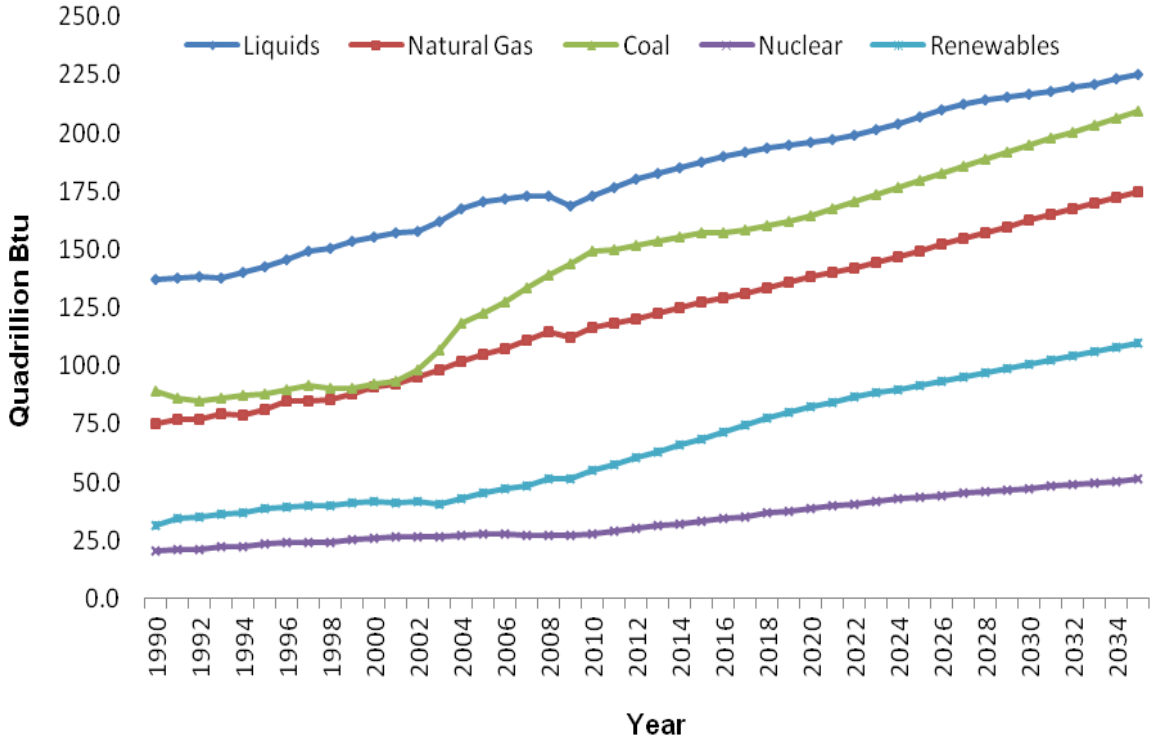

Figure 2.1: World energy consumption (Adapted from U.S. Energy Information Administration, 2011).

The significant increase in the consumption of liquid energy is quite noticeable in Figure 2.1; however, petroleum and other liquid fuels are the world's slowest-growing source of energy, with given expectations that world oil prices will remain relatively high through most of the projection period shown in Figure 2.1 (U.S. Energy Information Administration, 2011b). These concerns have shifted considerable attention towards efficient production of gas oil derived from bitumen in the Canadian oil sands, which is used for the production of synthetic crude oil.

The Oil and Gas Journal reported on a revision to Canada's proven reserves of crude oil to an estimate of 175.2 billion barrels of proven reserves (97% from unconventional deposits such as bitumen), placing it third globally, only behind Venezuela and Saudi Arabia. These unconventional deposits place Canada as one of the central sources of non-OPEC production growth in the coming decades (U.S. Energy Information Administration, 2011c).

2.2 Characterization of Gas Oil

2.2.1 Oil Sand, Bitumen, and Heavy Gas Oil Characterization

Oil sands often referred to as tar sand or bituminous sands are a naturally occurring deposits containing approximately 10–12% bitumen, 4-6% water and 80-85% sand and clay (Yui, 2008). The synthetic crude derived from the oil sand contains large amounts of middle distillate in comparison to conventional crude, with approximately 44% gas oil and 56% vacuum bottoms (Yui, 2008).

The term bitumen can be defined as "any natural mixture of solid and semi solid hydrocarbons" (Gray, 1994), with a high viscosity and a composition consisting of highly condensed molecules. Conventional crude oil, bitumen and heavy gas oil fractions can be characterized in terms of their physical properties as illustrated in Table 2.1.

Table 2.1: Characteristics of conventional crude oil, bitumen, and heavy gas oil (Gray, 1994; Lee et al., 2007).

	Viscosity [mPa.s]	**Density [g/cm^3]**	**API Gravity**
Conventional Crude Oil	10	-	25 - 37
Bitumen	$> 10^5$	> 1.00	< 10
Heavy Gas Oil	10^2 - 10^5	0.934 - 1.0	20 - 10

Table 2.1 illustrates the significant differences in viscosity, density, and API gravity between conventional crude oils and bitumen derived heavy gas oils; properties that considerably increase the difficulty of treatment of heavy gas oil.

Heavy gas oil is the fraction that is obtained through vacuum distillation of crude petroleum, with feedstocks acquired from Kuwait having a boiling range of 321-365 °C, Arabian heavy crude having a range of 345-565 °C (David and Pujadó, 2006), and athabasca bitumen

derived heavy gas oil having range very similar to that of the Arabian feed, 343-525 °C (Yui, 2008). Heavy gas oil obtained from atmospheric distillation units is often used to heat oil blending pool, gas oil pool, or fuel oil pool (David and Pujadó, 2006); whereas, heavy gas oil obtained through vacuum distillation of crude oil is often used as feedstock for catalytic cracking (Ancheyta and Speight, 2007).

2.2.2 Chemical Compounds Present in Heavy Gas Oil

The physical and chemical compositions of heavy gas oil vary by location, age of the oil field, and depth of the individual oil; while observing from a molecular perspective, it is a mixture of hydrocarbons, organic compounds such as nitrogen, sulphur, and oxygen, and metallic constituents such as nickel, vanadium, copper, and iron (Ferdous, 2003a).

The nitrogen and sulphur content of the heavy gas oil feed derived from Athabasca bitumen, as shown in Table 2.2, is significantly higher than conventional feeds; thus, making it much more difficult to process than light crude oils. It is also observed that it has a higher density, which is due to the high aromatic content (Duan, 2005).

Table 2.2: Characterization of heavy gas oil derived from Athabasca bitumen (Ferdous, 2004).

Characterization Parameters	Amount
Boiling Range (°C)	340 - 550
Sulphur Content (ppm)	40370
Nitrogen Content (ppm)	2986
Basic Nitrogen Content (ppm)	1043
Non-basic Nitrogen Content (ppm)	1943
Aromatic Content (ppm)	3720
Density (g/ml)	0.98

It is also imperative to consider the characteristics of light gas oil derived from Athabasca bitumen, due to the fact that there seems to be a significant difference in the hydrodesulphurization and hydrodenitrogenation of the two gas oil streams. Table 2.3 given below illustrates the characteristics of light gas oil derived from Athabasca bitumen.

Table 2.3: Characterization of various light gas oils derived from Athabasca bitumen (Owusu-Boakye, 2005).

	N (wppm)	**BN (wppm)**	**S (wppm)**	**C (wt%)**	**H (wt%)**	**^{13}C NMR**	**Density (g/cm^3)**
HLGO	1773	1211	7149	86.50	12.89	24.00	0.97
VLGO	634	285	26780	85.40	11.92	23.90	0.94
ALGO	290	153	15020	85.70	12.66	15.50	0.89
BLGO	461	247	17420	85.50	12.06	17.10	0.90

The feed streams shown in Table 2.3 represent hydrocrack light gas oil (HLGO), vacuum light gas oil (VLGO), atmospheric light gas oil (ALGO), and blended light gas oil (BLGO). It is interesting to note that in comparison to the characteristics of heavy gas oil shown in Table 2.2, light gas oil tends to have approximately 45% non-basic nitrogen compounds; whereas, heavy gas oil has approximately 65% non-basic nitrogen compounds; thus a 20% higher non-basic nitrogen content. Nitrogen and sulphur being the predominant and most influential compounds are further discussed below.

2.2.3 Heterocyclic Nitrogen Compounds

The presence of nitrogen bearing species in heavy gas oil is exceedingly detrimental during the hydrotreatment process. This is due to the poisoning of cracking catalysts and the contribution towards gum formation (Speight, 2000).

Nitrogen is predominantly present in the form of heterocyclic aromatic compounds, with aliphatic amines and nitriles being present in smaller amounts. The reactivity of aliphatic amines

and nitriles is very strong, allowing them to denitrogenate much more rapidly (Girgis and Gates, 1991). The heterocyclic nitrogen compounds can generally be divided in two groups: basic nitrogen compounds and non-basic nitrogen compounds. Basic nitrogen compounds are mostly six membered pyridine groups, while non-basic nitrogen compounds are usually five membered pyrrole groups (Ferdous, 2003a). The two main types of aromatic nitrogen compounds that have been identified in the Athabasca bitumen are non-basic (neutral) pyrrole benzologues and basic pyridine benzologues. It is also known that alkyl-substituted carbazoles are the major type of non-basic nitrogen compounds in synthetic crude oil. Based on this information, the nitrogen compounds present can be classified into two categories: basic and non-basic (neutral) heterocyclic compounds, such as pyridine, acridine, carbazole, quinoline, and indole (Ferdous, 2003b). Figure 2.2 given below illustrates some common basic and non-basic nitrogen compounds found in gas oil. Non-heterocyclic organonitrogen compounds such as aliphatic amines and nitriles are also present, but in considerably smaller amounts and can denitrogenated much more rapidly than the heterocyclic compounds (Ferdous, 2003b).

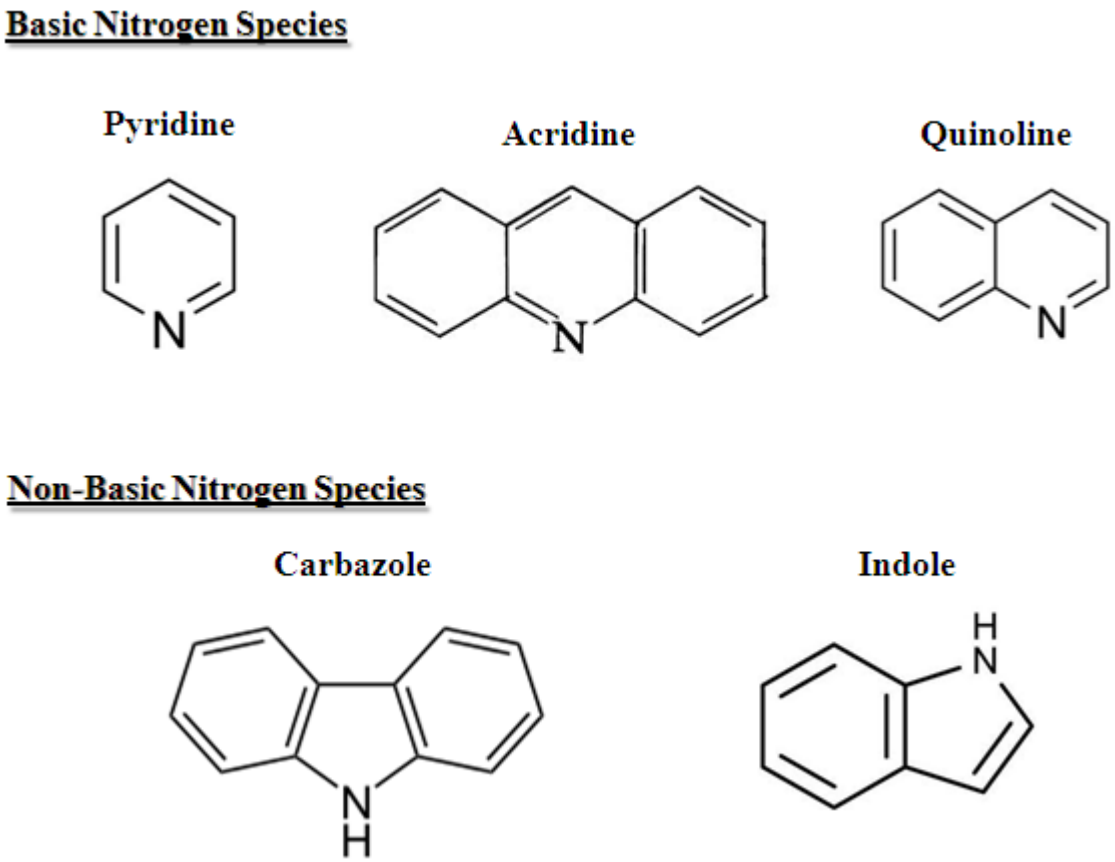

Figure 2.2: Typical basic and non-basic nitrogen compounds in gas oil (Adapted from Wikipedia, 2011).

The basicity of the nitrogen compounds exists due to the lone pair of electrons found on the nitrogen atom, making it readily available for reaction with acidic catalyst such as lewis base (Botchwey, 2003). In the case of non-basic nitrogen compounds, the electrons on the nitrogen atom tend to be delocalized within the ring containing the atom making them electron rich, but difficult to react with the acidic catalyst.

2.2.4 Heterocyclic Sulphur Compounds

Concentration of sulphur compounds found in petroleum feedstocks can vary significantly – 0.04 wt% for light crude oil to 5 wt% for heavy crude oil (Speight, 1999). The most abundant heterocyclic sulphur compounds identified in petroleum includes sulfides, thiophenes,

benzothiophenes, dibenzothiophenes, and naphthobenzothiophenes. Figure 2.3 illustrates several sulphur compounds found in crude oil.

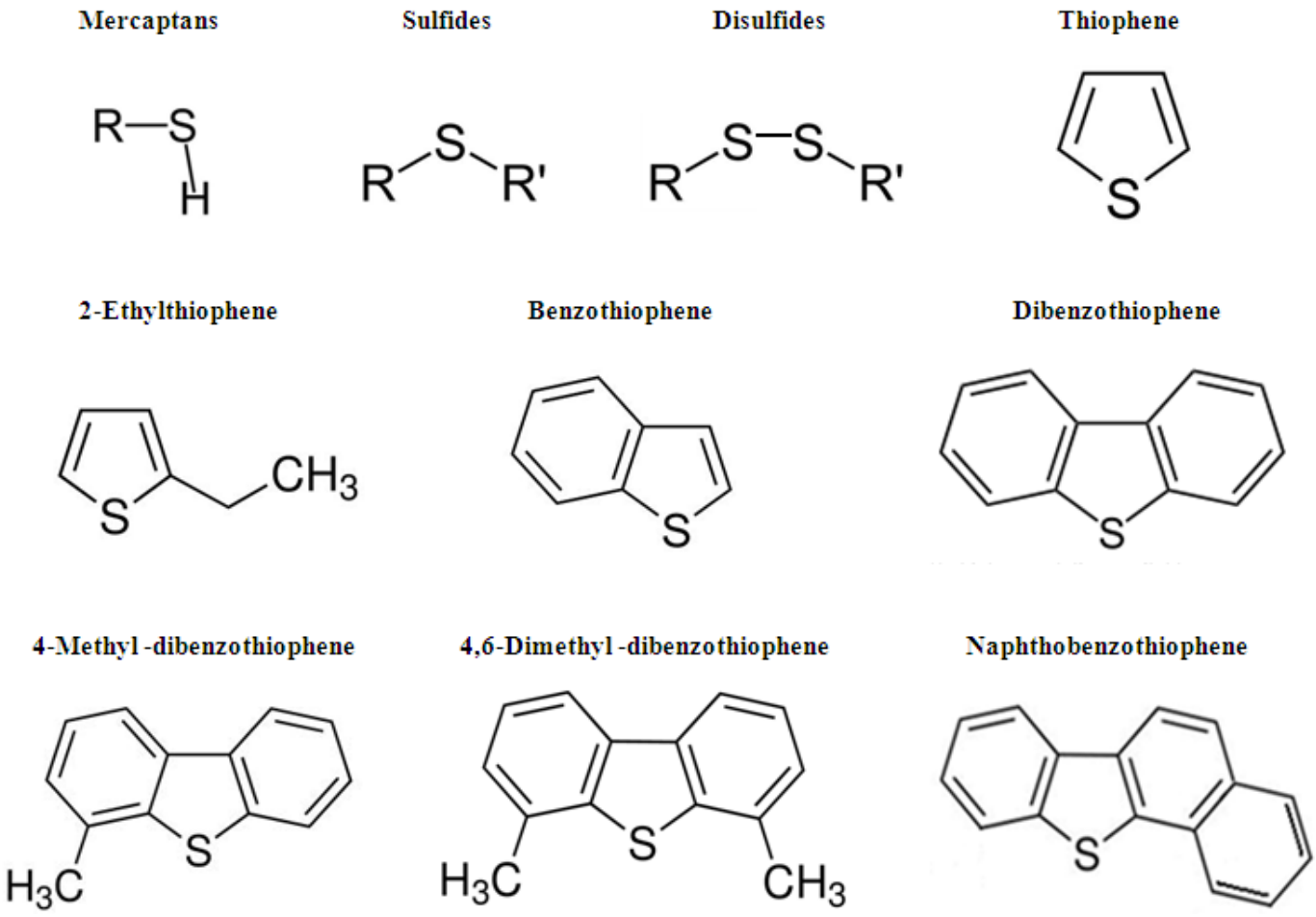

Figure 2.3: Typical sulphur compounds present in petroleum feedstock (Adapted from Topsøe et al., 1996).

During the hydrotreatment process, some sulphur species are readily hydrotreated or removed, while others such as thiophenic compounds are known to have the least reactivity (Girgis and Gates, 1991).

2.3 The Hydrotreating Process

2.3.1 Definition of Hydrotreating

Hydrotreating is an integral part of the oil refining process involving thermal treatment of the feedstock with hydrogen under high pressures. Its importance has continuously increased over the years. As an example of the necessity of hydrotreating, data collected in 1998 showed that of a total worldwide daily refinery capacity of approximately 81,500,000 bbl of oil, approximately 8,500,000 bbl/day is dedicated to catalytic hydrorefining and approximately 28,100,000 bbl/day is dedicated to catalytic hydrotreating (Speight, 2002).

The hydrotreating process makes use of the principle that the presence of hydrogen during mild thermal treatment reaction of a petroleum feedstock removes the heteroatoms and metals. The feedstock is reacted with hydrogen at temperatures, in the range of 300 – 400 °C, and elevated pressures in the range of 1200-1300 psi, under the presence of a catalyst, typically containing nickel-molybdenum (Ni-Mo) on γ-alumina (γ-Al_2O_3) support. During the hydrotreatment process the heteroatoms are removed in the form of hydrogen sulphide (H_2S), ammonia (NH_3), and water (H_2O), and metal species such as vanadium (V) and nickel (Ni) are simultaneously removed by hydrometallization reactions (Speight, 2002). Figure 2.4 given below illustrates a simplified schematic of the applications of hydrotreating in a modern refinery.

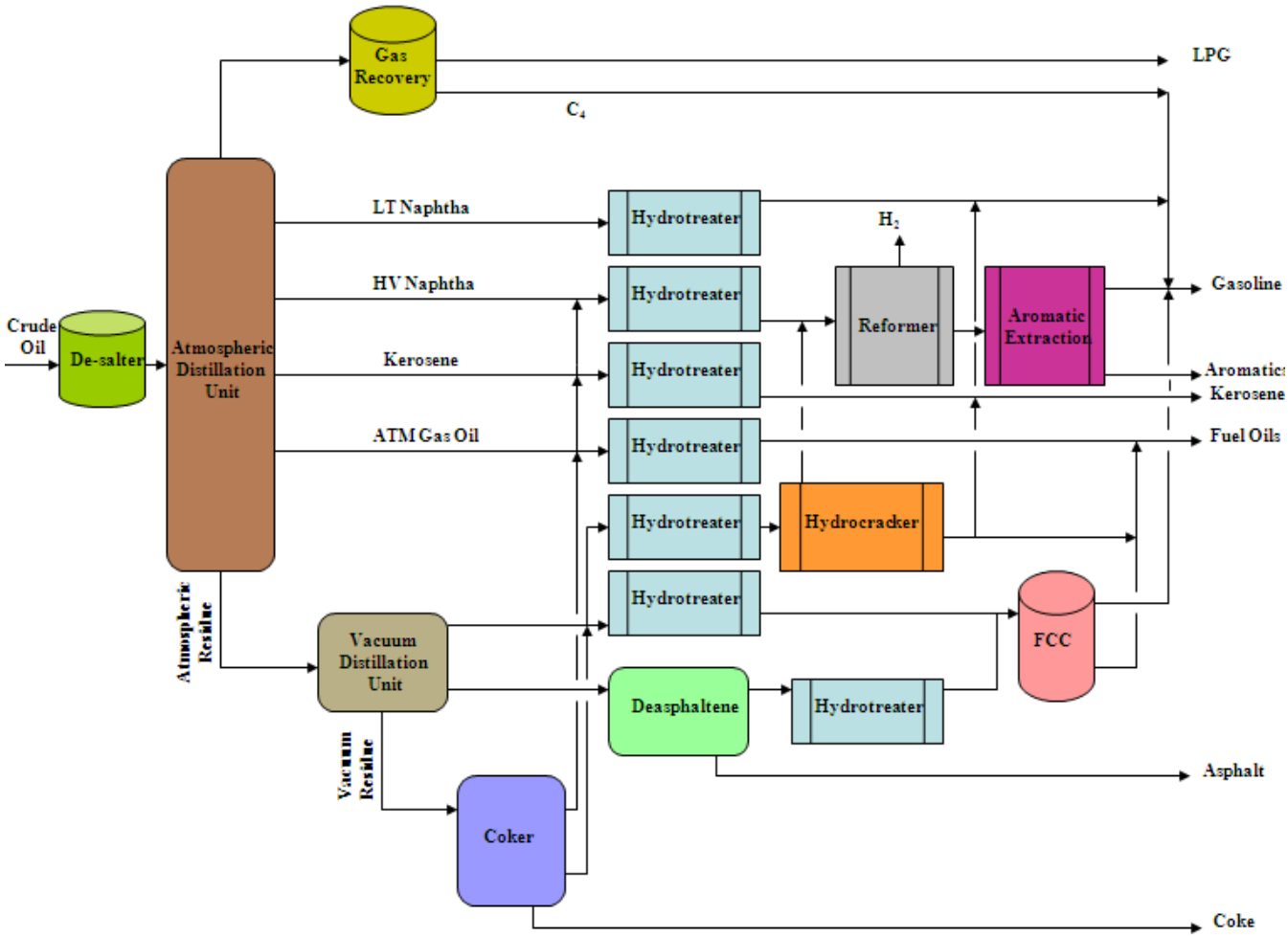

Figure 2.4: Application of hydrotreating in a modern refinery (Adapted from Mochida and Choi, 2004).

2.3.2 Objectives of Hydrotreating

The hydrotreating process consists of numerous reactions that occur simultaneously; however, one of the most distinguishing features is that the final product meets the required specifications for its particular purpose (Speight, 2002). Hydrotreating of various gas oils and residue can contribute to the following benefits (Bhattacharyya, 2005):

1. Improvement of FCC feed stock quality.
2. Reduction of coke yield in delayed coker and increase in liquid product yield.
3. Increase coke selling price as a result of lower sulphur and metal content.
4. Production of superior quality fuel oil.
5. Reduction of construction material cost for FCC and coker processing due to lower sulphur feedstock.
6. Increase in the capability of processing a wide variety of crudes.

2.4 Hydrotreating Reaction Mechanisms

The hydrotreatment process involves the removal of undesirable compounds from the petroleum fraction through selective reaction with hydrogen at high temperatures and pressures. This process can be generalized as shown in equation 2.1 (Boahene, 2011).

$$\text{Feed} \xrightarrow{\text{Catalyst, } H_2\text{, T, P}} \text{H/C} + H_2S + NH_3 + H_20 \qquad \text{(Eqn. 2.1)}$$

Emission regulations for sulphur and catalyst poisoning caused by nitrogen species present in the feedstock make hydrodesulphurization (HDS) and hydrodenitrogenation (HDN) the principle processes of interest during the hydrotreatment of bitumen derived gas oils.

2.4.1 Hydrodesulphurization

The removal of sulphur from the petroleum stream is greatly dependent on the structure of the sulphur compound, with the rate of removal varying several orders of magnitude (Mochida and Choi, 2004). Generally, acyclic sulphur compounds such as thiols and disulphides are highly reactive and can be removed under very mild conditions. Saturated cyclic sulphur compounds and aromatic systems in which sulphur is present in six-membered rings are also very highly reactive. However, compounds in which the sulphur atom is incorporated into the five-membered aromatic ring structure – such as thiophene, are much less reactive and the reactivity decreases as the ring structure becomes increasingly condensed (Mochida and Choi, 2004).

The sulphur compounds present in petroleum fractions can be classified into one of the following six sulphur types: mercaptans, sulfides, di-sulfides, thiophenes, benzothiophenes, and di-benzothiophenes. Figure 2.5 given below illustrates typical reaction mechanisms for these organosulphur molecules during the hydrotreatment process.

Mercaptans

Sulfides

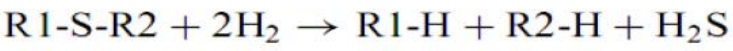

Di-sulfides

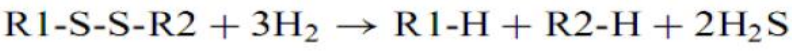

Thiophenes

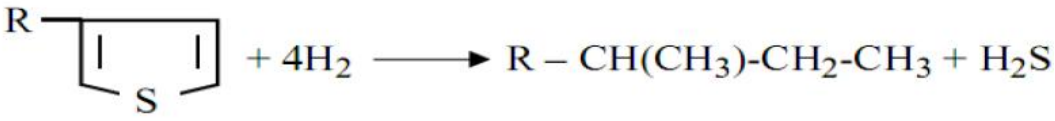

Benzo-thiophenes

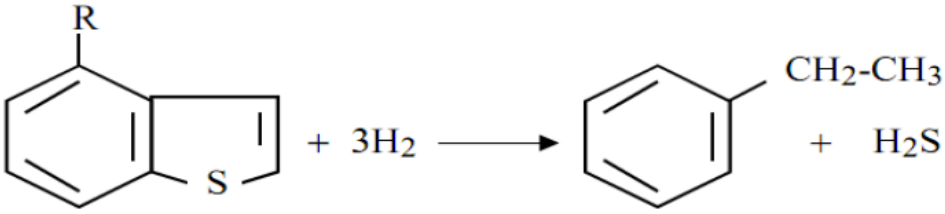

Di-benzo-thiophenes

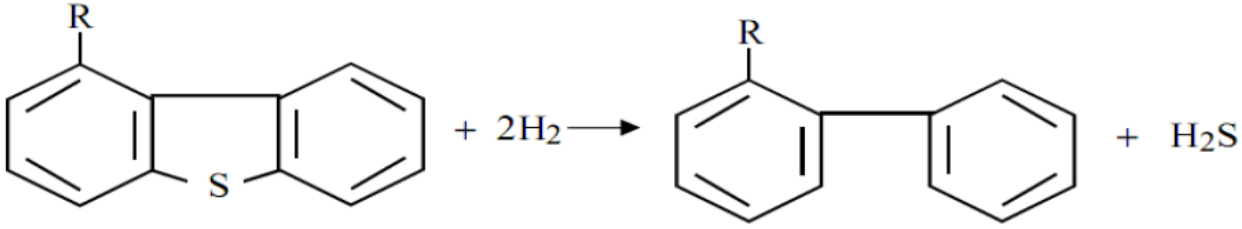

Figure 2.5: Typical reactions mechanisms for organosulphur molecules in petroleum crude (Adapted from Gruia, 2006).

There are several reaction pathways through which sulphur can be removed, and the preferred pathway changes depending upon the specific structure of the compound (Mochida and Choi, 2004). The two major reaction pathways that may occur during desulphurization include the hydrodesulphurization route and the hydrogenation route. In the first reaction mechanism, the sulphur atom is removed from the structure and replaced by a hydrogen atom. In this reaction scheme, there is no hydrogenation of any of the other carbon-carbon double bonds. The second reaction pathway referred to as the hydrogenation route, assumes that at least one aromatic ring adjacent to the sulphur containing ring is hydrogenated before the sulphur atom is removed and replaced by a hydrogen atom. The hydrogenation route destabilizes the aromatic ring system; thus weakening the sulphur-carbon bond and provides a less sterically hindered environment for the sulphur atom (Mochida and Choi, 2004).

The hydrogenation route is subject to thermodynamic equilibrium constraints, which results in maxima in the observed rates of hydrodesulphurization via the hydrogenative route, as a function of temperature, and allows hydrodesulphurization to be limited at low pressures and high temperatures. (Mochida and Choi, 2004). Figure 2.6 illustrates the hydrodesulphurization reaction mechanism during sequential and simultaneous desulphurization schemes.

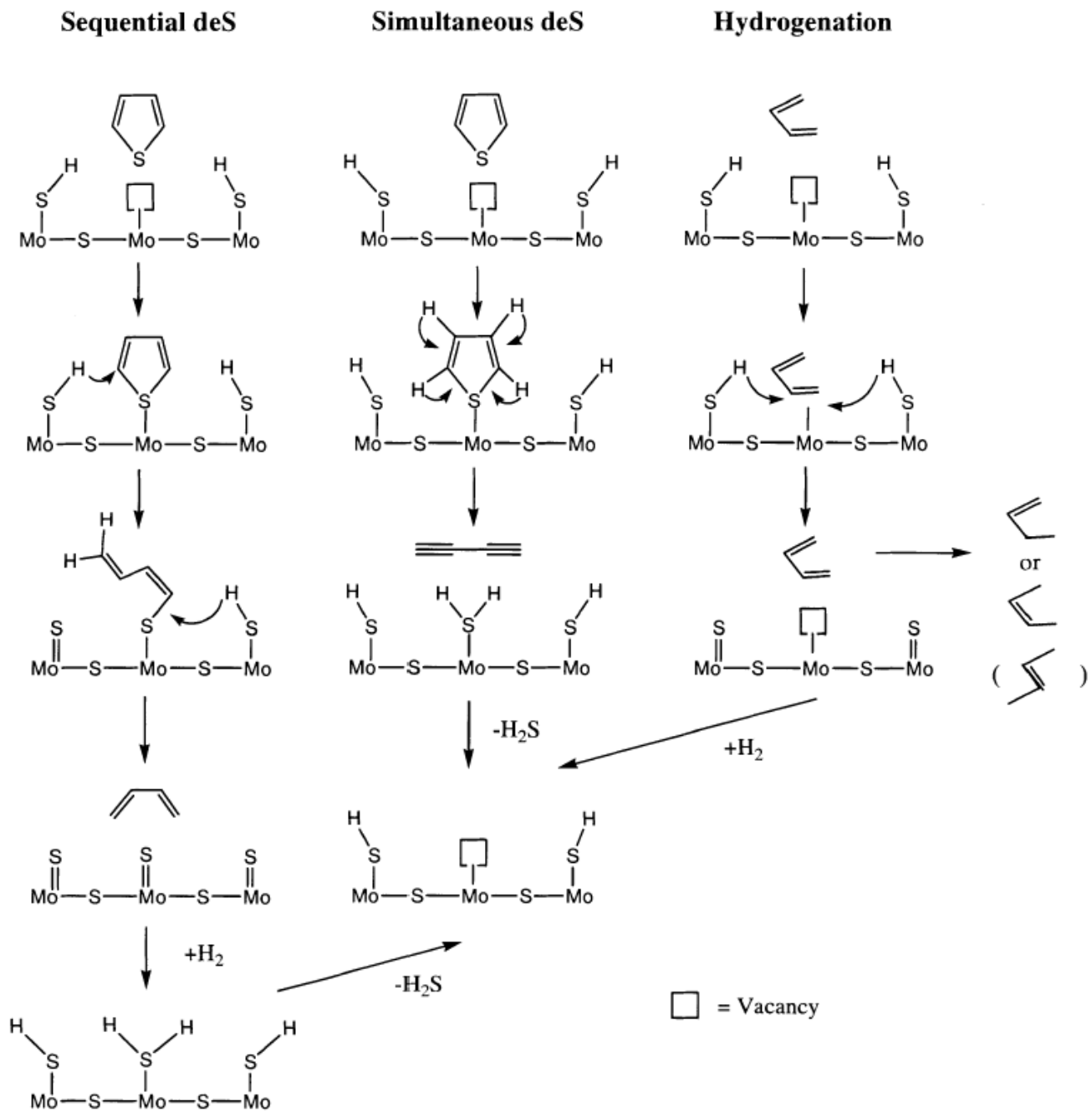

Figure 2.6: Sequential and simultaneous hydrodesulphurization reaction mechanism (Mochida and Choi, 2004).

The direct pathway towards desulphurization becomes more and more difficult with larger aromatic structures due to their increase in stability; as well, the insertion becomes sterically hindered in more condensed rings. Another complication is the proximity of the alkyl groups to the sulphur atom in the aromatic ring; with increasing adjacent alkyl groups the reactivity decreases due to steric hindrance of the sulphur during adsorption on the catalyst surface Consequently, hydrogenative routes are not significantly affected by alkyl substitution on the aromatic ring; whereas, the direct route becomes less important due to the presence of adjacent alkyl groups (Mochida and Choi, 2004).

2.4.2 Hydrodenitrogenation

There are several classes of reactions which simultaneously occur during the hydrotreatment process, with hydrodesulphurization and hydrodenitrogenation being the two prominent reaction mechanisms of interest. It has been well established based on numerous studies (Prins, 1997; Lu, 2007) over the years that the hydrodenitrogenation reaction network is much more complicated than the hydrodesulphurization reaction network, due to the fact that the heterocyclic ring has to be hydrogenated prior to the cleavage of the carbon-nitrogen bond. The reasoning is that the dissociation energy of double bonds in the heterocyclic rings is approximately twice that of the single bond in the hydrogenated heterocyclic rings (Lu, 2007). Quinoline – a basic nitrogen compound has often been used in representing the HDN process, since it offers many advantages over other nitrogen-containing hydrocarbons. Due to its bicyclic molecular structure, all reactions which take place in industrial HDN occur in the HDN reaction network of quinoline as well, for instance carbon-nitrogen bond cleavage, hydrogenation of an aromatic heterocyclic ring, and hydrogenation of a phenyl ring (Prins, 1997). Figure 2.7 given

below represents the reaction network of quinoline. According to Prins (1997), there is a general consensus on the given mechanism based on studies performed by several groups.

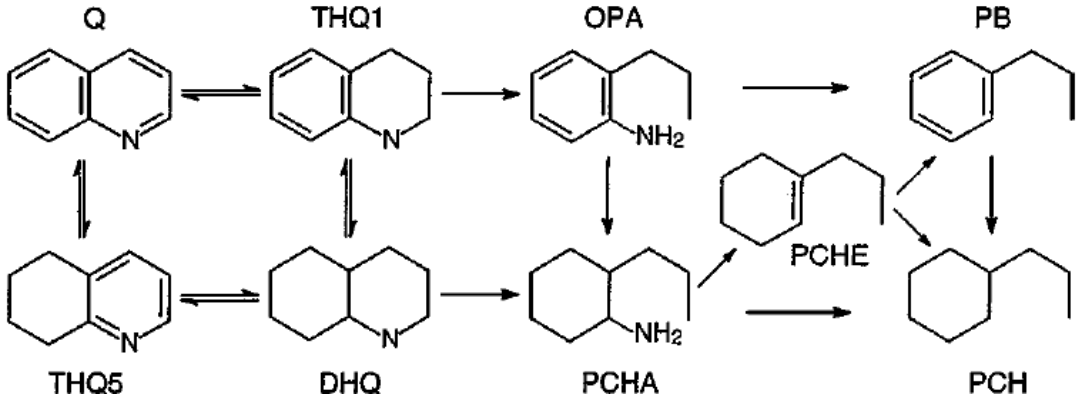

Figure 2.7: Reaction network of quinoline. Q = Quinoline; THQ5 = 5,6,7,8 Tetrahydroquinoline; DHQ = Decahydroquinoline; THQ1 = 1,2,3,4-Tetrahydroquinoline; OPA = *Ortho*-propylaniline; PCHA = 2-Propylcyclohexylamine; PCHE = Propylcyclohexene; PCH = Propylcyclohexane; PB = Propylbenzene (Prins, 1997).

Based on Figure 2.7, there are two ways to remove the nitrogen atom from quinoline, via OPA or via DHQ. In the first path, the heterocycle in quinoline (Q) is hydrogenated to THQ1 followed by ring opening to OPA. OPA is then hydrogenated to PCHA, and the nitrogen atom is removed from PCHA by elimination. In the second HDN path, quinoline is fully hydrogenated to DHQ which then reacts to PCHA and on to the hydrocarbons (Prins, 1997).

The reaction network shown in Figure 2.7 for quinoline is for a basic nitrogen containing compound, it is also crucial to study the reaction network of a non-basic nitrogen containing compound in order to understand the comparable characteristics followed during the HDN process. Figure 2.8 given below represents the reaction network of indole – a non-basic nitrogen containing compound.

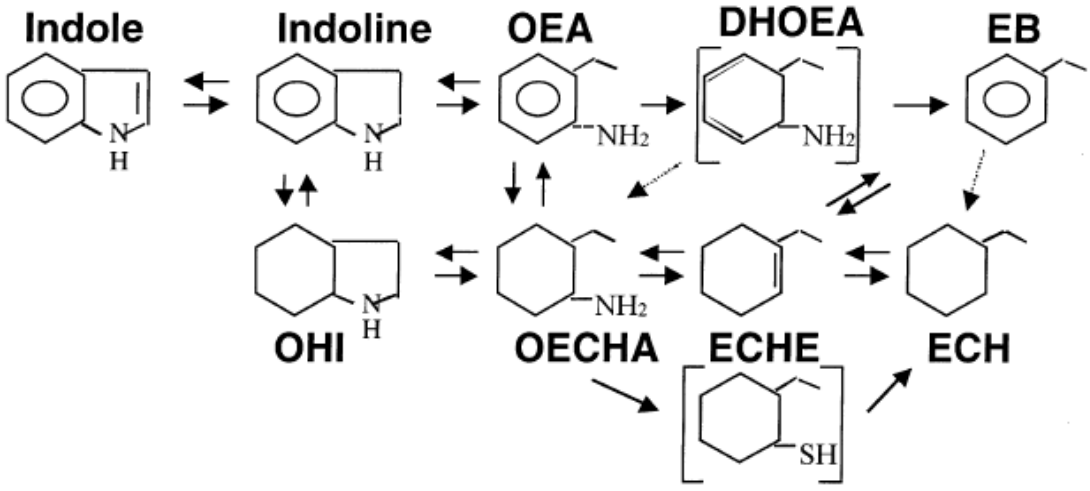

Figure 2.8: Reaction network of indole. OEA = O-ethylaniline; DHOEA = Dihydro-o-ethylaniline; EB = Ethylbenzene; OHI = Octahydro-indole; OECHA = O-ethylcyclohexylamine; ECHE = Ethylcyclohexene; ECH = Ethylcyclohexane (Bunch, 2000).

Based on Figure 2.8 there is a general consensus that the reaction network for indole HDN starts out with hydrogenation of the heterocyclic ring in a reversible step which leads to indoline formation, dictated by thermodynamic equilibrium under most conditions. Starting from indoline, the proposed reaction pathways in the literature were disputed (Bunch, 2000). Several of the previous reports on indole HDN suggest that *o*-ethylaniline (OEA) is the exclusive intermediate towards the formation of hydrocarbons, following indoline formation. On the other hand, one of the more recent studies (Callant et al., 1995) proposed that the reactivity of OEA is negligible in a mixture with indole/indoline so that the denitrogenation of indoline is via octahydroindole (OHI), an intermediate from the complete hydrogenation of the benzene ring. However, OHI has not been observed in any of the studies in the literature (Bunch, 2000).

Observing the reaction pathways illustrated in Figure 2.7 and 2.8, it can be seen that the removal of nitrogen for both basic and non-basic compounds involves the saturation of the nitrogen containing ring, followed by ring opening and then removal of nitrogen. In a number of

cases, it is also proposed that due to the reversibility of the intermediate compounds such as THQ1 and DHQ, and indoline and OHI, there is the possibility of full saturation of the compound before ring opening can occur, followed by nitrogen removal. Studies performed by Stern (Stern, 1979) also indicated that hydrogenation of the nitrogen containing compounds is the rate-determining step, and not the nitrogen removal stage.

2.5 Hydrotreating Catalysts

Hydrotreating technology and approach have had incremental changes over the last 70 years; however, the most important constituents have hardly changed. Alumina (Al_2O_3) supported Co-, Ni-, Mo-, and W-based catalyst are still highly favoured in the industry due to their chemical, physical, and mechanical properties, activity response, availability, and costs (Jong, 2009).

2.5.1 Typical Catalyst Composition

Typical hydroprocessing catalysts consist of Ni/Co-promoted Mo/W sulphides supported on an inorganic matrix of γ-alumina (γ-Al_2O_3). Acidic inorganic additives such as phosphorous (P) and zeolites are also widely applied. Co-Mo- and Ni-Mo-P based catalysts are typically used for HDS and HDN applications, while zeolites and amorphous SiO_2-Al_2O_3 containing catalysts are applied towards hydrocracking applications (Jong, 2009).

Suitable pore size distribution dependent on the type of feedstock is essential for maintaining the activity of the catalyst. The distillate HDS and HDN catalysts typically have a surface area between 150 and 250 m^2/g and a narrow pore size distribution, where 75% of the total pore volume is typically lower than 0.7 cm^3/g in order to obtain sufficient activity per reactor volume (Jong, 2009). In processing heavier feedstocks, larger average pore diameter is

required in order to ensure access to the internal area of the catalyst surface; as well, larger pore volume can result in higher metal deposition. In addition to these chemical properties, outstanding mechanical properties such as side and bulk crushing strength, and abrasion are also essential in order to ensure that the large catalyst beds do not collapse under their own weight or lead to catalyst fines resulting in pressure drop over the catalyst bed (Jong, 2009).

2.5.2 Catalyst Active Components

The most commonly used active components in commercial catalysts for the hydroprocessing of various petroleum fractions include Molybdenum (Mo) and Tungsten (W); these components are further promoted through Co and Ni; and then dispersed on a high surface area support (Lauritsen et al., 2007). According to Boahene (2011) the catalysts are active only in their sulphide forms, such as molybdenum sulphide (MoS_2) or tungsten sulphide (WS_2). Many researchers have proposed theories to facilitate the explanation of synergy existing between the active phase metals and sulphur that make these crystal structures effective catalysts for hydrotreating reactions (Boahene, 2011). Numerous models as mentioned below have been proposed explaining the sulphide Co-Mo or Ni-Mo phases as well as the location and functionality of Co or Ni for hydrotreating catalysts:

i. Co-Mo-S Model: It is proposed that Co-Mo-S phase consists of the MoS_2 structure and promoters are located on the edge planes of MoS_2 (Topsoe and Clausen, 1984).
ii. Rim-Edge Model: This model assumes that the selectivity of the reaction pathway – direct desulphurization and hydrogenation are affected by the morphology of the MoS_2 or WS_2 structure (Daage and Chianelli, 1994).
iii. Monolayer Model: This model assumes that a monolayer is formed as molybdenum species are bonded to the surface of the alumina (Schuit and Gates, 1973).

iv. Intercalation Model: This model assumes that MoS_2 slab consists of a plane of Mo(W) atoms sandwiched between two hexagonal closed-packed of sulphur atoms, and Co is assumed to interact with the layer structure of MoS_2 (Voorhoeve, 1971).

Among these models, the "Co-Mo-S model" and the Rim-Edge model" are the most accepted with respect to hydrotreating catalysts (Topsoe and Clausen, 1984). It has also been stated that the Co-Mo-S structure is not single phase, but a bulk phase with a fixed overall Co:Mo:S stoichiometry; hence, Co concentration in the structure can vary from almost none with only MoS_2, to full coverage of MoS_2 by Co (Delgado, 2002). Figure 2.9 illustrates the variations in which Co-Mo-S can be present: i) the catalytically active Co-Mo-S phase having MoS_2 like structure decorated by Co, ii) the thermodynamically stable Co_9S_8 structure (Co-sulfide), and iii) Co being dissolved into the Al_2O_3 support. It has been identified that from these varying structures, the Co-Mo-S structure is most associated with appreciable catalytic activity (Lauritsen et al., 2007; Delgado, 2002).

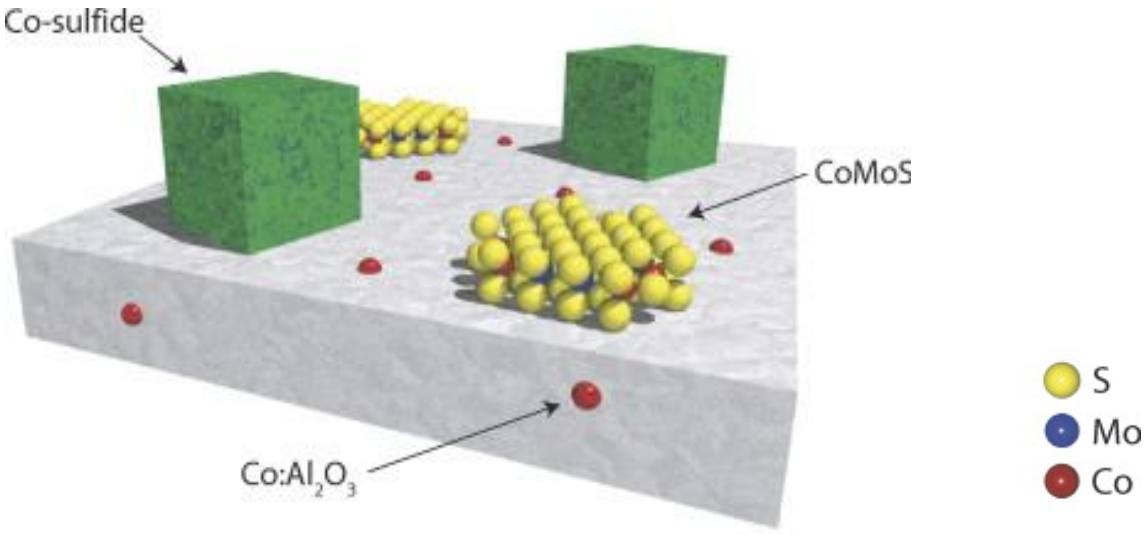

Figure 2.9: Co-Mo-S phase variations present on typical Al_2O_3 support (Adapted from Lauritsen et al., 2007).

Co-Mo-S phase is proposed to be present in either Type I or Type II phase structures on a typical Al_2O_3 support. Type I phase ($CoMoS_2$ I) mainly consists of highly dispersed monolayer MoS_2 particles interacting with the support by means of Mo-O-Al bond, and are supposedly incompletely sulphided; thus, have lower S coordination of Mo and Co (Ni). Type II phase ($CoMoS_2$ II) mainly consist of lower dispersed MoS_2 particles of higher stacking degree and are thought to be fully sulphided; hence, higher S coordination of Mo and Co (Ni) (Topsoe and Clausen, 1984).

In the Rim-Edge model it is assumed that the catalyst particles are stacked as discs, with the top and bottom discs described to be the "rim sites" and the discs in between are described as the "edge sites" (Daage and Chianelli, 1994). Figure 2.10 illustrates the concept of the Rim-Edge model, with the distinction between the rim and edge sites for stacked and unstacked MoS_2 particles.

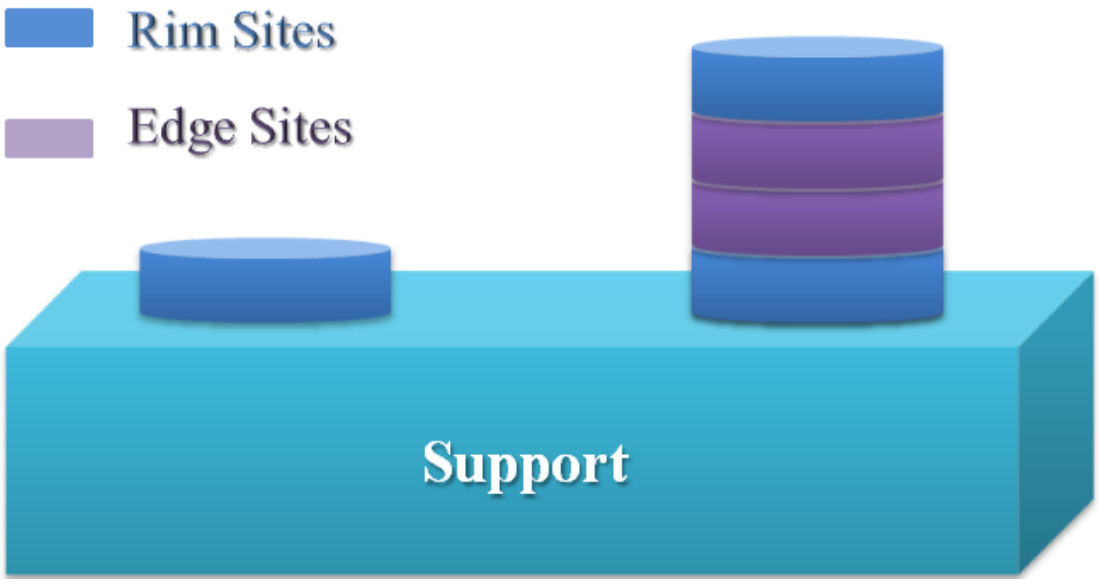

Figure 2.10: Rim-Edge model with stacked and unstacked MoS_2 particles (Adapted from Berhault et al., 2008).

The Rim-Edge model states that sulphur hydrogenolysis (C-S bond breaking) occurs at both the rim and edge sites; whereas dibenzothiophene (DBT) hydrogenation takes place on the rim site only (Daage and Chianelli, 1994).

2.5.3 Inhibition and Deactivation of Catalysts

The loss of catalytic activity and/or selectivity with time on stream leads to the gradual loss of the catalyst's ability to produce the desired product; this gradual loss is typically overcome by increasing the reactor temperature or reducing the feed rate (Gruia et al., 2006). Some of this loss in activity is related to the inhibiting effects of nitrogen containing compounds. Basic nitrogen compounds have been extensively studied and characterized as strong HDS inhibitors, with considerable amount of work being devoted to establishing their effect on the thiophene and dibenzothiophene reaction networks (Laredo et al., 2001). In comparison, little information has been published on the inhibiting effects of non-basic nitrogen compounds, usually considered less poisoning and inhibiting than the basic species (Furimsky et al., 1999). However, strong inhibiting effects have been reported for several known non-basic nitrogen compounds typically present in gas oil. According to Furimsky et al. (1999), a simple non-basic molecule such as indole as been found to have a long-time adsorption effect on the HDS by means of hydrogenation (HYD). Table 2.4 indicates the HDS and HYD conversion rates.

Table 2.4: HDS and HYD conversion with respect to the presence of indole (Furimsky et al., 1999).

	% Conversion	
	HDS	**HYD**
Before Indole	87	69
After Indole	64	21
After 2 days with DBT	80	39

Based on the results shown in Table 2.4, it can be seen that even after two days past the removal of indole, the HDS of dibenzothiophene did not entirely recover, and the HYD of naphthalene was still appreciably lower than before the addition of indole. This may be explained on the basis of relative reaction rates to desorption rates. A strongly adsorbed compound, having a slow rate of desorption compared to a given reaction, will experience only very slow recovery (Furimsky et al., 1999). Another critical point stated is that the basic strength is not necessarily the same as the adsorption strength on catalyst sites. Observing Table 2.5 it can be seen that according to pK_a values, piperidine is much more basic than pyridine, yet their overall adsorption on the CoMo catalyst is the same, implying that the degree of protonation of the adsorbed base is not directly related to its adsorption on the catalyst (Furimsky et al., 1999).

Table 2.5: Nitrogen compounds and their pK[a] and adsorption values (Furimsky et al., 1999).

Name	Structure	pK^a	Adsorbtion[c] (μmol/g)
Piperidine (PIP)	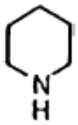	11.1	0.15
Pyridine (PY)		5.3	0.16
2,6-Lutidine (26L)	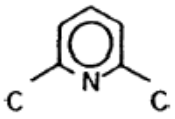	7[b]	0.045
3,5-Lutidine (35L)	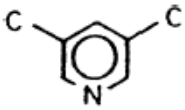	6.2	0.215
Aniline (AN)	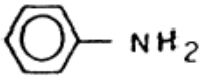	4.6	0.13
N,*N*-dimethylaniline (NAN)	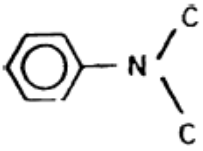	5.2	0.085
Quinoline (Q)	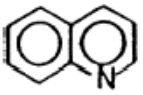	4.9	0.25
Quinaldine (MQ)	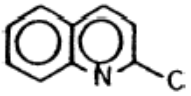	5.8	0.08

[a] Handbook of Chemistry and Physics, 60th ed., p. D-161.
[b] Estimated from data of susbstituted puridines.
[c] Amount adsorbed on catalyst at 0.25 kPa pressure of N-compound at 623 K, in presence of 1.06 kPa thiophene, 1.73 kPa H_2S and 83.3 kPa H_2.

A few studies have reported strong inhibiting effect of non-basic nitrogen, carbazole, on the thiophene and dibenzothiophene HDS reactions; comparable to those of the basic nitrogen compounds pyridine, piperidine and acridine (Vopa et al., 1988; Nagai et al., 1983). A study conducted by Laredo et al. (2001) considered the inhibiting effect of indole and carbazole (non-basic) and that of a mixture of quinoline (basic) and indole and carbazole, in order to simulate the effects of compounds found in real feedstock for diesel production. The dibenzothiophene HDS reactions were carried out at 320°C and 5.3 MPa in the presence of different concentrations of quinoline, indole or carbazole. The results of the experiments were fitted to a pseudo-first-order rate equation, as shown below.

$$r_{HDS} = k'_{DBT} \, C_{DBT} \qquad \text{(Eqn. 2.2)}$$

where k'_{DBT} is the pseudo-first order rate constant for dibenzothiophene HDS reaction inhibited by nitrogen compounds (Laredo et al., 2001). An inhibition factor (Θ) was also calculated in order to determine the degree of inhibition for each experiment, as shown below.

$$\Theta = \frac{k_{DBT} - k'_{DBT}}{k_{DBT}} \qquad \text{(Eqn. 2.3)}$$

Table 2.6 illustrates the inhibiting effects of the nitrogen compounds on dibenzothiophene HDS. It can be seen that there is a strong inhibiting effect caused by nitrogen compounds even at concentrations as low as 5 ppm; this effect increases with increasing nitrogen concentration, and tailing off at higher concentrations. The inhibiting strength based on the obtained results is as follows: Carbazole < Quinoline < Indole (Laredo et al., 2001).

Table 2.6: Inhibiting effects of nitrogen compounds on Dibenzothiophene HDS (Laredo et al., 2001).

Quinoline				Indole				Carbazole			
Initial concentration		$k'_{DBT} \times 10^{-2}$ (min^{-1})	R^2	Initial concentration		$k'_{DBT} \times 10^{-2}$ (min^{-1})	R^2	Initial concentration		$k'_{DBT} \times 10^{-2}$ (min^{-1})	R^2
mmol/l	ppm[b]			mmol/l	ppm[b]			mmol/l	ppm[b]		
0.276	5	0.96	0.9954	0.270	5	0.89	0.9970	0.270	5	1.19	0.9894
1.37	25	0.87	0.9974	1.31	24	0.77	0.9836	1.37	25	1.05	0.9861
2.76	51	0.84	0.9934	2.61	48	0.59	0.9923	2.72	50	0.94	0.9910
5.48	101	0.76	0.9849	5.24	97	0.39	0.9913	5.47	101	0.75	0.9879
				10.48	194	0.34	0.9901				

[a] DBT initial concentration — 0.0232 mol/l; 980 ppm as sulfur.
[b] As nitrogen.

The experimental results are represented quite strongly by the pseudo-first order rate equation, implying that the inhibition effect is approximately constant during each of the tests. It is also proposed that the inhibiting strength does not seem to be affected by the conversion of the parent nitrogen compounds, the formation or the disappearance of basic compounds or the degree of organic nitrogen removal; entailing that the coverage of active sites by nitrogen compounds is established in the early stages of the reaction and remains nearly constant throughout the experiment, probably due to the slow kinetics of desorption of these compounds (Laredo et al., 2001).

A second study was undertaken by Laredo et al. (2003) in order to determine whether the inhibiting behaviour observed from non-basic nitrogen compounds was due to the strong adsorption of the parent compound onto the catalyst active sites or the result of hydrogenation products that resulted during the hydrotreatment process. Indole and its hydrogenation products indoline and o-ethylaniline were used as the nitrogen compounds during hydrodesulphurization of dibenzothiophene. Similar experiments as those shown in the earlier study were conducted, with the results given in Table 2.7. It can be seen based on these results that as the nitrogen concentration was increased the inhibiting effect increased as well, tailing off at higher concentrations. The inhibiting strength based on the obtained experimental results was as follows: Indole < Indoline < o-ethylaniline. The higher inhibiting effect of indoline and o-ethylaniline suggests that the indole inhibiting effect could not be attributed only to hydrogenation reactions converting it into basic compounds, as has been suggested by a few studies, because if that was the case, all three of the nitrogen compounds should have shown the same strength at the same nitrogen concentrations. Therefore, the inhibition behaviour seems related to the strong adsorption of the specific nitrogen compound directly on the catalyst surface

(Laredo et al., 2003). Based on the kinetic studies, Table 2.8 illustrates the apparent adsorption constants for the nitrogen compounds. It can be seen that the highest adsorption constant K_N was obtained for o-ethylaniline (1.88 l/mmol), which proved to be a stronger inhibitor than indole and indoline. Furthermore, according to the results illustrated in this work, the inhibiting effect does not seem to be attributable to the basic strength of the nitrogen compounds because neither the pK_a nor the gas-phase basicity values follow the same trend as the adsorption constants (Laredo et al., 2003).

Table 2.7: Inhibiting effects of nitrogen compounds on Dibenzothiophene HDS (Laredo et al., 2003).

Indole				Indoline				*o*-Ethylaniline			
Initial concentration		$k'_{DBT} \times 10^{-2}$	R^2	Initial concentration		$k'_{DBT} \times 10^{-2}$	R^2	Initial concentration		$k'_{DBT} \times 10^{-2}$	R^2
(mmol/l)	(ppm)[b]	(min^{-1})		(mmol/l)	(ppm)[b]	(min^{-1})		(mmol/l)	(ppm)[b]	(min^{-1})	
1.57	28	0.55	0.96	1.57	28	0.50	0.98	1.57	28	0.45	0.98
3.16	57	0.45	0.95	3.05	56	0.41	0.98	3.11	55	0.35	0.99
6.20	112	0.38	0.98	6.10	110	0.31	0.95	5.99	109	0.28	0.97
12.41	224	0.33	0.98	12.20	221	0.27	0.95	12.43	217	0.23	0.98
17.81	323	0.28	0.98	17.57	318	0.22	0.99	17.87	313	0.19	0.95

[a] DBT initial concentration 0.0163 mol/l, 675 ppm as sulfur.
[b] As nitrogen.

Table 2.8: Apparent adsorption constants for the nitrogen compounds (Laredo et al., 2003).

Nitrogen compound	pK_a	Gas-phase basicity (kcal/mol)	n	Apparent adsorption constant		R^2
				K_N^n $(l/mmol)^n$	K_N (l/mmol)	
Indole	−3.6	215.6	0.5	0.86	0.74	0.9707
Indoline	5.0	221.4	0.5	1.14	1.30	0.9887
o-Ethylaniline	4.3	205.8[a]	0.5	1.37	1.88	0.9914

[a] Estimated from available data

There are several reasons that can lead to catalyst deactivation, including i) poisoning of the catalyst due to the presence of impurities such as sulphur and nitrogen in the feedstock, ii) sintering of the catalyst, and iii) changes in the catalytic activity due to intermediate formations (i.e. carbonations) which are a constituent part of the mechanism (Boahene, 2011).

The long-term deactivation effects on HDS catalysts can be classified into three different regimes as follows, i) initial rapid fouling due to coke formation ii) subsequent gradual fouling due to metal deposition, and iii) final catastrophic fouling due to pore mouth plugging (Boahene, 2011). Accordingly, four main factors are responsible for the long-term deactivation of the catalyst and can be classified as follows (Furimsky and Massoth, 1999):

1. Active site poisoning by a strongly adsorbing species (i.e. nitrogen).
2. Active site coverage by deposition (i.e. coke, nickel, vanadium).
3. Pore mouth constriction and/or blockage from coking.
4. Sintering of the active phase.

Poisoning of the catalyst is predominantly due to nitrogen based compounds strongly adsorbing onto the unsaturated active sites, with additional organic compounds such oxygen and sulphur having a less significant impact towards catalyst active site poisoning (Sigurdson et al., 2009). The poisoning can be reversible or irreversible depending on the characteristics of the feedstock and the operating conditions. In the case of irreversible poisoning, polymer formation occurs around the adsorbed nitrogen heteroatom causing the active site to become permanently deactivated. It is also known that the Athabasca derived bitumen gas oils have considerably high organonitrogen

concentrations which lead to poisoning during not only HDN reaction, but HDS reactions as well (Boahene, 2011).

2.5.4 Inhibition & Deactivation Based on Narrow-Boiling Fractions of Gas Oil

Considerable research efforts have been devoted towards studying the kinetics of overall gas oil feedstocks; however, gas oils with similar physical properties can exhibit unique kinetic behaviour, due to differences in chemical structures and heteroatom functionality (Trytten et al., 1990). It has also been well established that there is competitive adsorption for the catalyst active sites, in which, nitrogen containing compounds tend to competitively adsorb onto the active sites. Sundaram et al. (1988) stated that in a batch reactor containing naphthalene and quinoline or dibenzothiophene and quinoline, the hydrodenitrogenation rate of quinoline was nearly unchanged; however, the hydrogenation rate of the aromatic compounds and the hydrogenoloysis rate of the sulphur compounds became significantly inhibited; confirming the fact that these compounds indeed compete for the same catalyst active sites. Kanda et al. (2004) performed a detailed study to determine whether the trends in hydrodenitrogenation activity for different narrow-boiling fractions were simply the result of increasing molecular weight or due to the nitrogen species contained in the feedstock. The study was performed using three fractions (light fraction #2, boiling point (b.p.) 343-393 °C; middle fraction #4 b.p. 433-483 °C; and heavy fraction #8, b.p. 524 °C +) of the Athabasca coker gas oil. Table 2.9 and 2.10 illustrate the narrow fraction boiling range and elemental analysis, and the physical properties of the three fractions.

Table 2.9: Narrow fraction boiling range and elemental analysis of fractions #2, #4, and #8 (Kanda et al., 2004).

	boiling range (°C)	wt % of feed	mol wt.	S content (ppm)	N content (ppm)	C content (wt %)	H content (wt %)
feed				40700	3900		
Fraction 2	343/393	19.1	266	38600	2400	85.4	10.7
N-extract				24300	16300		
Fraction 4	433/483	21.2	362	41300	4200	85.1	10.5
N-extract				13800	10400	79.9	8.8
Fraction 8	>524	9.1	590	46100	6800	85.2	9.3
N-extract				38300	16200	79.3	8.7

Table 2.10: Physical properties of fractions #2, #4, and #8 (Kanda et al., 2004).

	asphaltenes (%, in pentane)	MCR (%)	ext mat (% Res)	total acid number	aromatic carbon content (%, from ^{13}NMR)
feed	1.55	1.98	0.003		38.12
Fraction 2	0.10	0.07		2.1	34.25
Fraction 4	0.20	1.18		2.5	35.89
Fraction 8	12.67	19.12	0.80	1.9	43.05

Based on nitrogen speciation analysis, which was performed using mass spectroscopy with N_2O chemical ionization and direct injection electrospray ionization, it was determined that fraction #2 (b.p. 343-393 °C) was dominated by alkyl-carbazoles and tetrahydrobenzocarbazoles; fraction #4 (b.p. 433-483 °C) was dominated by alkyl-naphthenopyridines; and fraction #8 (b.p. 524 °C +) had an even distribution of nitrogen compounds (Kanda et al., 2004). A clean feed, which comprised of hydrotreated gas oil, blended with 1 wt% quinoline to give a corresponding total nitrogen concentration of 1080 ppm, was used as the baseline reactant feed. Figure 2.11 illustrates the conversion of quinoline at 350 °C based on the reactor feed which was blended to contain a total nitrogen concentration of approximately 3000 ppm, with 1080 ppm nitrogen due to quinoline and 1900 ppm nitrogen due to the nitrogen species present in the different narrow-boiling fractions (Kanda et al., 2004).

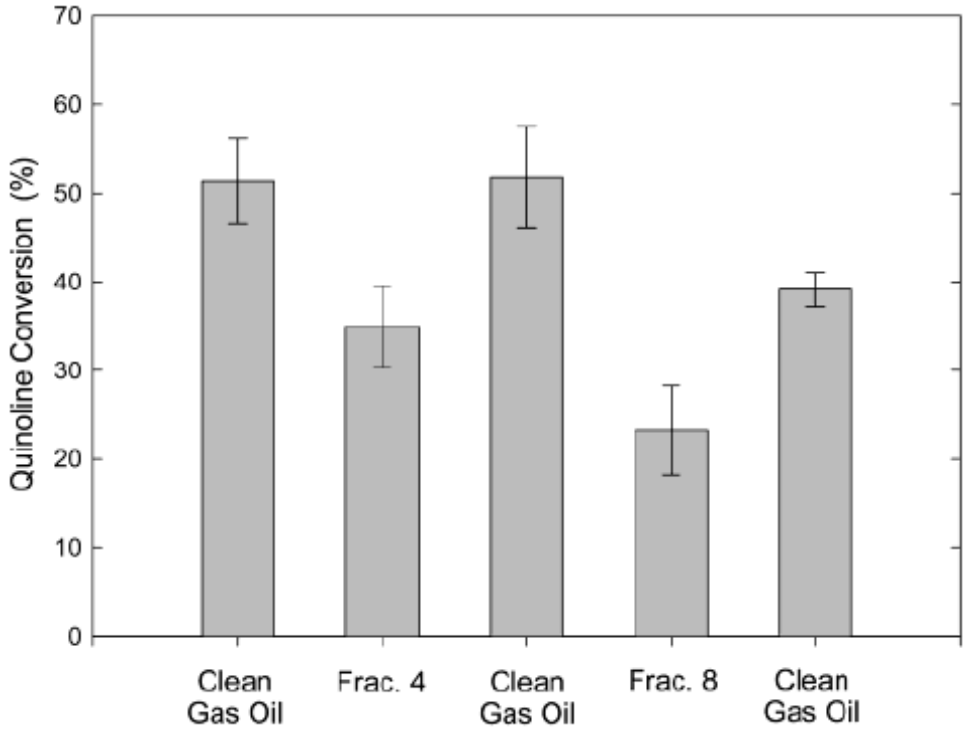

Figure 2.11: Conversion of quinoline at 350 °C and 3000 ppm total nitrogen (Kanda et al., 2004).

Based on these results, it can be seen that quinoline conversion in the clean feed was 51.3%; however, when fraction 4 was introduced, the conversion went down to 34.9%, and subsequently returned to the original conversion rate of 51.3% when the clean feed was re-introduced. This behaviour suggests that although there is an observable inhibitory effect caused by fraction 4 on quinoline conversion, this effect is reversible and no permanent catalyst deactivation is noticeable. When fraction 8 was introduced, the quinoline conversion decreased to 23.3%, suggesting higher levels of inhibition caused by this fraction. Once again, the clean feed was re-introduced into the system; however this time the conversion only increased to 39.1%; suggesting that fraction 8 caused inhibition, as well as, slight deactivation of the catalyst.

Further experiments were conducted to determine the effects of temperature on inhibition and deactivation caused by different narrow-boiling fractions. At a higher temperature of 380 °C, quinoline increased very slightly to 52.2%; however, when fraction 4 was introduced, similar inhibitory pattern as before was noticeable, as the conversion decreased to 35%. Upon re-introducing the clean feed, the conversion once again jumped back to 51.3%. When fraction 8 was introduced, the conversion decreased to 29.2%, which was only 5.8% lower than the conversion observed for fraction 4. Once again, when the clean feed was re-introduced, the quinoline conversion jumped to 47.3%, which was very similar to the original level of quinoline conversion. This behaviour suggests that the higher temperatures are able to regenerate the catalyst and eliminate a certain amount of catalyst deactivation caused by the compounds in fraction 8. The most interesting behaviour however, is that noticeable for fraction 2, which consists of the low-boiling compounds, meaning smaller molecular weight compounds than fraction 4 and

fraction 8. It can be seen that when fraction 2 was introduced, the quinoline conversion significantly decreased to 17.5%, which is 32.9% lower in comparison to 17.2 observed for fraction 4 and 22.1% observed for fraction 8. When the clean feed was re-introduced, the quinoline conversion only increased to 28.9%, suggesting a significant amount of deactivation of the catalyst. These results clearly indicate that the catalysts activity and the catalyst active sites are more sensitive to the type of components present in the gas oil rather than temperature and molecular weight, which are only partially responsible for the inhibition of catalyst activity. Fraction 2, being dominated by non-basic nitrogen compound such as carbazole, inhibited the catalyst activity by approximately 11.4% and deactivated the catalyst by approximately 21.5%; further illustrating the fact that although there is noticeable deactivation due to higher molecular weight compounds, the inhibition and deactivation due to certain types of nitrogen containing compounds is more severe then the size of the compounds.

2.6 Functionalized Polymers for Pre-treatment of Gas Oil

2.6.1 Poly(glycidyl methacrylate) as Polymer Support

Linear polymers grafted onto cross-linked polymer resin particles offer numerous potential applications due to the combination of the non-solubility resin and the flexibility of the graft polymer side-chains as the functional group carrier. The flexible side-chains can provide pseudo-homogeneous reaction conditions and better accessibility of the involved functional groups (Senkal, 2007).

The epoxy group present on the synthesized polymers have a unique reaction capability, as they are capable of undergoing ring opening with various compounds possessing hydroxyl, amine, or activated methylene groups. Hence, polymers with epoxy

(oxirane) groups offer numerous functionalization possibilities in mild reaction conditions. Epoxidized polybutadiene and phenol-formaldehyde resins with glycidyl groups are common examples of such polymers, with glycidyl methacrylate being the only commercially available vinyl monomer carrying oxirane group (Senkal, 2007).

Polymers with structural units containing such functional groups capable for further reactions are considered reactive. Heterogeneously cross-linked polymers are characterized by high porosity even in dry state. Reactions of their functional groups occur on a large internal surface, usually independent of the thermodynamic quality of the solvent (Svec, 1975). The polymer poly(glycidyl methacrylate) (PGMA) is a reactive macroporous copolymer that can be prepared by direct polymerization of the reactive monomers glycidyl methacrylate (GMA) and ethylene dimethacrylate (EDMA). Figure 2.12 illustrates the synthesis of PGMA from monomers GMA and EDMA.

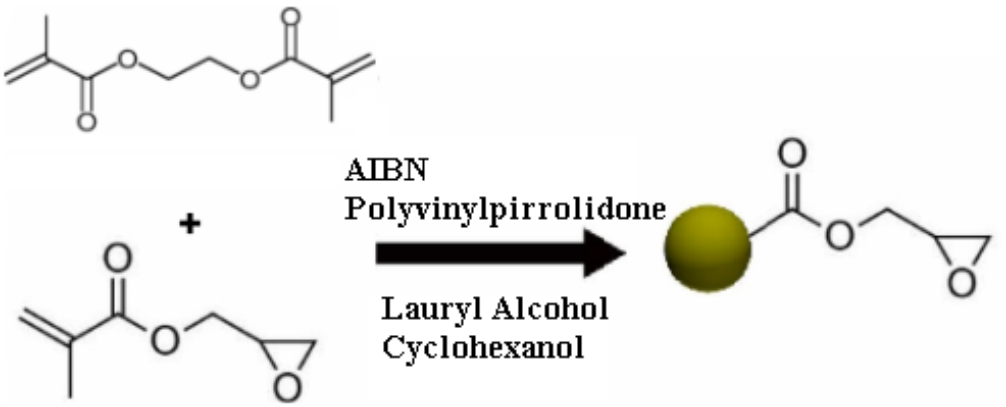

Figure 2.12: Synthesis of polymer poly(glycidyl methacrylate).

The epoxy group present on the polymer allows for substitution to take place with a number of compounds such as minerals, carboxylic acids, amines, diamines, amino acids, etc (Svec, 1975). Their spherical shape and rigidity also allows for the copolymers to be suitable in large scale industrial applications.

2.6.2 Selective Charge Transfer Complex Formation

In order to achieve deep desulphurization, stringent process conditions such as higher temperatures and higher hydrogen flowrates are required; however, these conditions lead to shorter catalyst life and costly processes. The use of electron deficient molecules to form charge transfer complexes (CTCs) with electron rich compounds (π-donors) present in gas oil such as Alkyldibenzothiophene (alkylDBT) and several non-basic nitrogen species is a novel technique for selective removal of these compounds prior to hydrotreatment. Studies performed by Milenkovic et al. (1999) looked into the removal of alkylDBT by forming CTCs with suitable π-acceptor molecules. Gas oil contains a large variety of aromatic compounds, most of which are capable of forming CTCs with the π-acceptor molecules; thus, can compete with the DBT derivatives. The experimental determination of their oxidation potential and the calculation of their HOMO (highest occupied molecular orbital) can allow a rough classification of their complexing abilities. It was also assumed that the higher the level of a molecules HOMO, the lower their oxidation potential, and therefore the stronger their association with the π-acceptor molecules (Milenkovic et al., 1999). Table 2.11 illustrates the HOMO and oxidation potential of several sulphur species.

Table 2.11: Oxidation potential and HOMO values of dibenzothiophene derivates (Milenkovic et al., 1999).

	AROMATIC COMPOUND	E^{ox} (V/SCE)	HOMO (eV)
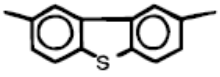	2,8-DMDBT	1.44	-8.44
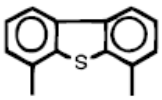	4,6-DMDBT	1.53	-8.51
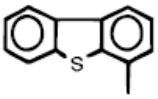	4-MDBT	1.57	-8.55
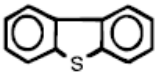	DBT	1.60	-8.60
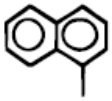	MN	1.63	-8.71
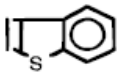	Benzothiophene	1.70	-8.80
	Fluorene	1.79	-8.84

CTCs are easily detected by UV-vis spectroscopy because their formation generally induces the appearance of a new absorption band usually reported as the Benesi-Hildebrand band; using the method of Foster-Hammick-Wardley, this phenomenon allows the calculation of the association constant (and hence the Gibbs' free energy) characterizing the complex (Milenkovic et al., 1999).

Several π-acceptor molecules were selected and tested in order to determine the highest selective removal of 4,6-DMDBT against other non-heteroatom containing aromatics. Figure 2.13 shows a listing of the potential π-acceptor molecules.

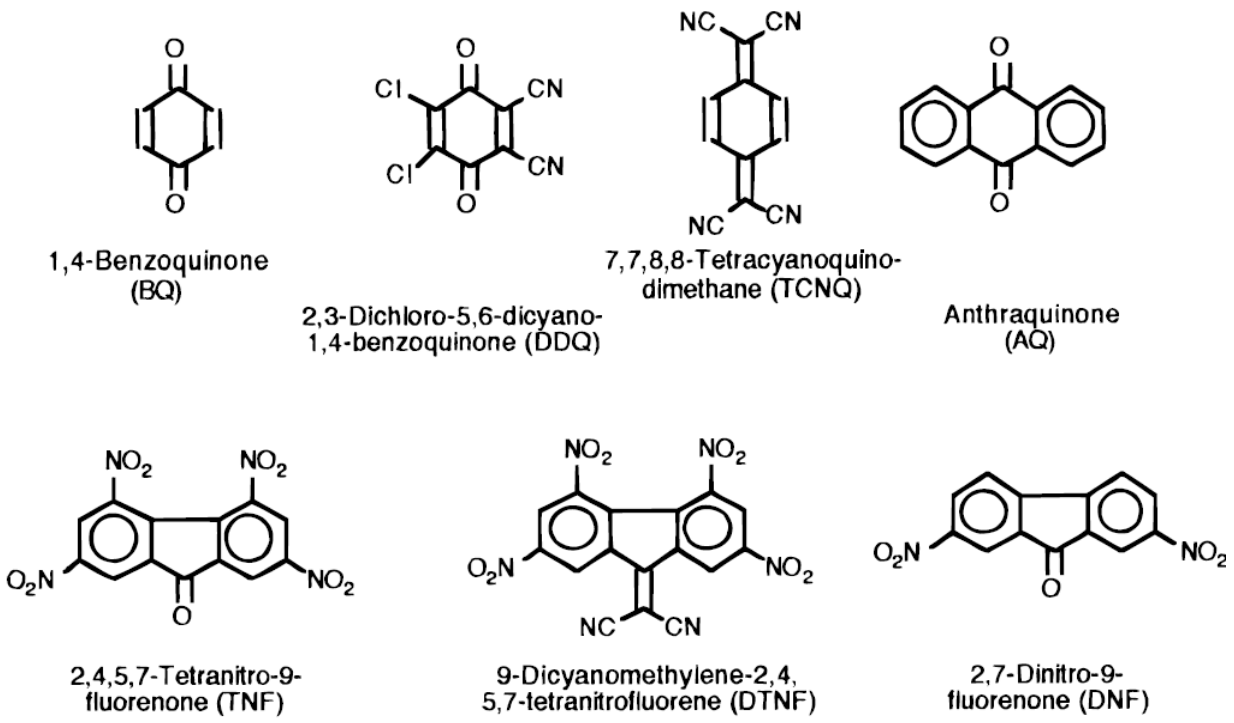

Figure 2.13: Structure of potential π-acceptor molecules for charge transfer complexation (Adapted from Milenkovic et al., 1999).

The obtained experimental results indicated TNF having the highest selective capabilities towards 4,6-DMDBT with a proven complex of 1:1 stoichiometry. This can in turn be correlated to the geometry and the shape of TNF's LUMO orbital (Milenkovic et al., 1999).

2.6.3 Functionalized Polymer for Non-Basic Nitrogen Removal

It is well known that basic nitrogen compounds tend to act as strong inhibitors during the hydrodesulphurization process, with extensive research already dedicated towards the study of the effects of basic nitrogen compounds on real feedstocks and model sulphur compounds, such as 4, 6 - dimethyldibenzothiophene; however, strong inhibitory effects have also been exhibited by non-basic nitrogen compounds such as

carbazoles and indoles. This is due to the hydrogenation reactions occurring during the hydrotreatment process, converting the parent compounds to their basic derivatives, as well as, the strong adsorption of the non-basic parent compounds themselves onto the catalyst active sites. The removal of basic nitrogen compounds by non-catalytic processes has been studied using numerous processes, such as ion-exchange resins (Cronauer et al., 1986; Prudich et al., 1986), volatile carboxylic acids (Qi et al., 1998a), metal complexation (Qi et al., 1998b), activated carbon (Almarri et al., 2009), etc. Some of these methods tend to be moderately efficient in the removal of basic nitrogen compounds; however, none of them seem to be selective or efficient enough for the removal of non-basic nitrogen compounds.

Macaud et al. (2004) stated that due to the planarity and electron-rich structure of the non-basic nitrogen compounds, they can form charge transfer complexes with suitable π-acceptor molecules. However, diesel fuel contains a large variety of aromatic compounds, with and without heteroatoms, capable of forming CTCs which could in turn compete with indole and carbazole. Accordingly, theoretical calculations and experimental studies on synthetic and real feeds have shown that selectivity of CTCs can be correlated to the spatial overlap of the frontier molecular orbitals of the lowest unoccupied molecular orbitals (LUMO) of the π-acceptor molecules and the highest occupied molecular orbitals (HOMO) of the donor molecules (Macaud et al., 2004).

It is also stated that the HOMO values of dibenzothiophene and carbazole are closed; as well as, the sulphur compound derivatives tend to be 20 times more concentrated than nitrogen compounds in feedstocks; thus, the carbazole / dibenzothiophene selectivity can be very low. However, the hydrophobic character of a

compound can be a key attribute in determining its interaction with a solid. The log P measurement provides a thermodynamic measure of its hydrophilicity. Hence, the log P value of dibenzothiophene is determined to be 4.59 and carbazole to be 3.77. Furthermore, the log P values for anthracene, phenanthrene, and pyrene are 4.63, 4.53, and 4.88. It is then expected that, using synergistic interactions between π-acceptor molecules and hydrophilic polymer, as shown in Figure 2.14, there is enhanced selectivity of charge transfer complex formation toward nitrogen-containing compounds (Macaud et al., 2004).

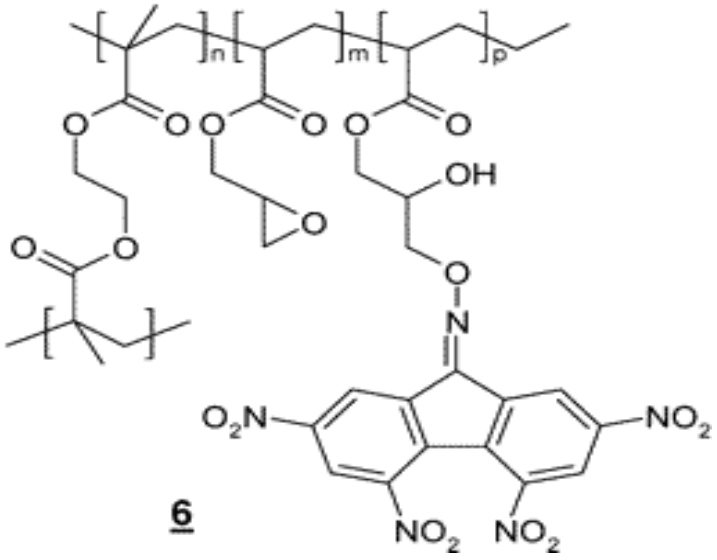

Figure 2.14: Structure of hydrophilic polymer (6) with π-acceptor molecule (TENF) attachment (Macaud et al., 2004).

The feasibility of the polymer was initially examined using model fuel containing equimolar quantities of each of the five nitrogen compounds (indole, carbazole, quinoline, acridine, and aniline) and 4,6-dimethyldibenzothiophene (4,6-DMDBT). Figure 2.15 illustrates the distribution coefficient of nitrogen and sulphur compounds from 30 grams of model fuel by 1 gram of the polymer. It can be seen that polymer 6 tends to be quite selective towards the non-basic nitrogen compounds such as indole and

carbazole, with a very low selectivity towards basic nitrogen compounds, and almost no selectivity towards the sulphur compounds (Macaud et al., 2004). This shows that the structure of the polymer functionalized by the π-acceptor molecule, creating a synergistic hydrophilic balance, is of significant importance for selective formation of charge transfer complexes with non-basic nitrogen molecules, which act as electron rich donors.

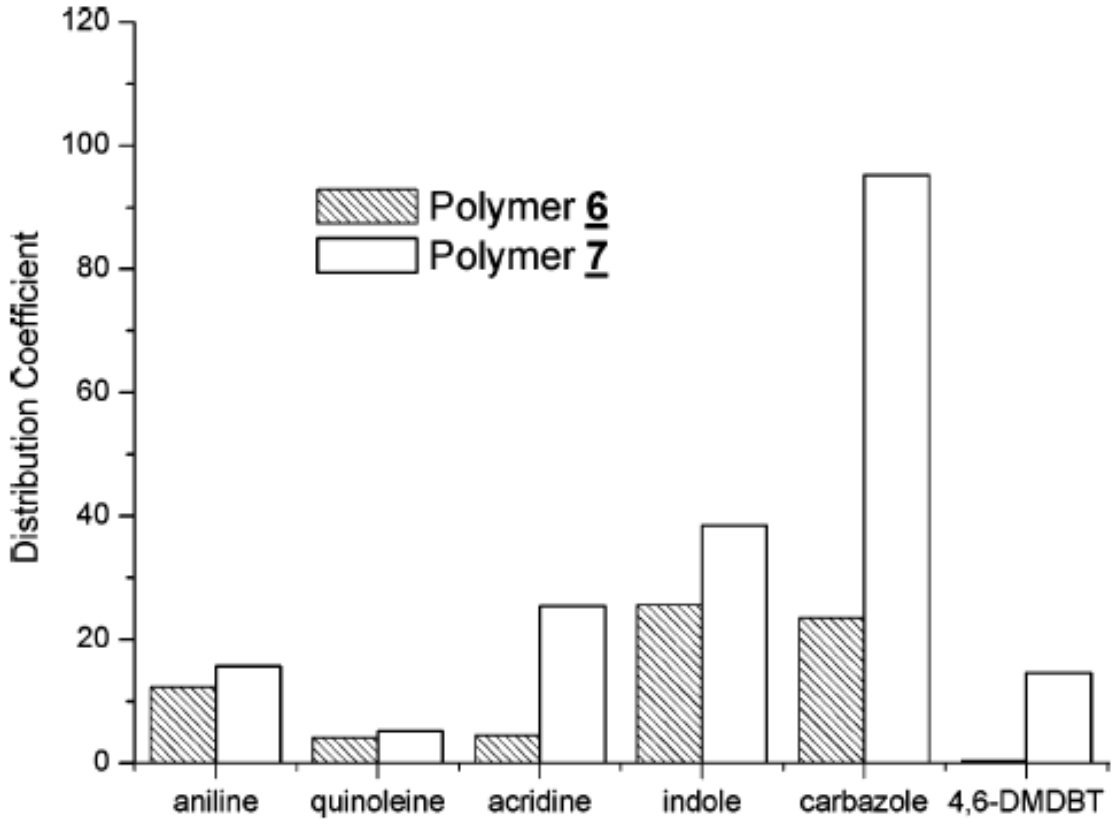

Figure 2.15: Distribution coefficient of nitrogen and sulphur compounds by 1 g of polymers (Macaud et al., 2004).

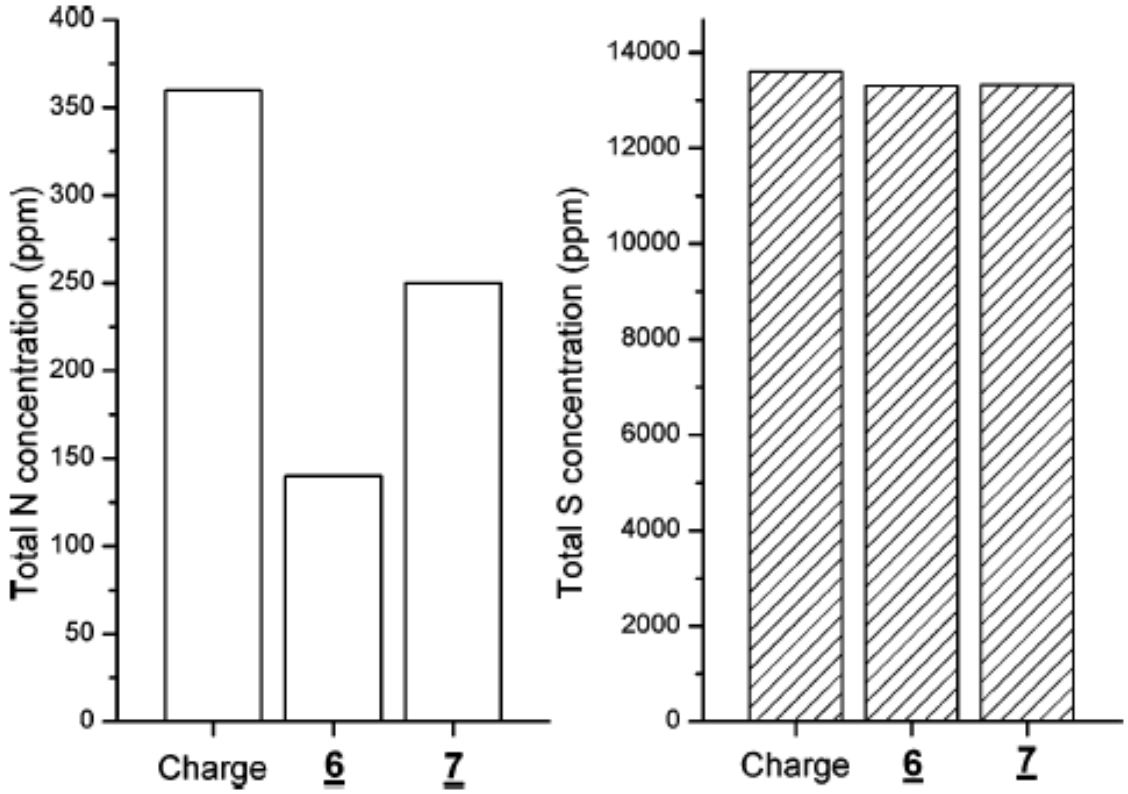

Figure 2.16: Total concentration of nitrogen and sulphur before & after contact with polymers (Macaud et al., 2004).

Figure 2.16 illustrates the experimental results obtained for both sulphur and nitrogen removal using Iranian straight run. It can be seen that approximately 60 wt% of nitrogen removal was accomplished in a single contact with polymer 6, where the resin to feed ratio was 8.2 by weight. Examining the sulphur levels, it is observed that these levels reduced by less than 3 wt% (Macaud et al., 2004); thus, proving that for both model and real feedstock, the immobilization of π-acceptor molecules on polar polymers can greatly enhance the selectivity of non-basic nitrogen molecules adsorption. These results indicate that a polar polymer with suitable π-acceptor molecules is a feasible technique for selective removal of non-basic nitrogen compounds from real feedstock.

2.7 Kinetic Study and Model Development

Kinetic studies offer an insight with respect to information regarding process parameters, operating conditions, and performance of catalysts through kinetic model development. The following section describes the external and internal mass transfer limitations as these two resistances play a major role in the transfer rate of reactants to heterogeneous catalysts; and thus the study of intrinsic rates of reaction. As well as, the development of the power law model.

2.7.1 External and Internal Mass Transfer Limitations

External and internal mass transfer is dependent on the rate of diffusion in each phase when observing the reaction rate of heterogeneous catalytic reactions. Figure 2.17 illustrates an overview of the mass transfer in each phase and the reaction steps.

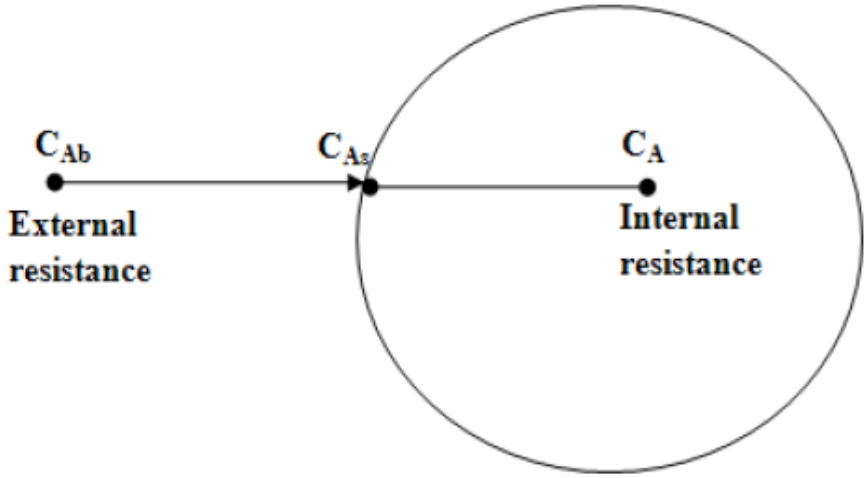

Figure 2.17: External and internal mass transfer and reaction steps.

As shown in Figure 2.17, external diffusion is represented by the difference in concentration from C_{Ab} to C_{As}, and occurs as the reactants diffuse from the bulk phase of the fluid to the surface of the catalyst pellet. Internal diffusion is represented by the

difference in concentration from C_{As} to C_A, and occurs when the reactants diffuse from the surface to the internal areas of the catalyst pellet. Both external and internal diffusion play a significant role in influencing the rate of transfer in heterogeneous catalysts.

It is known that the rate of mass transfer of bulk reactants and products in industrial reactors, between the bulk fluid and the catalyst surface is small; hence, the overall rate of reaction is limited. Generally, pilot scale reactors should be operated at high fluid velocities or using smaller catalyst pellets in order to eliminate external mass transfer limitations (Boahene, 2011). The following Mears criterion is proposed for studying the effects of external mass transfer limitations (Fogler, 2006);

$$C_m = \frac{-r'_A \rho_b Rn}{k_c C_{Ab}} < 0.15 \qquad \text{(Eqn. 2.4)}$$

Where, C_m is the ratio of reaction rate to the external diffusion rate, r_a, ρ_b, R, n, k_c, and C_{Ab} are the reaction rate per unit mass of catalyst (kmol/kg-s), bulk density of the catalyst bed (kg/m^3), catalyst particle radius (m), reaction order, mass transfer coefficient (m/s), and bulk concentration (kmol/m^3) respectively, and

$$\rho_b = (1 - \varepsilon)\rho_c \qquad \text{(Eqn. 2.5)}$$

Where ε = catalyst bed porosity, and ρc = catalyst density. If C_m value is less than 0.15, then external diffusion resistance is negligible (Fogler, 2006). Internal mass transfer considers the limitations due to the difference in concentration of a particular reactant between the outer surface area of a catalyst pellet and the inner channels of the pellet, as shown in Figure 2.18.

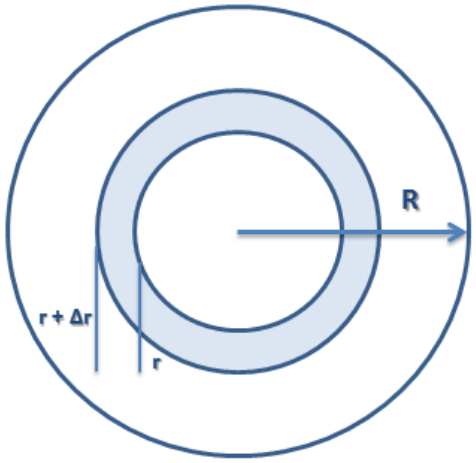

Figure 2.18: Internal mass transfer shell balance.

Internal mass transfer can limit the overall rate of reaction if diffusion through the channels is slow, with low diffusion mass transfer coefficients. The effectiveness factor (η) describes the effect of internal diffusion resistance on the overall rate of reaction; it is the ratio of the actual overall rate of reaction to the rate of reaction that would result if the entire interior surface were to be exposed to the external pellet surface conditions (C_{As}, T_S) (Fogler, 2006). It can be expressed as follows;

$$\eta = \frac{3}{\phi_1^2}\left(\phi_1 \coth \phi_1 - 1\right) \qquad \text{(Eqn. 2.6)}$$

Where ϕ_n refers to the Thiele modulus for the n^{th} order reaction and is given by:

$$\phi_n^2 = \frac{k_n \rho_c S_a C_{As}^{n-1} R^2}{D_e} = \frac{Surface\ \ reaction\ \ rate\ \ of\ \ "A"}{Diffusion\ \ rate\ \ of\ \ "A"} \qquad \text{(Eqn. 2.7)}$$

And k_n = rate constant of n^{th} order reaction (mol/m^3)(m/s); C_{As} = concentration of A at the catalyst surface (mol/m^3); ρ_c = catalyst density (kg/m^3); S_a = catalyst surface area (m^2/kg catalyst); R = radius of catalyst particle (m); and D_e = effective diffusivity (m^2/s) which is defined as;

$$D_e = \frac{D_{AB}\phi_P\sigma}{\xi} \qquad \text{(Eqn. 2.8)}$$

Where D_{AB} = bulk or Knudsen diffusivity of A in B; ϕ_P = pellet porosity (volume of void space / total volume); σ = constriction factor; and ξ = tortuosity (actual distance a molecule travels between two points / shortest distance between those points) (Fogler, 2006).

If the Thiele modulus is large ($\varphi > 3$) and effectiveness factor, η, is less than 0.3, then internal diffusion limits the rate of the reaction. However, if the Thiele modulus is small ($\varphi < 1$) and effectiveness factor is greater than 0.7, then surface reaction is rate limiting. In order to determine whether internal diffusion is significant or not, the Weisz-Prater criterion can be calculated as follows;

$$C_{WP} = \frac{-r_{Aobs}\rho_c R^2}{D_e C_{As}} \qquad \text{(Eqn. 2.9)}$$

$$C_{WP} = \eta\phi_n^2 = \frac{Actual\ \ reaction\ \ rate\ \ of\ \ "A"}{Diffusion\ \ rate\ \ of\ \ "A"} \qquad \text{(Eqn. 2.10)}$$

If $C_{WP} << 1$ then internal diffusion resistance is negligible; however, if $C_{WP} >> 1$ then internal diffusion limits the reaction (Fogler, 2006).

2.7.2 Power Law Model

Power law model is a more simplified approach to generate the basic kinetic information, such as reaction order, reaction rate constant, activation energy, effect of operating condition on conversion (Marroquín et al., 2005). Due to its simplicity, the power law model is very popular to generate basic kinetic information, such as reaction order, reaction rate constant, activation energy, effect of operating condition on conversion (Ferdous et al., 2006a). In comparison to the Langmuir-Hinshelwood or the

multi-parameter model, the power law model contains fewer parameters that need to be calculated. The following power-law model has been proposed for evaluating the removal of sulphur and nitrogen species present in HGO (Ferdous et al., 2006b).

$$-r_A = k_A C_A^n = \frac{dC_A}{dt} \qquad \text{(Eqn. 2.11)}$$

Where, $-r_A$ = rate of HDS or HDN reaction, k_A = apparent rate constant, C_A = sulphur or nitrogen content, n = reaction order, and t = residence time. Integrating and solving equation 2.11 analytically yields three solutions depending on the value of n, as shown below:

$$k_A = LHSV\ [C_0 - C_p] \qquad \text{for n = 0} \qquad \text{(Eqn. 2.12a)}$$

$$k_A = LHSV\ \ln\left[\frac{C_0}{C_p}\right] \qquad \text{for n = 1} \qquad \text{(Eqn. 2.12b)}$$

$$k_A = LHSV\ \left[\frac{1}{n-1}\right]\left[\frac{1}{C_p^{n-1}} - \frac{1}{C_0^{n-1}}\right] \qquad \text{for } n \neq 0, 1 \qquad \text{(Eqn. 2.12c)}$$

Where, k_A = apparent rate constant; LHSV= liquid hourly space velocity; C_0 = nitrogen and sulphur in heavy gas oil, C_P = nitrogen and sulphur in hydrotreated product, and n = reaction order. The apparent rate constant is used in the above kinetic expressions since it takes into account the effect of diffusion due to mass transfer limitations. The derived power law equations allow for the determination of the reaction order (n) and the apparent rate constant (k). The activation energy (E_a) which is the minimum amount of

energy that must be overcome for a chemical reaction to proceed can be expressed using the Arrhenius equations as follows;

$$k_A = k_0 e^{(-E/RT)} \quad \text{(Eqn. 2.13)}$$

Where k_0 = Arrhenius constant; E = activation energy (kJ/mol); R= gas constant (kJ/mol); and T = temperature (K). It is known that the values of the reaction order and activation energy are highly dependent on the type of feedstock, catalyst, operating conditions, and experimental set-up (Biswas, 2011). The reaction order for HDN reactions using the power law model have been reported in the range of 1.0 – 2.0 (Bej et al., 2001a); whereas the reaction order for HDS reactions have been reported in the range of 1.0 – 2.5 (Ferdous et al., 2006b). Table 2.12 provides a summary of kinetic studies performed on real feedstock from several sources of open literature; it should be noted however that all of the heavy gas oil feedstocks refer to those derived from Athabasca Bitumen and utilize a NiMo catalyst support.

Table 2.12: Kinetic parameters derived using power law model for numerous HDN and HDS studies (Biswas, 2011).

References	Feed	Catalyst	Boiling Range,°C	Order of Reaction		Activation Energy kJ/mol	
				HDS	HDN	HDS	HDN
(Ferdous et al., 2006b)	Heavy Gas Oil	NiMo/γ-Al_2O_3	185-576	1.5	1	87	74
(Bej et al., 2001b)	Heavy Gas Oil	NiMo/γ-Al_2O_3	210-655	2	1.5	28	80
(Yui and Dodge, 2006)	Heavy Gas Oil	NiMo/γ-Al_2O_3	242-566	1.5	1	94	79
(Diaz-Real et al., 1993)	Heavy Gas Oil	NiMo/ zeolite-alumina-silica	345-524	PS 1st	PS 1st	176	208
(Yui and Sanford, 1989)	Heavy Gas Oil	NiMo/γ-Al_2O_3	196-515	1.5	1	138	92
(Mann et al., 1988)	Heavy Gas Oil	NiMo/zeolite-alumina-silica	345-524	1.5	2	87	105
(Botchwey et al., 2004)	Heavy Gas Oil	NiMo/γ-Al_2O_3	210-600	PS 1st	PS 1st	122	96
(Marin et al., 2002)	LCO+SRGO	NiMo/faujasite modified γ-Al_2O_3	209-369	PS 1.5	PS 1st	77.8	51.4
(Ancheyta et al., 2002a)	Middle distillate blend	NiMo/γ-Al_2O_3	156-344	1.5-2.0	-	58-175	-
(Mapiour et al., 2010a)	HGO	NiMo/γ-Al_2O_3	258-592	2.0	1.5	101	79

Where, PS = Pseudo

CHAPTER 3

EXPERIMENTAL METHODOLOGY

This chapter highlights the experimental procedure carried out for the synthesis of polymer poly(glycidyl methacrylate) incorporated with tetranitrofluorenone. The synthesis has been categorized into four subsections detailing each of the four steps carried out during the procedure. In addition, the chapter also outlines the experimental procedure and reactor set-up during the hydrotreatment process.

3.1 Preparation of Poly(glycidyl methacrylate) Incorporated with Tetranitrofluorenone

The following four steps outline the synthesis procedure followed for developing the polymer support PGMA and attaching the organic compound TENF; thus obtaining the desired polymer.

3.1.1 Step 1: Synthesis of Polymer Support Poly(glycidyl methacrylate)

Synthesis of polymer PGMA-TENF required a four step synthesis procedure, with each step involving a modified experimental setup. Step 1 entailed synthesis of the copolymer PGMA as described by Svec et al. (1975), with slight modifications. A three-neck flask incorporated with a mechanical stirrer, and a valve for expelling air from the system using pure nitrogen was utilized. The reactants were mixed in three different sets, with 57.2 g of glycidyl methacrylate and 24.5 g of ethylene glycol dimethacrylate being mixed with 0.8 g of the radical initiator azobisisobutyronitrile. Separately, the inert phase was prepared consisting of 98.6 g of cyclohexanol and 9.8 g of dodecanol; and finally, a solution consisting of 6.0 g of polyvinylpyrrolidone in 600 ml of distilled water was

prepared. The three solutions were then stirred in the 3-neck flask, and air was expelled from the system to give a nitrogen rich environment. The reaction was performed at 70°C for the first 2 hours, and then at 80°C for another 6 hours. Once the reaction was completed, the system was allowed to cool for 2 hours, while it was still stirred; the synthesized copolymer was then washed multiple times with distilled water and then ethanol to remove any soluble components. The PGMA beads were then dried at 90°C for 24 hours.

3.1.2 Step 2: Substitution of Epoxy Ring with Acetone Oxime

Second step of the synthesis procedure involving substitution of the epoxy ring utilized a similar experimental setup without the valve for nitrogen intake. The process as described by Lemaire et al. (2002) was followed with slight modifications. Using a three-neck flask incorporated with a mechanical stirrer, 37.8 g of acetone oxime was dissolved in 329.2 ml of N,N-dimethylformamide; after which 78.7 g of potassium carbonate was added and the system brought to 100°C. Finally, 61.5 g of synthesized PGMA beads were added, and the system stirred at 400 RPM for 24 hours. Upon completion of the reaction, the polymer beads were washed several times with distilled water, then ethanol, and left for drying at 90°C for another 24 hours.

3.1.3 Step 3: Synthesis of Tetranitrofluorenone

Tetranitrofluorenone (TENF) was synthesized following the procedure described by Newman et al. (19) with slight modification. A three neck flask was fitted with an all-glass funnel and condensers on each side; the flask was kept in a temperature controlled oil bath. 110 ml of concentrated (95-98%) H_2SO_4 was initially added to the system, and

then 239 ml of fuming (70%) HNO_3 was slowly added. The system was allowed to reach reflux temperatures and kept at that condition for about 2 hours. Separately a solution consisting of 120 ml of concentrated H_2SO_4 with 10.3 g of dissolved 9-fluorenone was prepared and added drop wise, over a 1 hour period, into the refluxing system. Finally, a third solution consisting of 160 ml of H_2SO_4 and 175 ml of HNO_3 was prepared and added drop wise via the funnel over a period of 8.5 hours. After this time period, the heating was turned off, and the system was simply allowed to stand for 10 hours. The prepared solution was then poured very slowly into 2700 ml of distilled water. It is important to note that this step should be carried out with caution and in a fume hood, as the fumes are very hazardous. The formed yellow precipitate is then decanted, filtered and washed several times with water and allowed to dry in the oven at 80°C for another 10 hours.

3.1.4 Step 4: Coupling of Tetranitrofluorenone On Poly(glycidyl methacrylate)

Final step of the synthesis involved coupling of the organic compound with the oxime functionality of the modified PGMA beads. The process outlined by Lemaire et al. (2002). for the coupling of these compounds was used with slight modifications. Using the optimized parameters, 15.9 g of TENF was dissolved in 270 ml of acetic acid at temperatures of about 100°C. Then 14.7 g of p-toluene sulfonic acid monohydrate was added to the system and dissolved as well. The solution was then transferred to a three-neck flask equipped with two condensers, and 58.7 g of modified PGMA beads were added to the system, which was then allowed to gently reflux for 3 days. Once the reaction was completed, the modified beads were filtered and washed several times with toluene, and allowed to dry at 90°C for 24 hours.

3.2 Polymer Characterization Techniques

Several characterization techniques as described below were employed to ascertain the structure, morphology, and presence of certain chemical groups for both the intermediate and finalized polymer.

3.2.1 Nitrogen Adsorption/Desorption (BET)

Surface area, pore volume, and pore size measurements of the intermediate and final polymer were determined using nitrogen physisorption isotherms through Micromeritics ASAP 2000 analyzer at liquid nitrogen (N_2 at 99.995% purity) temperature of 77 K. The analysis is based on the theory established by Brunauer, Emmett, and Teller (BET) for predicting the surface characteristics of a substance using size of the adsorption monolayer of an adsorbate (Gregg et al., 1967). The analyses were performed using approximately 0.20 g of the sample, which was then degassed at 200°C for 2 hours in a vacuum of 550 Torr in order to remove any moisture. The specific surface area (m^2/g) was obtained using the N_2 adsorption and desorption isotherms, while the pore volume (cm^3/g) and average pore size (nm) were obtained using the BJH algorithm (developed by Barrett–Joyner–Halenda, using the Kelvin equation for calculation of pore volume and pore sizes) for adsorption and desorption of nitrogen.

3.2.2 Scanning Electron Microscopy (SEM)

Scanning electron microscopy uses focused beam of high energy electrons in order to generate a variety of signals at the surface of the solid specimen, which are then collected and can reveal information about the specimen such as external morphology and crystalline structure. The JEOL 840A scanning electron microscope at the electron

microscopy laboratory in the department of geological sciences, at the University of Saskatchewan was employed for imaging the various polymer samples. The samples were examined by mounting them onto aluminum slabs using carbon paint, then applying a gold coating through vacuum sputtering to improve secondary electron signals and reducing charging. SEM was utilized in order to examine the shapes of the synthesized polymer beads.

3.2.3 Fourier Transform Infrared Spectroscopy (FTIR)

Fourier transform infrared spectroscopy (FTIR) is a technique which emits infrared radiation through a sample, allowing some of the radiation to get absorbed and some to transmit through. The spectrum which is then generated from the transmitted radiation represents the molecular absorption and transmission, creating a unique fingerprint of the molecular structure. JASCO FTIR 4100 spectrometer was employed for analyzing the polymer samples. The samples were generated by mixing the polymer with KBr and developing pellets that were analyzed at room temperature. The generated spectra were in the range of 400 – 2000 cm^{-1} with a resolution of 4 cm^{-1} and average scans of 32.

3.2.4 Thermo Gravimetric/Differential Thermal Analysis (TG/DTA)

Thermogravimetric analysis is a technique used for determining changes in weight with respect to changes in temperature. Simultaneous TG/DTA measures both heat flow and weight changes in a material as a function of temperature or time. The analyses were performed using 5 mg of the polymer samples in a PerkinElmer Diamond TG/DTA instrument, where data was collected at 20 second intervals at a heating rate of 5°C/min under an argon atmosphere.

3.2.5 Nitrogen Elemental Analysis (CHNOS)

The amount of nitrogen content present on the polymer after step 2 synthesis as the acetone oxime was substituted in place of the epoxy ring was measured using Vario EL III CHNOS elemental analyzer.

3.2.6 Hydrochlorination for Determining α-epoxide Content

The most specific and practical methods for the determination of the α-epoxide content of uncured resins are based on the addition of hydrogen chloride to the epoxy group, producing a chlorohydrin (Kline, 1959), as shown below;

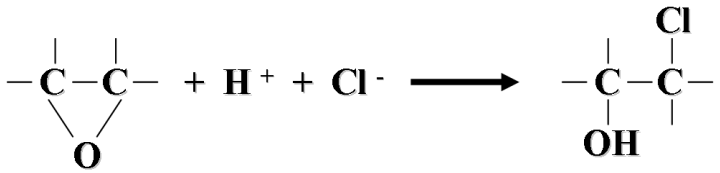

(Eqn. 3.1)

The difference between the amount of acid added and the amount unconsumed, as determined by titration with standard base, is a measure of the epoxide content.

The titration was performed following the method described by Kline (1959), with the initial preparation of three solutions; the sodium hydroxide solution, which was a standard in a 0.1 N methanol, the HCl-dioxane reagent, and the neutral ethyl-alcohol-cresol red solution as the indicator. The titration was performed using 2 g of the sample in a 250 ml flask. 25 ml of purified dioxane was then added to the flask and the system swirled for a few minutes. Then, 25 ml of the prepared HCl-dioxane was poured into the flask and the system swirled for a few minutes and allowed to stand for about 15 minutes. The content of the flask was filtered, and an aliquot portion of the obtained solution (approximately 40 ml) was further used by adding 25 ml of the cresol red neutralized

solution. This solution was then titrated using the prepared standard 0.1 N methanolic sodium hydroxide solution until a violet end point colour was reached.

3.3 Hydrotreating Experimental Set-up

The following sections detail the experimental set-up of the trickle bed reactor used during the hydrotreatment studies, and the product analysis.

3.3.1 Hydrotreating Trickle Bed Reactor

The schematic of the trickle bed reactor used for the hydrotreatment studies is shown in Figure 3.1. The system can be divided into three sub-sections, the feed section, the reaction section, and the gas-liquid separation section. The feed section includes the feed tank which rests on a weight scale, and is connected to an Eldex syringe feed pump; it also has an inlet for He (not shown in the diagram) which acts as an inert gas to assist in the flow of the feed to the pump. The reaction section consists of a 304 stainless steel tubular micro scale trickle bed reactor (240 mm length and 10 mm diameter), and a heater with a temperature controller (Eurotherm controls, model No. 2216e) used for controlling the temperature of the catalyst bed. During reaction, the reactor is packed with the desired catalyst (combination of catalyst and silicon carbide mesh) and pressurized using inert helium and regulated using a back pressure regulator, while having hydrogen flow into the system with the feed simultaneously over the catalyst bed. The final section being the liquid product and gas phase separation comprises of a water scrubber vessel, high pressure (HP) separator and an H_2S scrubber. After separation, the hydrotreated feed is collected downstream in a product vessel.

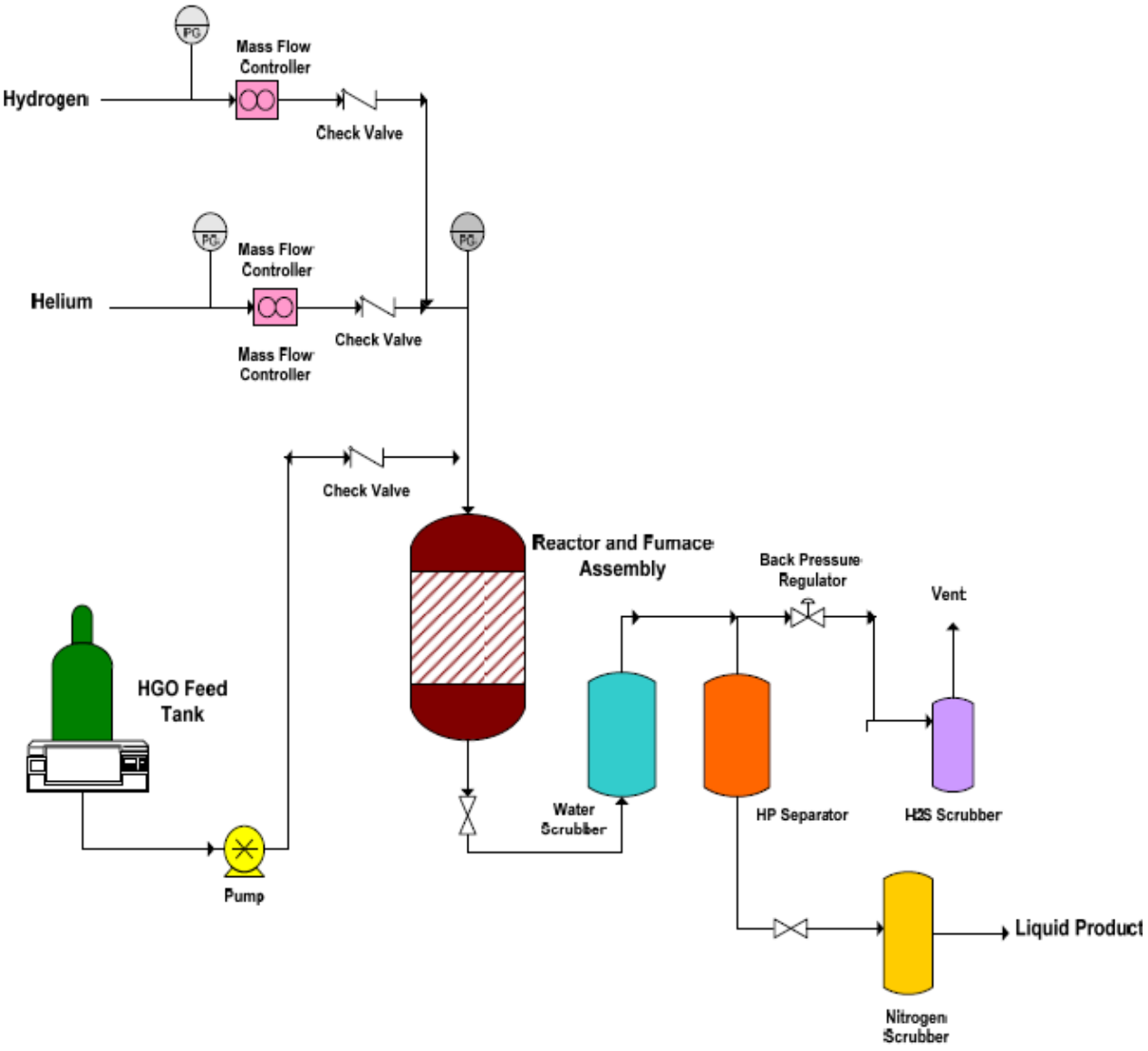

Figure 3.1: Schematic of the trickle bed reactor set-up for hydrotreatment (Adapted from Biswas, 2011).

3.3.2 Reactor Loading and Preparation

The loading procedure for the catalyst into the reactor vessel is shown in Figure 3.2. Before loading the catalyst, the bottom of the reactor vessel was fitted with a Swagelok filter and gasket to ensure the catalyst, mesh, and any particulates remain in the reactor vessel. Thereafter, the loading of the reactor vessel as shown in Figure 3.2 was performed. The catalyst was loaded in between the glass beads (33 mm diameter) and the silicone carbide (16, 46, and 60 mesh) to ensure even distribution of incoming feed. Earlier studies on this particular reactor indicated that such loading procedure led to the establishment of trickle flow in the catalyst bed (Bej et al., 2001b). Once the vessel had been loaded, it was fitted into the reactor system, and then the scrubber unit was filled with approximately 50 ml of distilled water. The system was then slowly pressurized to about 1300 psi using helium, and the reactor vessel was checked for any leaks. If there were no leaks, the system was kept pressurized for 24 hours; after which the sulfidation procedure was carried out, which involved wetting the catalyst with clean gas oil and 2.9 % by volume butanethiol at 100 °C. The initial rate of sulfidation was kept at 2.5 ml/min for 2 hours and then the flow was set to 5 ml/hr (LHSV 1 hr^{-1}). Hydrogen was then introduced into the system at 600 ml/ml of feed. The temperature of the reactor was raised in steps to 194 °C and kept at that temperature for 24 hours and then again in steps to 343 °C and kept at that temperature for another 24 hours. After sulfidation, precoking (preformed in order to stabilize the catalyst activity) was the next step, which involved switching the feed to the desired gas oil and running the system at a feed rate of 5 ml/hr. Precoking was performed for 4 days at 370 °C at an LHSV of 1 hr^{-1} with a hydrogen flow rate of 600 ml/ml of feed.

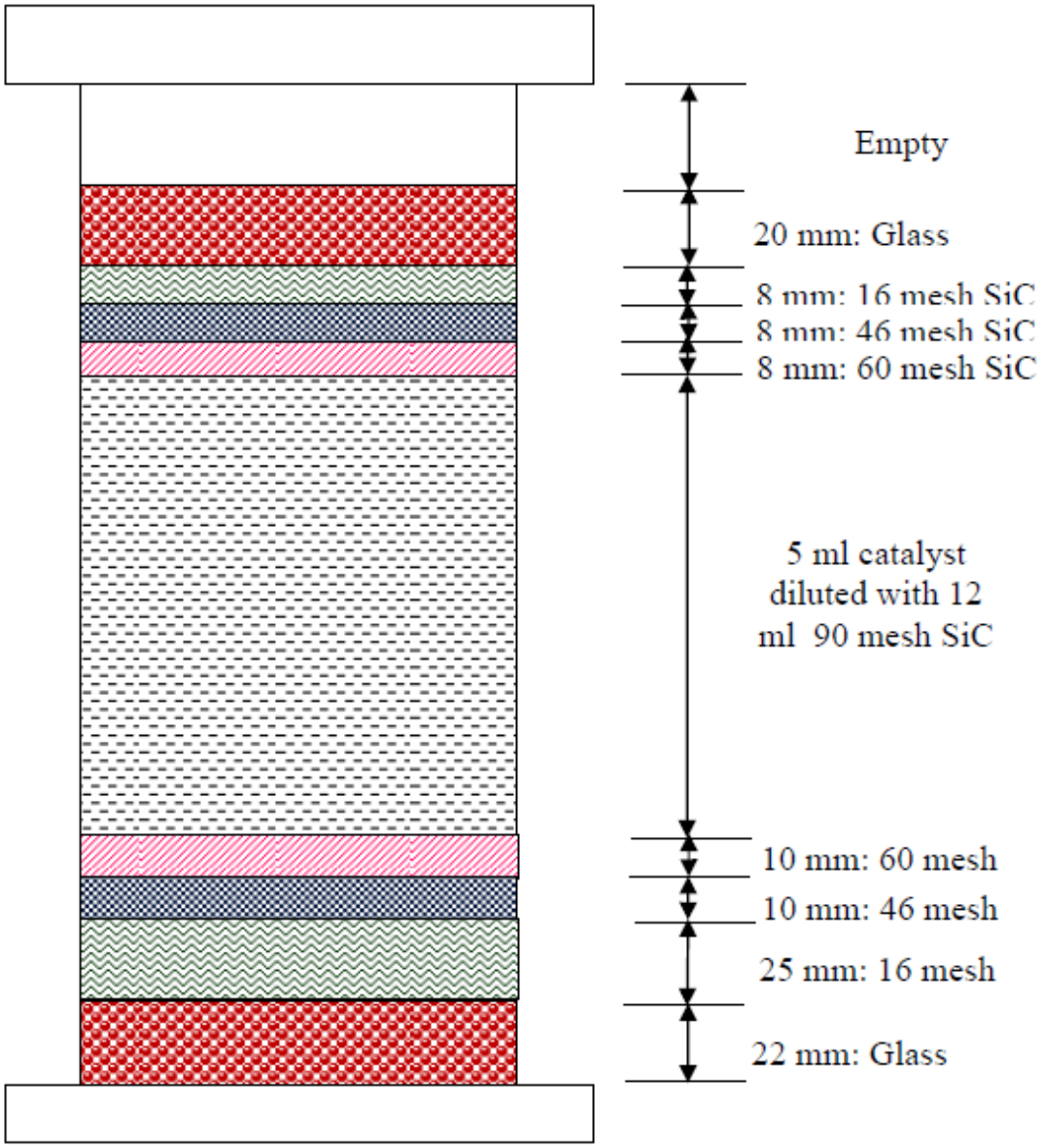

Figure 3.2: Reactor vessel loading procedure using the desired catalyst (Adapted from Biswas, 2011).

3.3.3 Heavy Gas Oil Feed and Product Analysis

The hydrotreatment tests were performed using the bitumen derived heavy gas oil provided by Syncrude Canada Ltd. The characteristics of the gas oil are given in Table 3.1 below.

Table 3.1: Characteristics of Athabasca's bitumen derived heavy gas oil

HGO Characteristics	
Sulfur (wt%)	3.4424
Nitrogen (wt%)	0.3081
Density (g/ml)	0.98
Simulated Distillation	
IBP (°C)	282
FBP (°C)	648
Boiling Range (°C)	wt%
IBP-310	2
310-350	6
351-400	17.2
401-450	27.2
451-500	26.3
501-600	19.2
600-FBP	2.1

The boiling point distribution of the feedstock was performed using simulated distillation ASTM D6352 method using a Varian Model CP 3800 Gas Chromatograph coupled with a Varian CP 8400 Auto sampler. It can be seen that the sulphur, nitrogen, and density levels are significantly high in comparison to conventional feedstocks; thus requiring high temperatures – 375 to 400 ºC and pressures – 1250 to 1300 psi for the hydrotreatment of this feedstock. Once the reaction has taken place inside the reactor vessel, the hydrotreated gas oil is sent to the water scrubber unit where ammonia and

ammonium sulphide are removed, and the liquid product is collected in the vessel. The collected samples were stripped using nitrogen gas (N_2) for the removal of any residual gases.

In order to analyze the concentrations of sulphur and nitrogen in both the feedstock and the hydrotreated product Antek 9000 NS analyzer was utilized. The sulphur content was measured using the combustion-fluorescence technique of the ASTM D5463 method, while the nitrogen content was determined by the combustion-chemiluminescence technique of the ASTM D4629 method. It should be noted however that an instrument error of approximately ±3% for sulphur and ±2% for nitrogen is observable based on the analyzed results.

CHAPTER 4

RESULTS AND DISCUSSION

4.1 Analysis and Optimization of Poly(glycidyl methacrylate) with Tetranitrofluorenone

Synthesis of the complexing agent poly(glycidyl methacrylate) incorporated with tetranitrofluorenone was carried out for the selective removal of polyaromatic compounds containing neutral nitrogen bearing species. The following sections detail the steps and analysis performed in synthesizing the desired polymer.

4.1.1 Investigation of Synthesized Polymer Support Poly(glycidyl methacrylate)

The heterogeneously cross-linked macroporous polymer was prepared by direct polymerization of reactive monomers glycidyl methacrylate (GMA) and ethylene glycol dimethacrylate (EDGMA). The composition of the monomers was selected based on the highest yield obtained for the formed spherical copolymer in the range of 100-400 μm. In addition, further increases in EDGMA resulted in more defective particles due to an increase in the cross-linking agent resulting from higher polymerization rates owing to increases in molar concentrations of the double bonds present (Svec et al., 1975). Table 4.1 illustrates the BET analysis, epoxy titration, and elemental analysis based on a number of parameters that were varied as indicated in the description.

BET analysis shown in Table 4.1 indicated that samples E and F generally had a higher surface area and epoxy content, which is a key determinant in the efficiency of the polymer synthesis, since higher substitution of the epoxy content is possible with more α-epoxide present. The pore diameter and pore volume were sufficient for all samples for the processing of heavy gas oil; however, epoxy content titration and elemental analysis

was not carried out for Sample D due to agglomeration of the monomers to sizes of 500 μm and greater; hence, making it unsuitable for further synthesis. The cause of these defects can be related to stirring speed which plays a significant role in the particle sizing. This has also been discussed by Svec et al. (1975) who reported similar changes with respect to stirring intensity. Accordingly, with increasing speed in stirring the particle size tends to decrease, while at decreasing stir speeds the particle size is increased and tends to agglomerate together; this can also be observed based on SEM analysis of the formed PGMA beads as shown in Figure 4.1, where sample E beads have a greater particle size in comparison to sample F. It was also observed that by mixing the reactants in a single batch, defectiveness was increased significantly, as non-uniformed shaped particles were formed, as illustrated in the SEM image of sample C. Hence, mixing the reactant in three different sets not only decreases the defectiveness of the particles, but at the same time increase the α-epoxide content as well. It should be noted that reproducibility of the BET analysis for samples E and F was performed, with the results being fairly consistent (± 2 m^2/g).

Table 4.1: BET analysis, epoxy titration, and elemental analysis of PGMA samples with varying parameters.

Sample	Description	BET Analysis			Epoxy Titration	Elemental Analysis
		Specific S.A. m^2/g	Pore Dia. Å	Pore Vol. cm^3/g	Content in Fraction wt%	Nitrogen Content %
Sample A	Mixed in a single batch; 300 RPM	34 ± 2	168 ± 3.5	0.14 ± 0.02	5.50 ± 0.5	0.005 ± 0.001
Sample B	(Mixed in a single batch) / 2; 300 RPM	30 ± 2	178 ± 3.5	0.14 ± 0.02	5.50 ± 0.5	0.006 ± 0.001
Sample C	Mixed in a single batch; 400 RPM	28 ± 2	182 ± 3.5	0.13 ± 0.02	4.08 ± 0.5	0.006 ± 0.001
Sample D	Mixed in a single batch; 200 RPM	36 ± 2	161 ± 3.5	0.14 ± 0.02	N/A	N/A
Sample E	Mixed in three sets; 300 RPM	35 ± 2	157 ± 3.5	0.14 ± 0.02	5.82 ± 0.5	0.006 ± 0.001
Sample F	Mixed in three sets; 400 RPM	39 ± 2	151 ± 3.5	0.15 ± 0.02	5.55 ± 0.5	0.003 ± 0.001

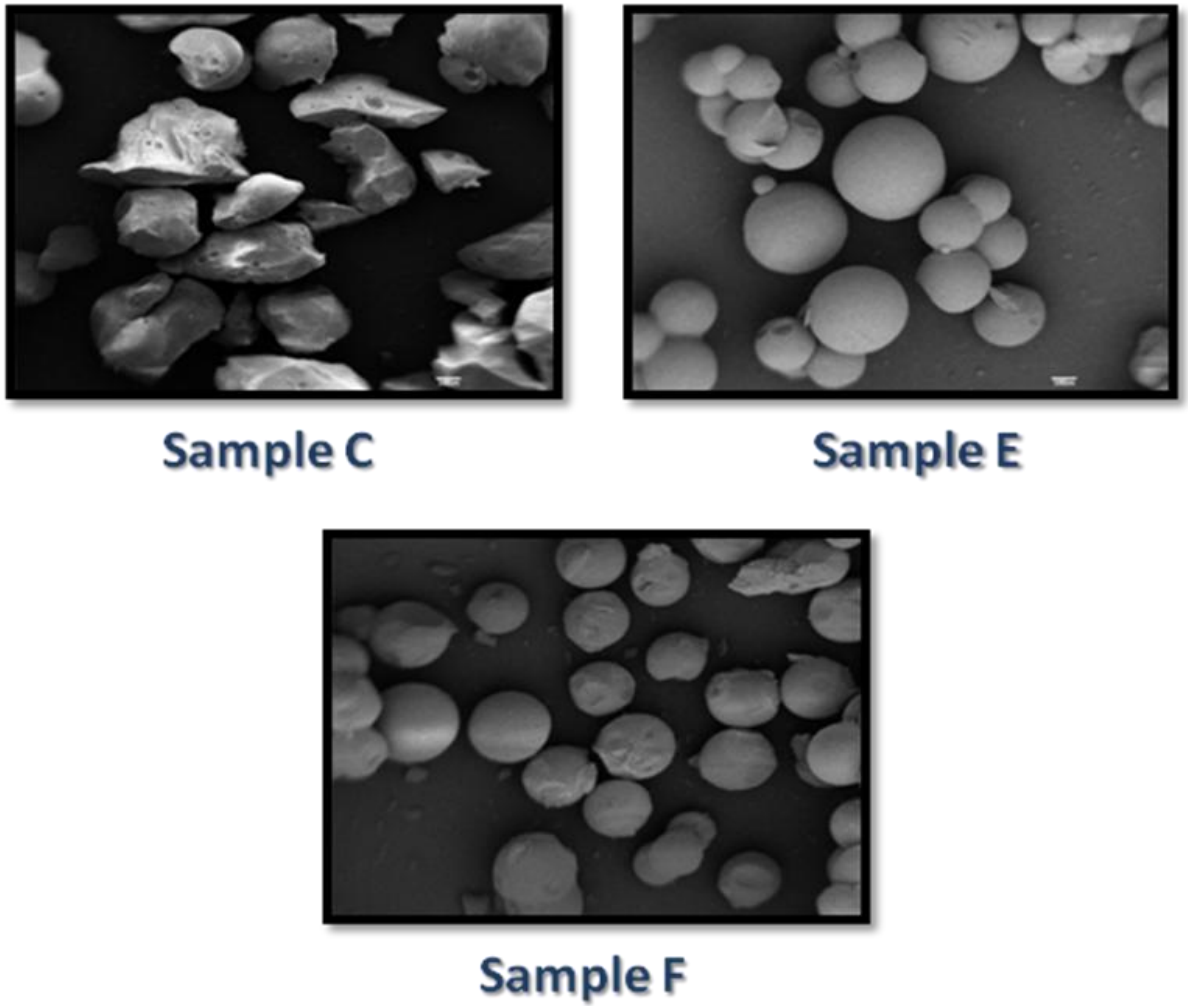

Figure 4.1: SEM images of samples C, E, and F at 100µm illustrating PGMA bead sizes and shapes.

FT-IR was also performed in order to establish the presence of the epoxy group on the synthesized polymer. It was observed that all six samples showed characteristic peaks in the range of 1250-1265 cm^{-1} and 810-950 cm^{-1} as shown in Figure 4.2, which is representative of the symmetrical and asymmetrical stretching of the epoxy ring; whereas, the strong band observed at 1736 cm^{-1} is due to the C=O stretching vibration (Okubo, 2001; and Tuncer, 2007). This shows that all of the synthesized samples had the presence of the α-epoxide, but at different concentration amounts. These results are in agreement with the titration analysis performed for the α-epoxide content, illustrating the presence of the epoxy ring at varying quantities in all samples as well.

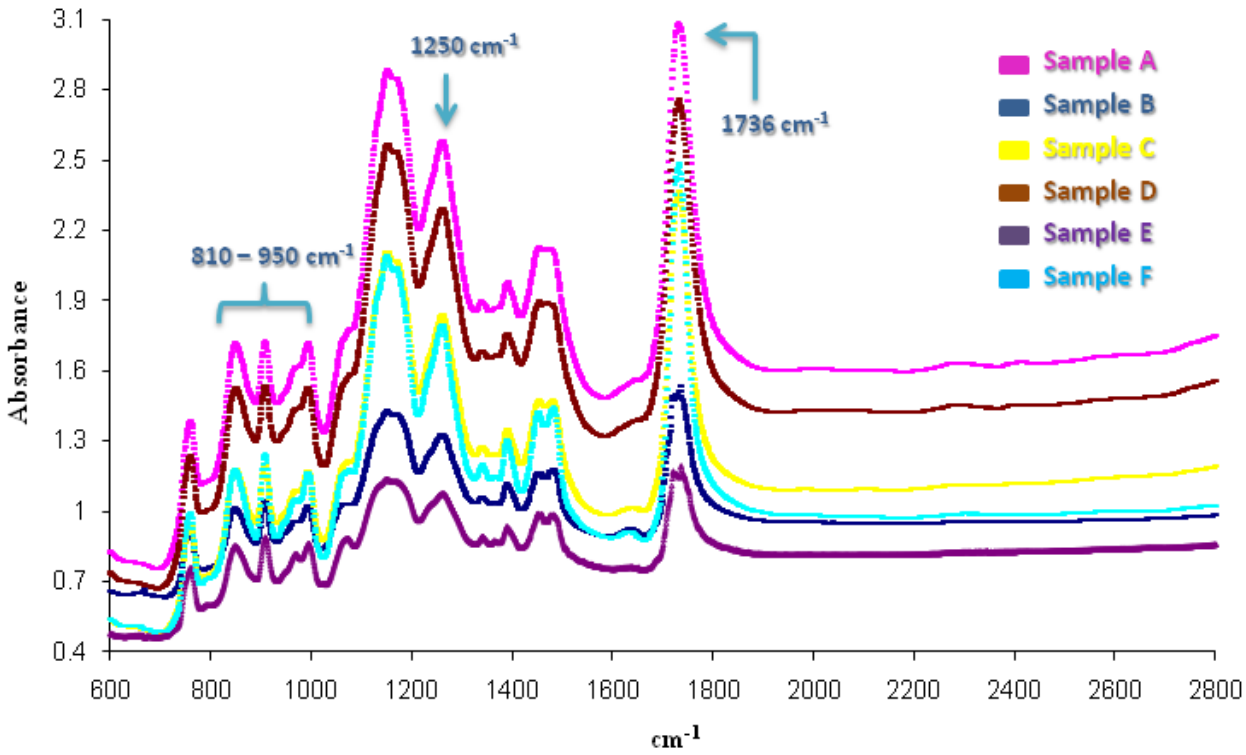

Figure 4.2: FT-IR of all six synthesized PGMA samples illustrating presence of the epoxy ring.

4.1.2 Investigation of Substituted Acetone Oxime

Second step of the synthesis procedure dealt with substitution of the oxime functionality in place of the epoxy ring. The conditions as specified by Lemaire et al. (2002) had to be modified due to extremely low conversion rates; consequently, several parameters as indicated in Table 4.2 were customized in order to determine the optimum conditions under which the highest oxime substitution could take place. A comparison of the results demonstrating the change in the epoxy content occurring in step 2 synthesis with respect to the α-epoxide content titration are illustrated in Figure 4.3. The excess amount of acetone oxime being used during this reaction can simply be determined through molar excess calculations; however, in order to do so, the average molecular weight of PGMA must be known. This value can be calculated using gel permeation chromatography, which is a technique often used for characterization of polymers and can be utilized for determining the viscosity molecular weight (M_v) of the polymer PGMA (Wikipedia, 2012).

The results indicate that sample J had the highest substitution of epoxy ring to acetone oxime occurring under the aforementioned conditions (approximately 33%); which in comparison to sample G, synthesized under the conditions discussed by Lemaire et al. (2002), more than doubled. This increase in substitution was solely due to an increase in temperature from 80°C to 100°C. The effect of time however, seemed to have had a detrimental impact, as can be noticed in sample H and K, in which the substitution decreased as time was doubled. The elemental analysis conducted to determine the nitrogen content for each sample were generally in agreement with the results of the epoxy content titration, with samples J and K illustrating the highest nitrogen content.

Table 4.2: Epoxy content determination and elemental analysis of step 2 modified beads.

Sample	Description	Epoxy Titration	Elemental Analysis
		Content Decrease	Nitrogen
		wt%	Content %
Sample G	Mixed at 300 RPM, 80°C, for 24 hours	15.1	0.716
Sample H	Mixed at 300 RPM, 80°C, for 48 hours	0.5	1.087
Sample I	Mixed at 300 RPM, 80°C, for 24 hours, DMF doubled	21.8	0.765
Sample J	Mixed at 400 RPM, 100°C, for 24 hours	32.7	1.376
Sample K	Mixed at 400 RPM, 100°C, for 48 hours	26.5	1.350
Sample L	Mixed at 400 RPM, 120°C, for 72 hours	6.4	0.994
Sample M	Mixed at 400 RPM, 120°C, for 48 hours	13.6	1.076

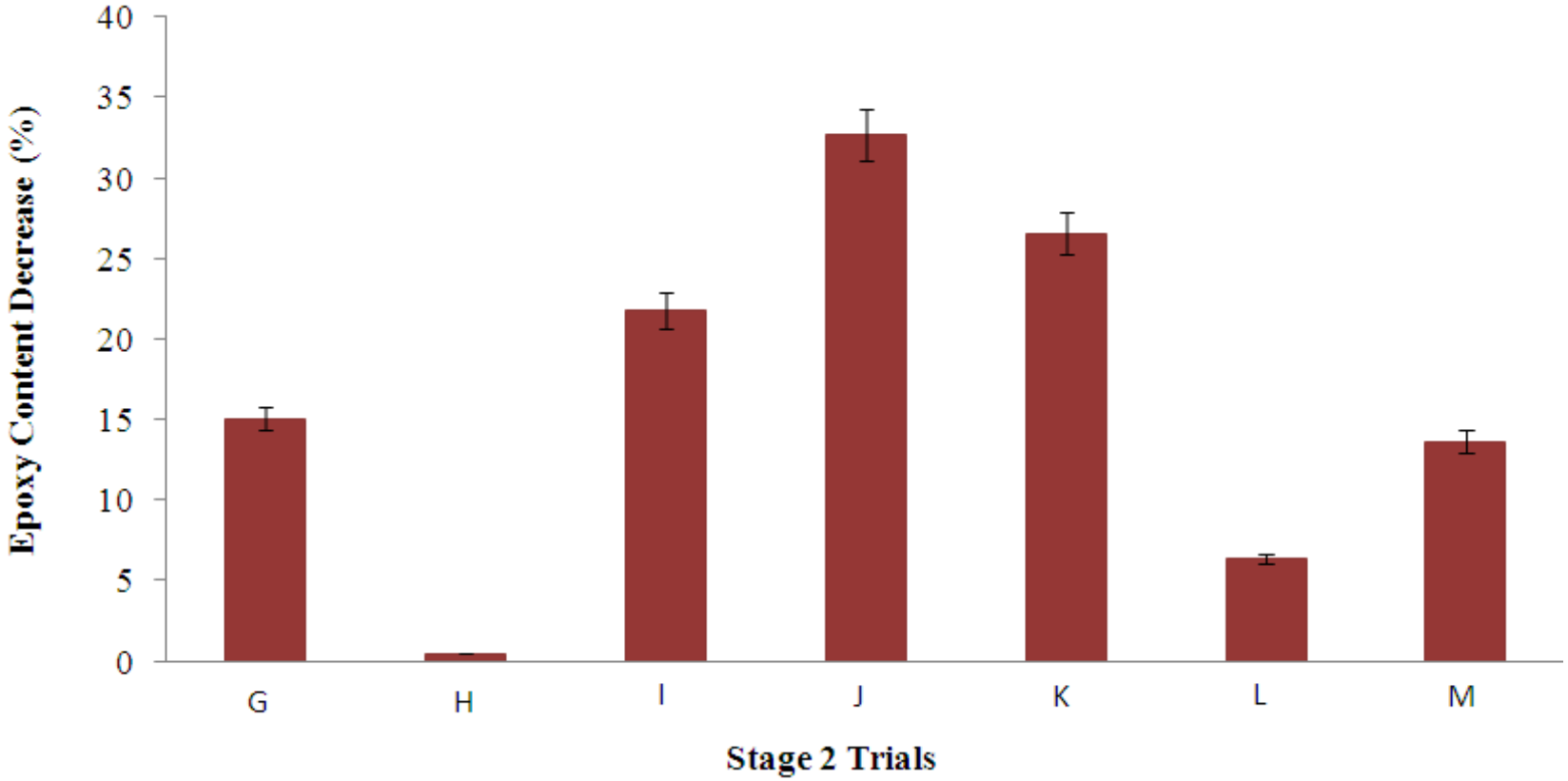

Figure 4.3: Epoxy content decrease due to substitution with acetone oxime.

FT-IR was also performed on all step 2 samples, as shown in Figure 4.4, in order to ascertain the presence of acetone oxime functionality onto the polymer. Characteristics peaks in the range of 1650 cm^{-1} (Nadine, 2007) for the acetone oxime functionality can be observed for all seven samples; however, the peak for sample G is very low, which in support of the titration and elemental analysis can e due to the lower substitution of the oxime functionality. Furthermore, characteristic peaks for the epoxide group are still present, indicating the fact that not all of the epoxide groups had been converted during the synthesis.

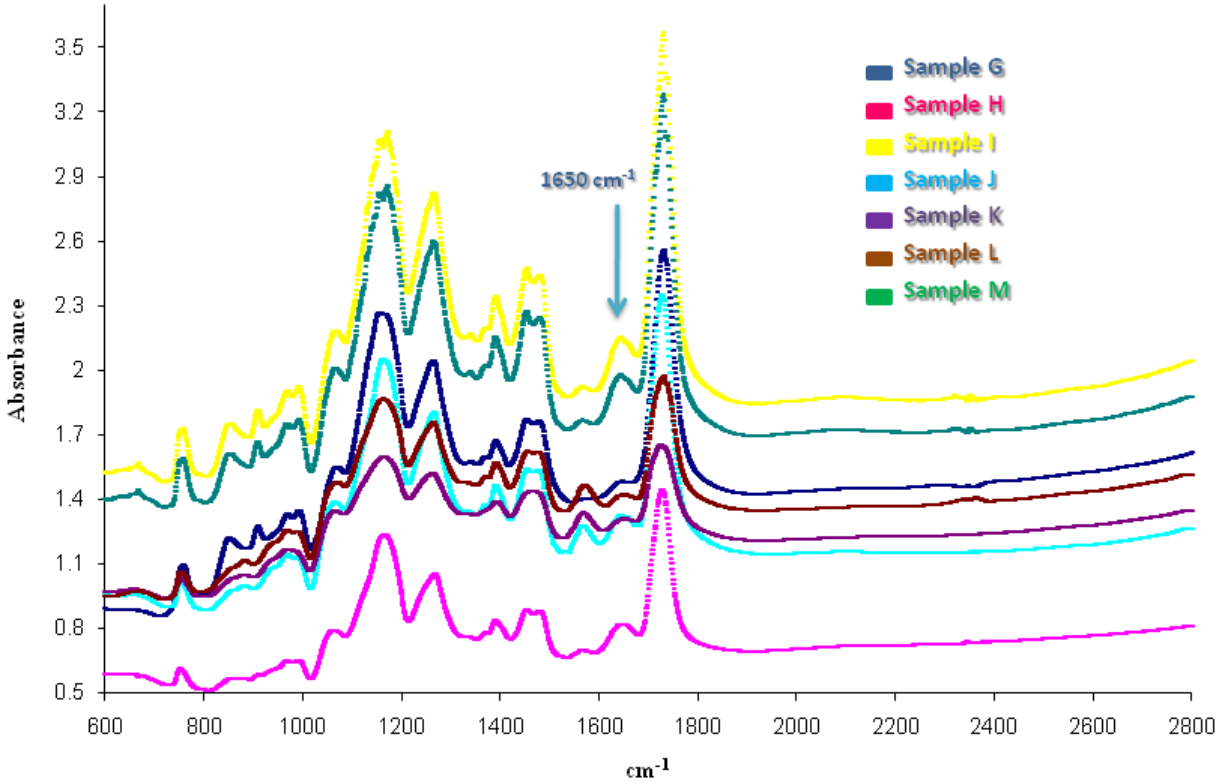

Figure 4.4: FT-IR of all seven step 2 synthesized samples illustrating the presence of acetone oxime.

4.1.3 Investigation of Tetranitrofluorenone Coupling

Prior to coupling of the organic compound tetranitrofluorenone, it had to be synthesized following the procedure described by Newman et al. (1956) through nitration of fluorenone. The light yellow precipitate formed was then used directly in step 4 synthesis; however, due to the lack of information provided in literature with regards to the synthesis, several parameters as shown in Table 4.3 were tested in order to determine the optimum conditions under which the highest yield for TENF coupling could be obtained.

Figures 4.5 and 4.6 illustrate TGA and DTG thermograms that were obtained for each of the step 4 synthesized samples to understand their thermal behaviour attributable to parameter modifications. Mass loss beginning at approximately 230°C is noticeable based on TGA curves for all seven samples and can be attributed to random PGMA chain scission (Tuncer et al., 2007). In addition, DTG curves indicate that degradation of the synthesized polymer for all samples took place in two steps as shown by the two distinct peaks at approximately 297°C and 348°C. An estimate of the coupling of TENF onto the oxime functionality was done based on the melting point range of the organic compound which is known to be 249-253°C (Newman et al., 1956). Table 4.3 indicates mass loss for each sample within that temperature range, with sample T demonstrating the highest mass loss, while sample R showing the lowest mass loss. These results suggest that the optimum conditions for the highest coupling of TENF onto the oxime functionality present on the polymer are those followed in sample T. Additionally, it can be noted that a more precise quantitative analysis of the coupling of TENF onto the polymer can be performed using solid-state NMR.

Table 4.3: Synthesis parameters of all seven step 4 samples and the amount of coupling of TENF onto oxime functionality.

Sample	Description	TGA (μg)
Sample N	Refluxed for 3 days; 9.78 g of beads; Sulfonic Acid (10% of beads); 1.76 g TENF	78 ± 3
Sample O	Refluxed for 3 days; 9.78 g of beads; Sulfonic Acid (10% of beads); 2 × TENF	70 ± 3
Sample P	Refluxed for 3 days; 9.78 g of beads; Sulfonic Acid (25% of beads); 1.76 g TENF	72 ± 3
Sample Q	Refluxed for 2 days; 9.78 g of beads; Sulfonic Acid (10% of beads); 1.76 g TENF	70 ± 3
Sample R	Refluxed for 3 days; 9.78 g of beads; Sulfonic Acid (5% of beads); 1.76 g TENF	66 ± 3
Sample S	Refluxed for 3 days at 10°C higher than the refluxing temperature; 9.78 g of beads; Sulfonic Acid (10% of beads); 1.76 g TENF	76 ± 3
Sample T	Refluxed for 3 days; 9.78 g of beads; Sulfonic Acid (25% of beads); 1.5 × TENF	127 ± 3

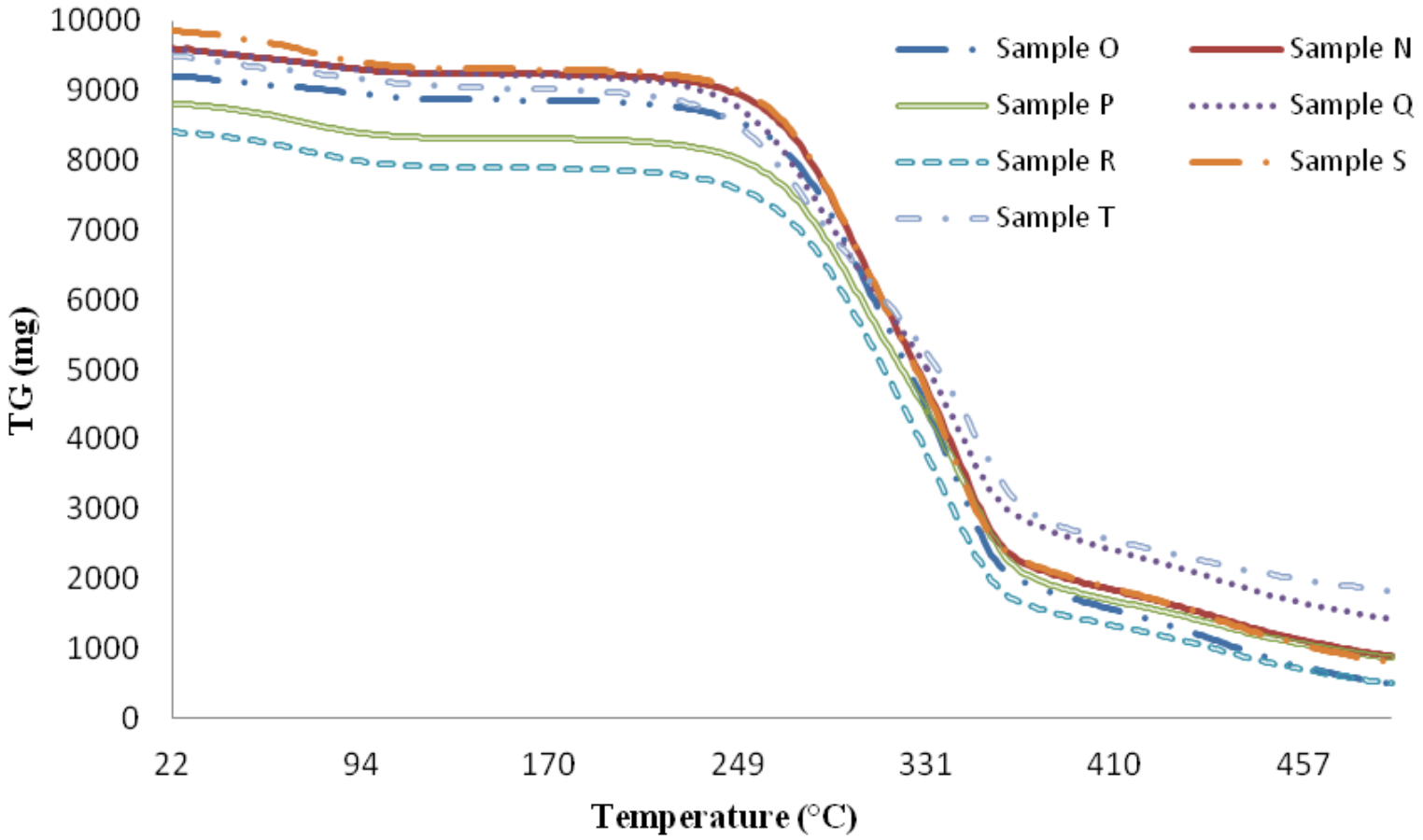

Figure 4.5: TGA thermograms of all seven step 4 synthesized samples.

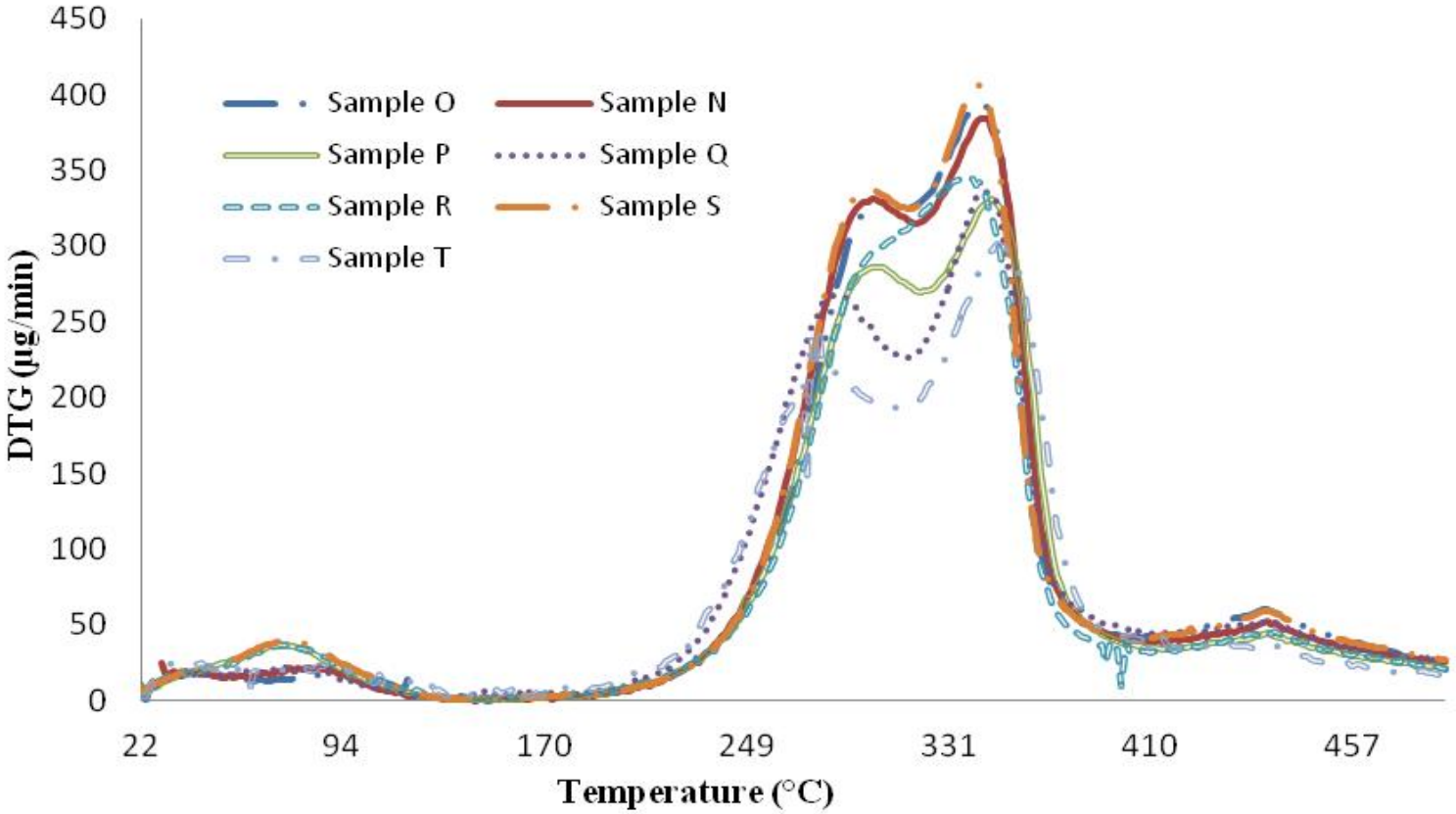

Figure 4.6: DTG thermograms of all seven step 4 synthesized samples.

4.2 Hydrotreatment Studies Using Pre-treated and Non-treated Heavy Gas Oil

The optimized polymer developed based on the numerous parameter studies from section 4.1 was then produced in greater quantity in order to perform pre-treatment of bitumen derived heavy gas oil for hydrotreatment studies. The following sections detail the contact time and reusability studies, as well as inhibition and deactivation studies performed using the pre-treated heavy gas oil with the respective polymer.

4.2.1 Investigation of Polymer Contact with Heavy Gas Oil

Feasibility of the synthesized polymer for the selective removal of neutral nitrogen compounds was tested using bitumen derived heavy gas oil; characterization of this gas oil is given in Table 4.4.

Table 4.4: Characterization of heavy gas oil derived from Athabasca bitumen.

Characterization Parameters	**Amount**
Boiling Range (°C)	350 - 600
Sulphur Content (ppm)	35337
Nitrogen Content (ppm)	5056
Non-Basic Nitrogen Content (ppm)	3286
Aromatic Content (ppm)	3720
Density (g/ml)	0.98

The nitrogen and sulphur content, as well as the density of this heavy gas oil is significantly higher in comparison to conventional feedstocks (Ferdous et al., 2004); thus,

making it much more difficult to pre-treat using the synthesized polymer. In order to determine the highest selectivity and extraction towards nitrogen bearing compounds, all seven synthesized samples from step 4 were tested using heavy gas oil for nitrogen and sulphur removal, with the results shown in Figure 4.7.

Percent removal of both nitrogen and sulphur present in bitumen derived heavy gas oil by means of contacting with the synthesized polymer was performed in order to determine whether changing the parameters as discussed in Table 4.3 would influence the selectivity and removal rate of nitrogen bearing compounds in heavy gas oil. The amount of polymer used was approximately 15 % by weight with respect to the amount of heavy gas oil; with further increases leading to higher viscosity and less contact occuring in the mixed stream. As shown in Figure 4.7, all seven samples were able to selectively target and remove nitrogen bearing compounds, with sample T having the highest nitrogen removal at 6.7 %, while having little to no influence on the sulphur or aromatic compounds also present in the heavy gas oil. Basic and non-basic nitrogen analysis of Sample T was also performed by Syncrude Canada Ltd. using acid-base titration, which showed that only 1.1% of the removed nitrogen species were of basic nature; thus, confirming the selectivity of the polymer towards non-basic nitrogen species. These results are in agreement with those of Table 4.3 which showed that sample T had the highest TENF coupling onto the oxime functionlity, while sample R had the lowest; thus, highest nitrogen removal being attained for Sample T and one of the lowest for sample R. Additionally, based on the mechanism of complexation, the structures of the extracted compounds should be those resembling neutral nitrogen such as carbazole and its derivatives, some polyaromatics capable of forming charge transfer complexes with the

immobilized π-acceptor, and dibenzothiophene derivatives. Basic nitrogen compounds such as quinoline and aniline and their derivatives are not complexed due to the difference in their molecular orbital symmetry (Macaud et al., 2004). It should also be noted that an instrument error of ± 3 % for sulphur and ± 2 % for nitrogen ought to be accounted for; as well, blank tests were performed to confirm that the removal of nitrogen was solely due to the performance of the synthesized beads. The tests were also performed three times for each sample in order to ensure reliability, and the average of the removal rate was then taken as the removal rate for both nitrogen and sulphur.

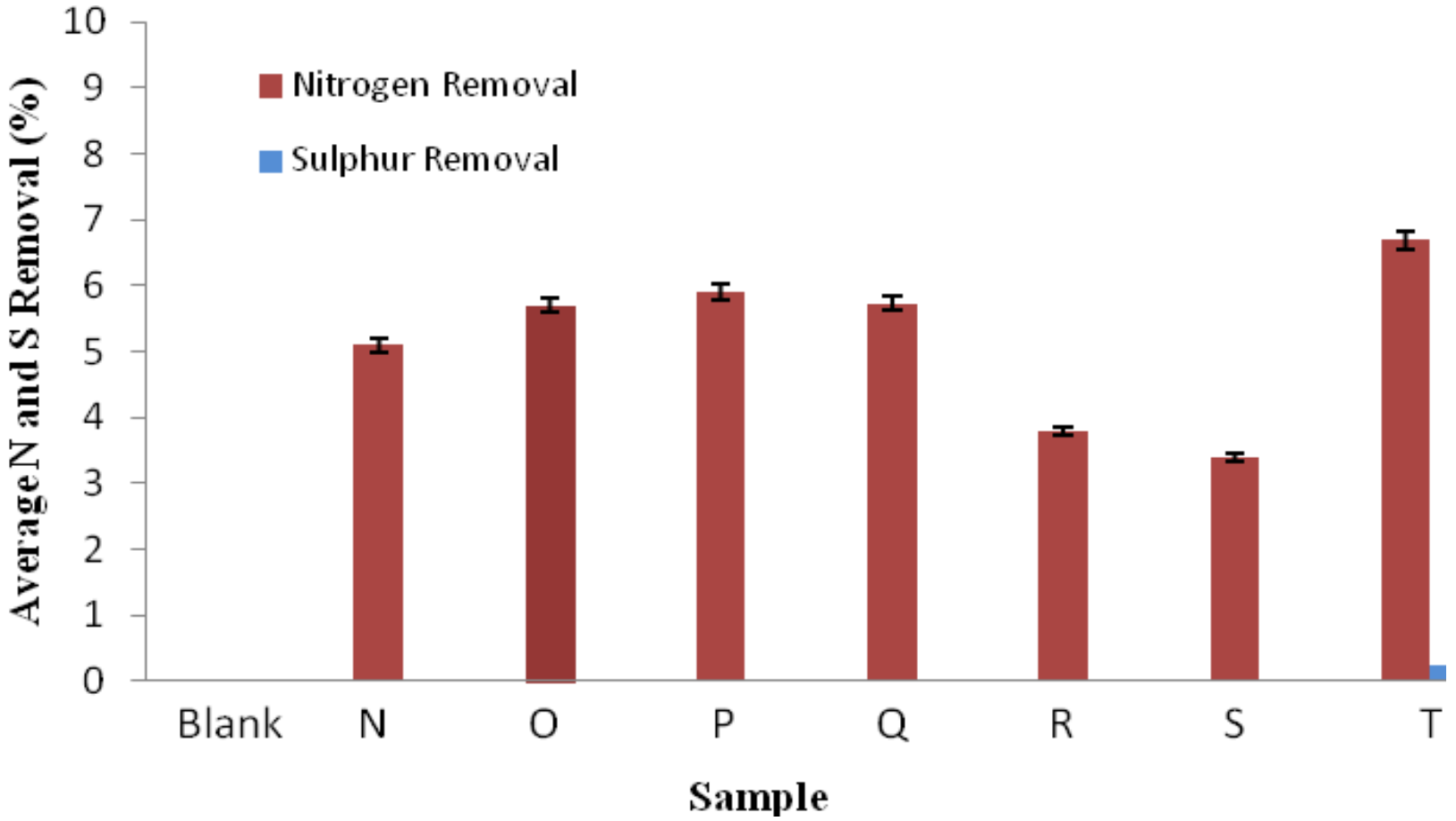

Figure 4.7: Percent removal of nitrogen and sulphur from heavy gas oil using step 4 synthesized polymer beads at 110°C for 1 hour at 400 RPM.

4.2.2 Investigation of Polymer Reusability

One of the advantages of using this polymer as a pre-treatment method is its known ability to be reused several times; hence, contact studies were performed in order to establish the effective reusability of the polymer. Figure 4.8 illustrates contact studies performed using sample T polymer.

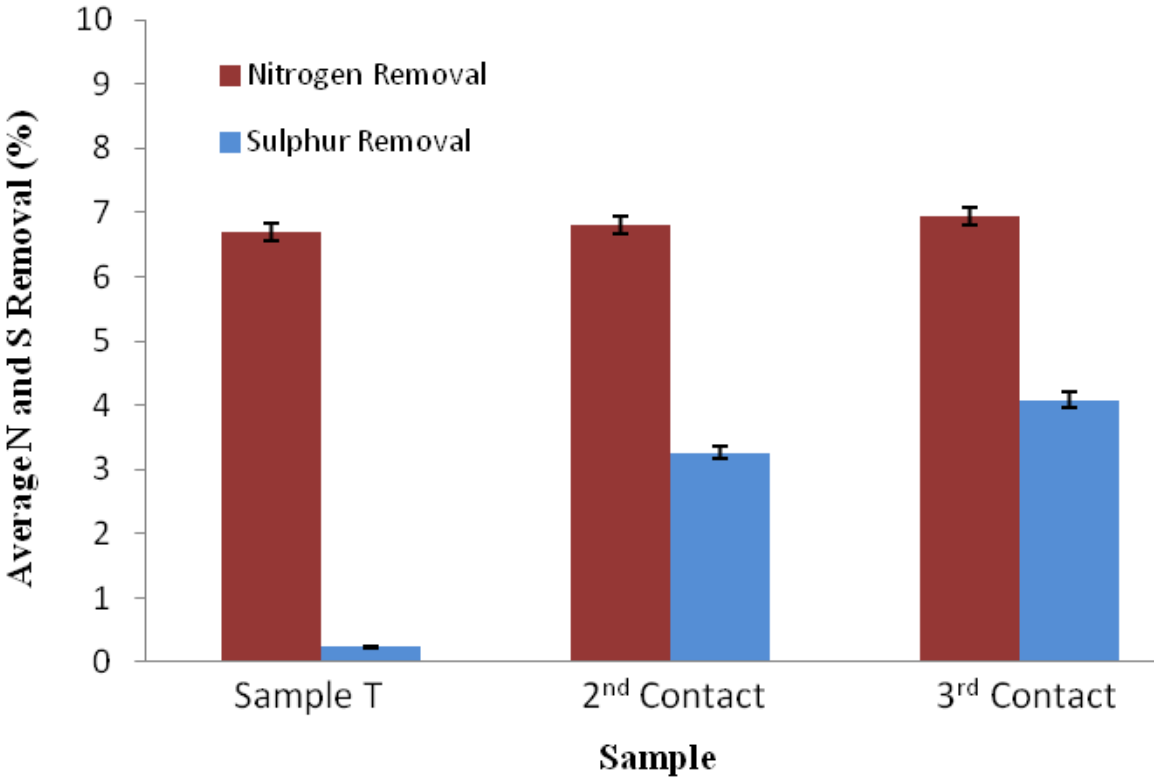

Figure 4.8: Contact study performed using sample T to determine reusability of the polymer.

As shown earlier in Figure 4.7, sample T had the highest nitrogen removal, and thus was further utilized by washing the once contacted polymer with toluene multiple times, and then contacting it again with heavy gas oil for the second and third time to determine its reusability. The results in Figure 4.8 show that the polymer can indeed be used multiple times for the removal of nitrogen bearing compounds, since the removal rate of

nitrogen stayed consistent in the range of approximtely 6.5 %. It was noticed however, that the removal of sulfur was increased after each contact, this may be due to the complexation of some dibenzothiophene derivatives as discussed earlier, and the polymer requiring further washing with toluene to fully remove any compounds attached that may have hindered the selectivity of the polymer during successive contacts. In addition, Table 4.5 illustrates BET analysis performed on the washed beads following second and third contact with HGO in order to determine whether any significant changes occurred in consequence of the successive contacts.

The results in Table 4.5 show that the surface area of the washed beads decreased slightly after the second contact, and stayed consistent after the third contact indicating that successive contact and washing does not significantly influence the surface of the spherical beads; as well, the pore volume and pore diameter stayed moderately consistent as well, further illustrating that no significant pore blockage or changes in pore volume occurred after the beads were washed and reused.

Table 4.5: BET analysis after 2nd and 3rd contact with HGO using sample T beads.

Sample	**BET Analysis**		
	Specific S.A. (m^2/g)	**Pore Dia.(Å)**	**Pore Vol. (cm^3/g)**
Sample T	58	125	0.18
After 2nd Contact	52	135	0.18
After 3rd Contact	53	136	0.18

4.2.3 Inhibition and Deactivation Due to Non-Basic Nitrogen Compounds

Long-term hydrotreatment study was performed in order to determine the level of inhibition and deactivation caused by non-basic nitrogen species in bitumen-derived heavy gas oil. In order to do so, trickle bed reactor was employed under the given conditions;

- Temperature: 375 ˚C
- Pressure: 1250 psig
- LHSV: 1.0 h^{-1}
- H_2/Feed Ratio: 600 ml/ml

Three heavy gas oil feeds at varying nitrogen levels (HGO A: 5% nitrogen removal, HGO B: 3% nitrogen removal, and HGO: no nitrogen removal) through contacting with the functionalized polymer, were used to determine inhibiting and deactivating effects of non-basic nitrogen species. Figure 4.9 illustrates the order in which the gas oil feeds were hydrotreated in a continuous reaction, and their conversion levels. It should be noted that clean feed refers to previously hydrotreated feed with an addition of 1 wt% dibenzothiophene and 1 wt% thiophene; furthermore, throughout all of the performed experiments, the proprietary trilobe-shaped NiMo/γ-Al_2O_3 commercial catalyst supplied by Syncrude Canada Ltd was employed.

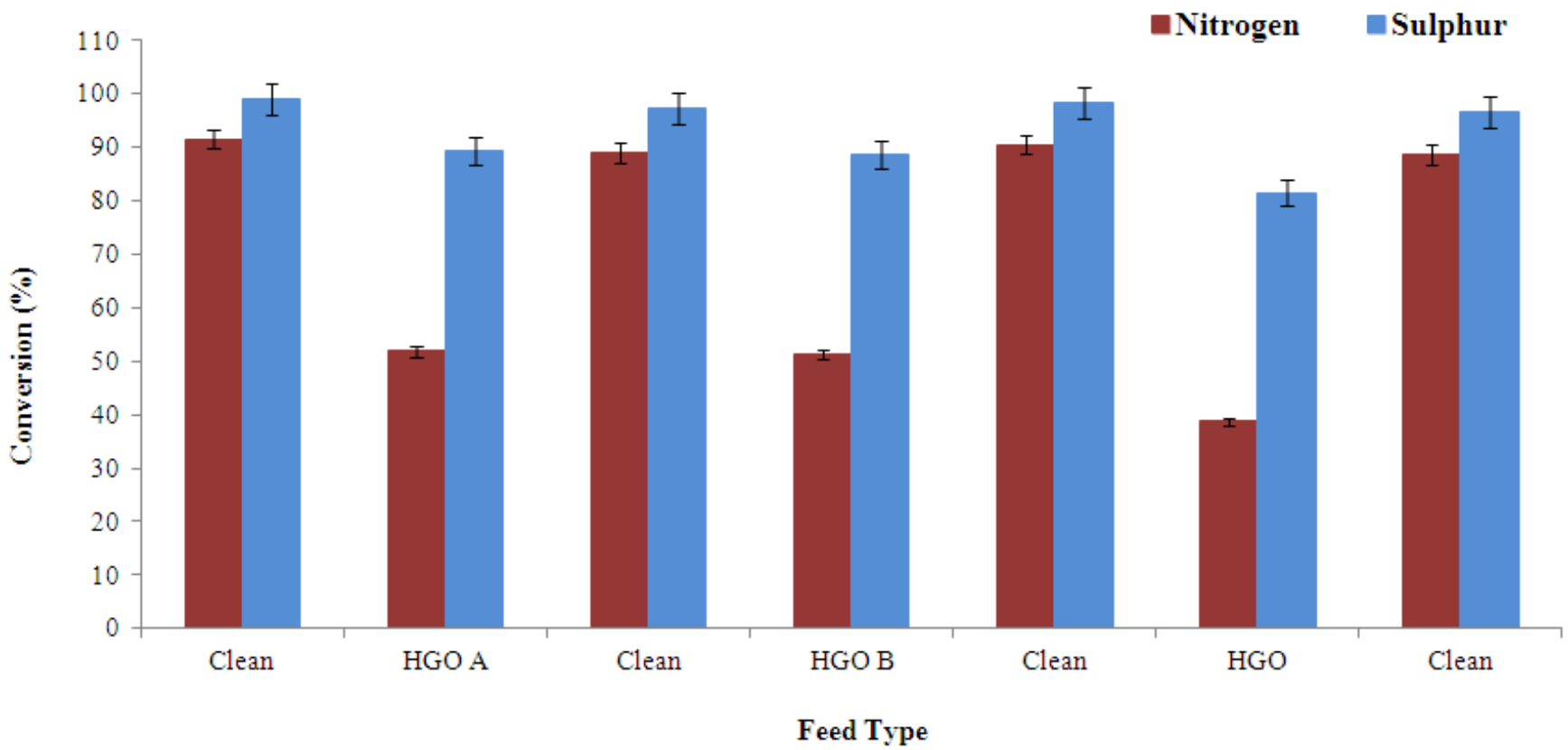

Figure 4.9: Nitrogen and sulphur conversion of HGO feeds at varying nitrogen levels.

The results shown in Figure 4.9 indicate that the removal of non-basic nitrogen species from heavy gas oil had a significant impact even at levels as low as 5%. The nitrogen and sulphur conversions of the clean gas oil feed stayed comparatively consistent after each of the HGO feed streams were put in; indicating that there was very little to no deactivation of the catalyst active sites due to non-basic nitrogen species. However, examining the change in conversion between HGO A with 5% non-basic nitrogen removal and HGO with no nitrogen removal, it was observed that sulphur conversion was inhibited approximately 9% and nitrogen conversion was inhibited approximately 20% (overall difference in conversion was 25%, with 5% removed before hydrotreatment using the functionalized polymer). Consequently, based on these outcomes it can be concluded that non-basic nitrogen species have a much more detrimental impact through inhibiting of catalyst active sites, and their selective removal prior to hydrotreatment can inturn significantly improve hydrodesulphurization and hydrodenitrogenation activity.

4.3 Hydrotreating Kinetics Study

The following sections describe the effects of reaction conditions during the hydrotreatment of both treated and non-treated heavy gas oil feedstocks, and the development of kinetic expressions using the power law model for the hydrodesulphurization and hydrodenitrogenation activity.

4.3.1 Effect of Temperature on Pre-treated and Non-treated Heavy Gas Oil Activity

The effect of temperature on the HDS and HDN activity of pre-treated and non-treated heavy gas oil was studied using commercial catalyst in the temperature range of 375 °C to 395 °C, while keeping other parameters such as hydrogen/oil ratio, pressure, and LHSV constant. The conversion of sulphur with respect to changes in temperature is shown in Figure 4.10, with results indicating that the conversion increased with increasing temperature. It is important to note however that the change in conversion was higher at the lower temperature range (375 – 385 °C) than in the higher temperature range (385 – 395 °C). This may be due to the fact that reaction temperature has an affect on both direct desulfurization (DDS) and hydrogenation (HYD) routes of refractory compounds; thus, refractory compounds such as 4,6-DMDBT which are more easily hydrogenated at lower temperatures tend to increase the activity at the lower temperature range rather than the higher temperature range (Xu et al., 2004). It was also observed that at all three temperatures the conversion of sulphur was significantly (approximately 7%) higher for treated HGO than for non-treated HGO. This implies that the removal of non basic nitrogen species from heavy gas oil had a significantly positive impact on the conversion on sulphur species during hydrotreatment. The highest sulphur conversion

obtained for treated HGO was 96.7% and 90.5% for non-treated HGO, both at the temperature of 395 °C, LHSV of 1.0 hr^{-1}, pressure of 1250 psig, and hydrogen/gas oil ratio of 600 ml/ ml.

The effect of temperature on the conversion of nitrogen was also studied, and the results are shown in Figure 4.11. Similar to the sulphur conversion, it can be seen that as the temperature was increased, the conversion increased as well for both treated and non-treated HGO, with higher changes in conversion being observed at the lower temperature range (375 – 385 °C). However, the impact of removing non-basic nitrogen species using pre-treatment was much more substantial in comparison to sulphur, as nitrogen conversions were increased approximately 15% (inclusive of the 5% nitrogen removal using pretreatment). This implies that the non-basic nitrogen species have a detrimental impact on the hydrotreatment of other nitrogen bearing compounds through competitive inhibition onto the catalyst active sites. The highest nitrogen conversion obtained for treated HGO was 70.1% and 60.5% for non-treated HGO, both at the temperature of 395 °C, LHSV of 1.0 hr^{-1}, pressure of 1250 psig, and hydrogen/gas oil ratio of 600 ml/ ml.

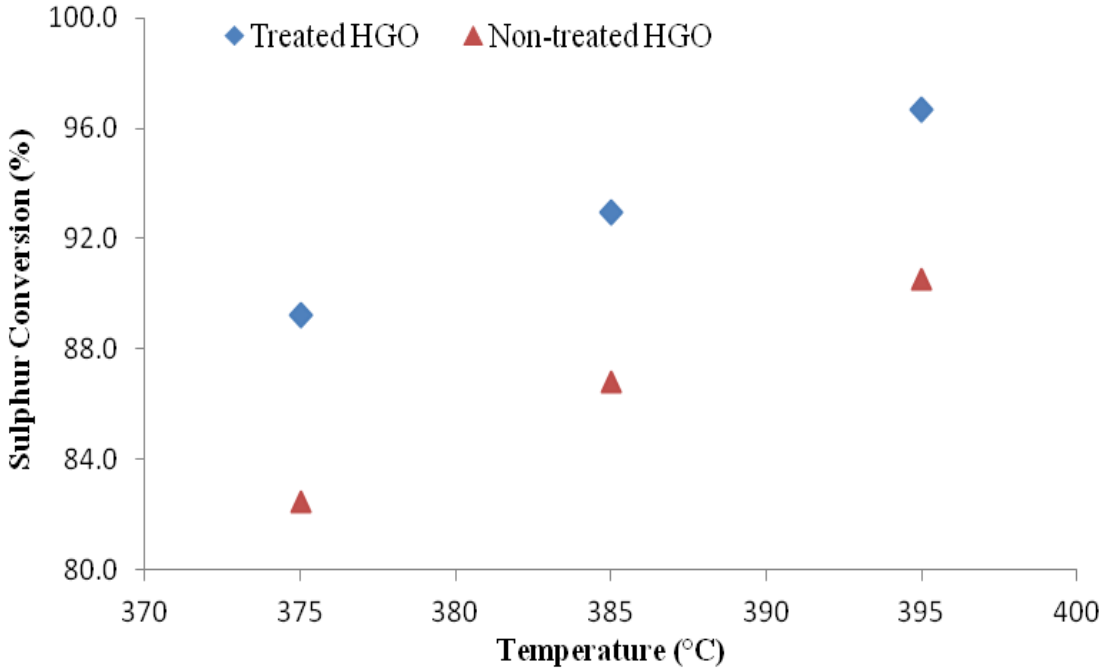

Figure 4.10: Effect of temperature on the conversion of sulphur for treated and non-treated HGO at LHSV of 1 hr^{-1}; hydrogen/oil raio of 600 ml/ml; and pressure of 1250 Psi.

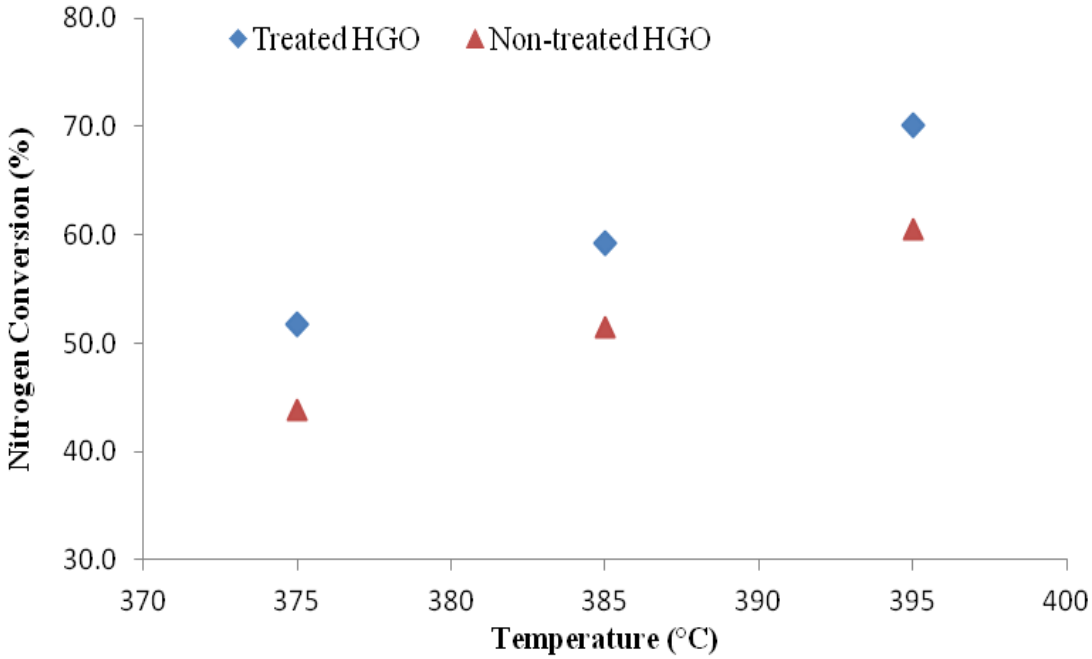

Figure 4.11: Effect of temperature on the conversion of nitrogen for treated and non-treated HGO at LHSV of 1 hr^{-1}; hydrogen/oil raio of 600 ml/ml; and pressure of 1250 Psi.

4.3.2 Effect of LHSV on Pre-treated and Non-treated Heavy Gas Oil Activity

The effects of liquid hourly space velocity (LHSV) on the HDS and HDN of pre-treated and non-treated heavy gas oil were studied using commercial catalyst, while keeping other parameters such as temperature, hydrogen/oil ratio, and pressure constant. The conversion of sulphur with respect to changes in the LHSV (range of 0.5 hr^{-1}, 1.0 hr^{-1}, and 2.0 hr^{-1}) is given in Figure 4.12. The results indicate that with increasing LHSV the conversion for both treated and non-treated HGO decreased; this is due to the fact that as LHSV is increased, so is the feed rate, which results in less contact time of feed with the catalyst, resulting in lower conversion rates. It is important to note that similar to the effects of temperature, LHSV conversation rates were also higher for treated HGO, implying that more catalyst active sites were available for conversion even at higher feed rates. Additionally, it can be observed from Figure 4.12 that the conversion for treated HGO at LHSV of 0.5 hr^{-1} and 1.0 hr^{-1} is very similar, implying that competitive adsorption by non-basic nitrogen species has been reduced; thus, allowing for higher conversion even at higher LHSV, as more catalyst active sites are available for conversion. The highest sulphur conversion obtained for treated HGO was 97.5% and 94.9% for non-treated HGO, both at LHSV of 0.5 hr^{-1}, temperature of 395 °C, pressure of 1250 psig, and hydrogen/gas oil ratio of 600 ml/ ml.

The effect of LHSV on the conversion of nitrogen was also studied, and the results are shown in Figure 4.13. Similar to the sulphur conversion, it can be seen that as the LHSV was reduced the conversion was increased for both treated and non-treated HGO, with treated HGO having higher conversion rates at LHSV of 0.5 hr^{-1} and 1.0 hr^{-1}. It was observed that for nitrogen and sulphur, the conversion for both treated and non-treated

HGO are equivalent, implying that at the high LHSV rate of 2.0 hr^{-1} the effects of non-basic nitrogen species acting as inhibitors is insignificant. The highest nitrogen conversion obtained for treated HGO was 90.3% and 78.3% for non-treated HGO, both at LHSV of 0.5 hr^{-1}, temperature of 395 °C, pressure of 1250 psig, and hydrogen/gas oil ratio of 600 ml/ ml.

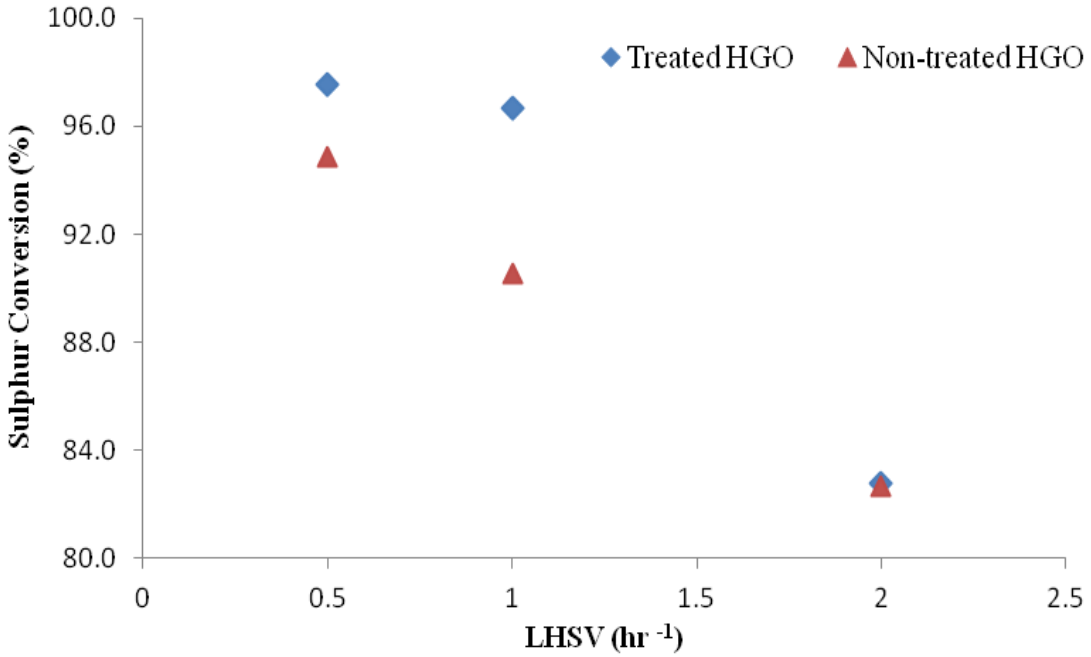

Figure 4.12: Effect of LHSV on the conversion of sulphur for treated and non-treated HGO at a temperaure of 395°C; hydrogen/oil raio of 600 ml/ml; and pressure of 1250 Psi.

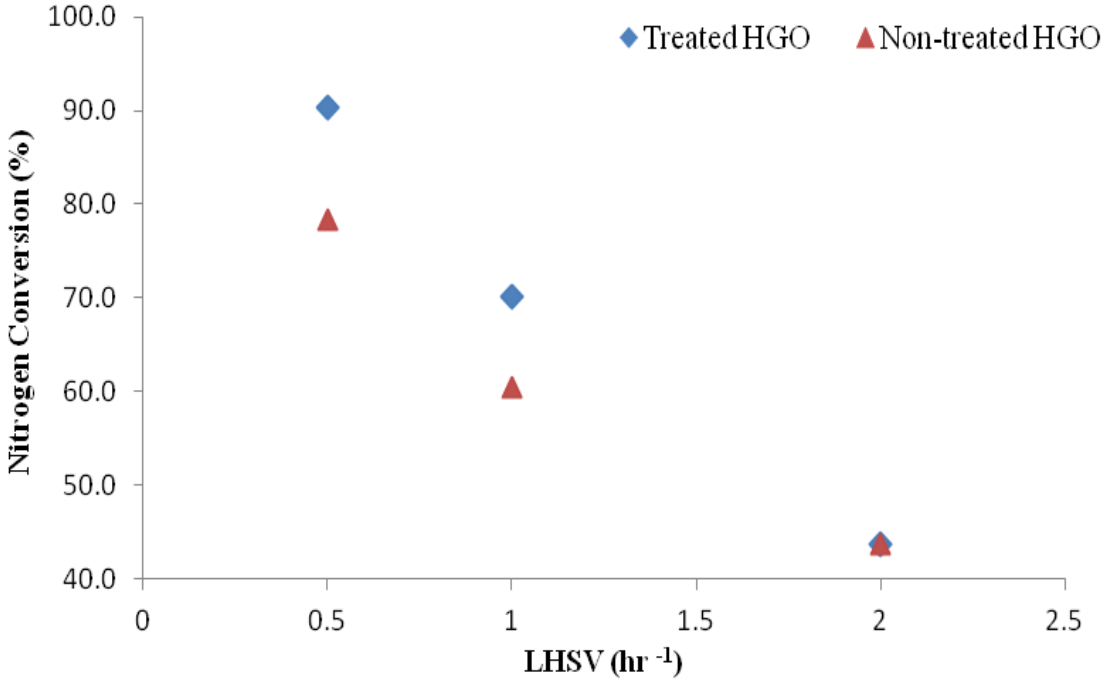

Figure 4.13: Effect of LHSV on the conversion of nitrogen for treated and non-treated HGO at a temperaure of 395°C; hydrogen/oil raio of 600 ml/ml; and pressure of 1250 Psi.

4.3.3 Rate Kinetics of Hydrodesulphurization and Hydrodenitrogenation

Kinetic analysis was performed in order to study the effects of reaction parameters and the selective elimination of non-basic nitrogen species from heavy gas oil. HDS and HDN activities over the commercial catalyst were investigated using both treated and non-treated heavy gas oil in a micro scale trickle bed reactor. Based on the obtained results, power law model was developed in order to predict the hydrotreating activities of treated and non-treated heavy gas oil. It should be noted that the following assumptions were taken into considerations for the kinetic analysis (Biswas, 2011):

1. Trickle bed micro reactor operations were considered as steady state isothermal and plug flow.
2. The effects of H_2S and NH_3 concentrations on both the mass transfer resistance and hydrotreating activities were considered negligible.
3. Axial dispersion and wall effects were neglected due to dilution of the catalyst bed with nonporous, inert particles during experimental run.
4. Complete wetting of catalyst.

The calculation method employed for the molar concentration of sulphur and nitrogen is given in Appendix A, along with the reaction rate calculation of HDS and HDN. Appendix B illustrates the calculated product concentrations of treated and non-treated heavy gas oil for HDS and HDN conversions obtained for kinetic studies.

The power law model was employed for studying the kinetic parameters due to its simplicity. Table 4.6 illustrates the order of the reactions (n), the kinetic equations based on the discussion in section 2.7.2, and the R^2 values generated for HDS and HDN from the respective kinetic equations. The values of the reaction order were determined based

on the best fit of experimental data. A trial and error approach was adopted by varying the value of n and solving for the power law equation described in section 2.7.2. The power law equations with the highest R^2 values were then chosen to represent the best fitted equations for HDS and HDN of both treated and non-treated heavy gas oil. The value of R^2 is generally regarded as a statistical measure of fitness; the closer this value is to unity the better is the fit for data. Based on the calculated R^2 values given in Table 4.6, it can be seen that for treated heavy gas oil both HDS and HDN have a reaction order of 1.50; whereas for non-treated heavy gas oil, HDS follows a reaction order of 2.25 and HDN follows a reaction order of 2.00. These reaction orders appear to be in agreement with those reported in literature, which states that for heavy gas oil, the reaction order for HDS should be in the range of 1.00 to 2.50; while for HDN the reaction order should be in the range of 1.00 to 2.00 (Ferdous et al., 2006b; Biswas, 2011). Figures 4.14 and 4.15 illustrate the fitting of rate data for the aforementioned selected order of reactions for HDS and HDN of both treated and non-treated heavy gas oil.

Table 4.6: Determination of reaction orders (n) of power law model for treated and non-treated heavy gas oil.

Order of Reaction (n)	Kinetic Equation	Value of R^2 (Treated HGO)		Value of R^2 (Non-treated HGO)	
		HDS	HDN	HDS	HDN
0.00	$k = [C_F - C_P] * LHSV$	0.9178	0.9954	0.9969	0.9952
0.50	$k = 2[C_P^{0.5} - C_F^{0.5}] * LHSV$	0.9266	0.9974	0.9971	0.9968
1.00	$k = \ln[C_F - C_P] * LHSV$	0.8165	0.9766	0.1741	0.9476
1.50	$k = 2[1/C_P^{0.5} - 1/C_F^{0.5}] * LHSV$	**0.9276**	**0.9984**	0.9981	0.9968
2.00	$k = [1/C_P - 1/C_F] * LHSV$	0.9179	0.9954	0.9980	**0.9982**
2.25	$k = 0.8[1/C_P^{1.25} - 1/C_F^{1.25}] * LHSV$	0.9128	0.9926	**0.9987**	0.9959
2.50	$k = 0.667[1/C_P^{1.5} - 1/C_F^{1.5}] * LHSV$	0.9083	0.9888	0.9961	0.9966
3.00	$k = 0.50[1/C_P^{2} - 1/C_F^{2}] * LHSV$	0.9014	0.9785	0.9865	0.9960

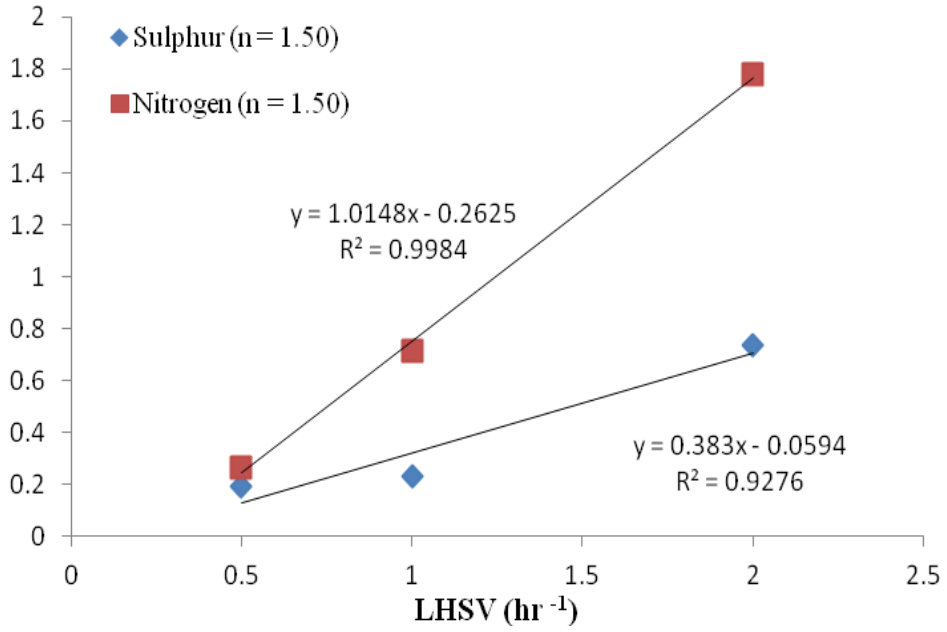

Figure 4.14: Fitting of treated HGO experimental data to the P-L model having reaction order 1.5 for HDS and HDN, respectively. (Catalyst = 5 cm^3, T = 395ºC, P = 8.6-8.8 MPa, LHSV = 0.5-2 hr^{-1} and H_2/Oil ratio = 600 mL/mL).

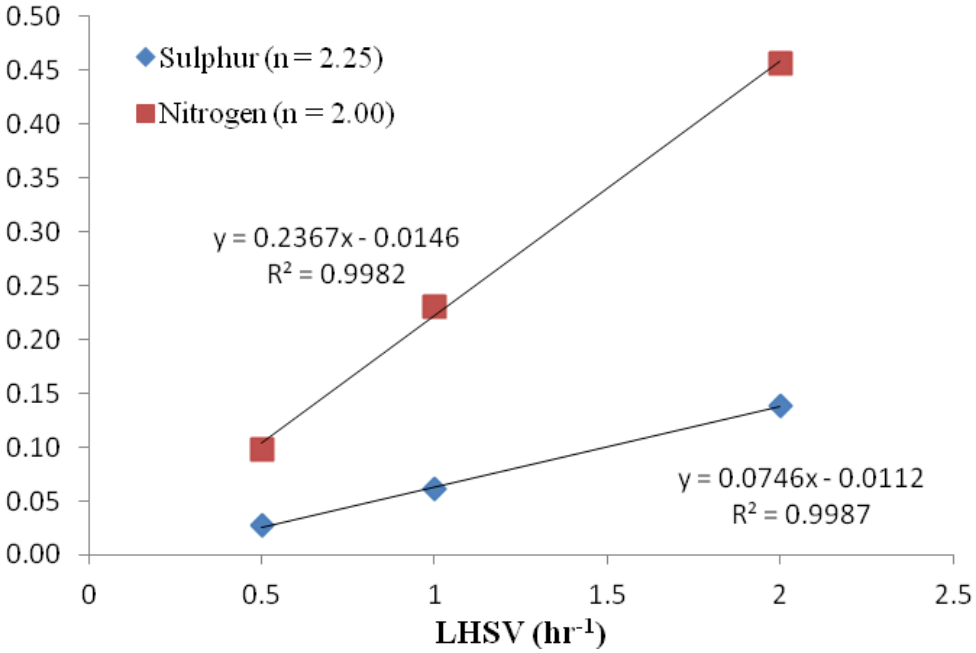

Figure 4.15: Fitting of non-treated HGO experimental data to the P-L model having reaction order of 2.25 for HDS and 2.00 for HDN, respectively. (Catalyst = 5 cm^3, T = 395ºC, P = 8.6-8.8 MPa, LHSV = 0.5-2 hr^{-1} and H_2/Oil ratio = 600 mL/mL).

The activation energies (Ea) for the treated and non-treated heavy gas oil HDS and HDN conversions were calculated based on the equations discussed in section 2.7.2. The calculated activation energy for treated heavy gas oil for HDS was 141.4 kJ/mol and for HDN was 113.8 kJ/mol. The activation energy for non-treated heavy gas oil for HDS was 150.4 kJ/mol and for HDN was 121.4 kJ/mol. These values are in agreement with those determined in literature for bitumen derived heavy gas oil (Boahene, 2011; Biswas, 2011). The lower activation energy for treated HGO implies that the chemical reactions required less energy for conversion; hence higher conversions were obtainable for treated heavy gas oil. It was also noticeable that for both treated and non-treated heavy gas oil HDS had higher activation energy than HDN, this is opposing the general trend observed where HDS has lower activation energy than HDN (Boahene, 2011; Biswas, 2011). This is solely due to the removal of non-basic nitrogen species prior to hydrotreatment, since those compounds are competitively adsorbed onto the catalyst active sites causing inhibition, and increasing the amount of energy required for their hydrotreatment. Table 4.7 provides a summary of the obtained kinetic parameters based on the power law model for both treated and non-treated heavy gas oil feedstocks.

Table 4.7: Summary of reaction orders (n), activation energies (E), and pre-exponential factors (A) derived using P-L model for treated and non-treated heavy has oil.

	Reaction Order (n)	**Activation Energy, E (kJ/mol)**	**Pre-exponential Factor (A)**
Treated HGO (HDS)	1.50	141.4	$9.44 * 10^{11}$
Treated HGO (HDN)	1.50	113.8	$2.16 * 10^{09}$
Non-treated HGO (HDS)	2.25	150.4	$7.39 * 10^{12}$
Non-treated HGO (HDN)	2.00	121.4	$1.33 * 10^{10}$

CHAPTER 5

CONCLUSIONS AND RECOMMENDATIONS

The objective of this thesis was to synthesize, optimize, and characterize an electron-deficient polymer capable of selectively removing non-basic nitrogen species from heavy gas oil prior to hydrotreatment. In addition, hydrotreatment studies were performed in order to evaluate the performance of treated heavy gas oil. Several key conclusions derived from the results and discussions are presented in the following section, along with recommendations for future studies related to this work.

5.1 Conclusions

The polymer poly(glycidyl methacrylate) incorporated with tetranitrofluorenone was successfully synthesized in a four step synthesis procedure. Characterization was performed during each of the intermediate steps, with the final results indicating that sample T was the optimized polymer due to the highest weight loss of approximately 126.9 μg during TGA analysis.

Feasibility of the synthesized polymer samples from step 4 for the selective removal of non-basic nitrogen compounds was tested, and the results showed sample T having the highest nitrogen removal of approximately 7%, while having little to no influence on the sulphur or aromatic compounds also present in the heavy gas oil. The reusability studies were also performed and showed that the polymer could indeed be used multiple times, with consistent removal of nitrogen compounds at approximately 6.5%.

The final phase involved performing kinetic studies to evaluate the performance of the treated gas oil in comparison to non-treated gas oil. The effect of parameters such as temperature and LHSV were tested, with higher temperatures and lower LHSV resulting in higher conversion rates. The highest sulphur conversion obtained for treated HGO was 97.5% and 94.9% for non-

treated HGO, both at LHSV of 0.5 hr^{-1} and temperature of 395 °C; while highest nitrogen conversion obtained for treated HGO was 90.3% and 78.3% for non-treated HGO, both at LHSV of 0.5 hr^{-1} and temperature of 395 °C.

The power law model was employed for determining the reaction order and calculating the activation energies. The results indicated that for treated HGO the reaction order for both HDS and HDN was 1.50; while for non-treated HGO the reaction order for HDS was 2.25 and for HDN was 2.00; these results were in agreement with those stated in literature. The calculated activation energy for treated HGO for HDS was 141.4 kJ/mol and for HDN was 113.8 kJ/mol; while for non-treated HGO the activation energy for HDS was 150.4 kJ/mol and for HDN was 121.4 kJ/mol.

The kinetic studies indicated that treated HGO had lower activation energy for both HDS and HDN in comparison to non-treated HGO, which signified that the removal of non-basic nitrogen species prior to hydrotreatment had a significant impact on improving the performance of the catalyst and allowing for higher conversion rates to be obtained under the same reaction conditions.

5.2 Recommendations

After observing the performance of poly(glycidyl methacrylate) with tetranitrofluorenone as a method of pre-treatment for heavy gas oil, the following recommendations are proposed for further studies.

- The polymer poly(glycidyl methacrylate) was used as the electron-deficient polymer support due to the presence of the epoxy ring on the polymer which can be utilized for attaching a number of different compounds (i.e. tetranitrofluorenone). Attachment of different compounds can allow for selectivity towards different species present in heavy gas oil, such

as sulphur; thus, further research into applicable compounds for selective removal of sulphur or oxygen species can prove to be beneficial towards catalyst performance.

- The synthesized polymer was employed for the selective removal of non-basic nitrogen species from bitumen derived heavy gas oil; however, it can supposedly be used for the removal of those species from other gas oils as well such as vacuum gas oil and light gas oil.
- The maximum selective removal of non-basic nitrogen species from heavy gas oil performed in this study was approximately 6%. This was due to the complexity of synthesizing the polymer and treating heavy gas oil in quantities applicable for hydrotreating studies; thus, it is suggested that higher nitrogen removal be performed in order to further study the inhibiting and deactivating effects of nitrogen species on catalyst active sites, and to quantify the detrimental effects of these species towards HDS and HDN conversion rates.
- The hydrotreatment studies were performed using the commercial NiMo/α-Al_2O_3 catalyst supplied by Syncrude Canada Ltd. It is suggested that further hydrotreatment studies be performed using treated HGO with varying catalysts in order to study the effects of non-basic nitrogen species on their activity.

CHAPTER 8

LIST OF REFERENCES

Almarri, M, Ma, X, Song, C, "Selective Adsorption for removal of nitrogen compounds from liquid hydrocarbon streams over carbon and alumina based adsorbents," Industrial & Engineering Chemistry Research. 48, 951-960 (2009).

Ancheyta, J., J.G. Speight, "Hydroprocessing of Heavy Oil and Residua," CRC Press, Taylor and Francis Group, Boca Raton, FL (2007).

Bej, S.K., A.K. Dalai and J. Adjaye, "Effect of hydrotreating conditions on the conversion of residual fraction and microcarbon residue present in oil sands derived heavy gas oil," Energy and Fuels. 15, 1103-1109 (2001a).

Bej, S.K, Dalai, A.K, Maity, S.K, "Effect of diluent size on the performance of micro-scale fixed bed multiphase reactor in up-flow and down-flow modes of operation", Catalysis Today 64, 333 (2001b).

Berhault, G., M. Perez De la Rosa, A. Mehta, M.J. Yácaman and R.R. Chianelli, "The single-layered morphology of supported MoS2-based catalysts-The role of the cobalt promoter and its effects in the hydrodesulphurization of dibenzothiophene," Applied Catalysis A: General. 345, 80-88 (2008).

Bhattacharyya, K.G., Talukdar, A.K., "Catalysis in petroleum and petrochemical industries," Narosa Publishing House PVT Ltd, 473-482 (2005).

Biswas, P, "Catalytic Performances of NiMo/Zr-SBA-15 Catalysts for the Hydrotreating of Bitumen Derived Heavy Gas Oil," Department of chemical engineering, University of Saskatchewan, 39-62 (2011).

Boahene, P.E, "Effect of Pore Diameter Variation of Fe-W/SBA-15 Supported Catalysts on Hydrotreating of Heavy Gas Oil from Athabasca Bitumen," Department of chemical engineering, University of Saskatchewan, (2011).

Botchwey, C, "Two-stage hydrotreating of heavy gas oil with inter-stage hydrogen sulfide removal," Department of chemical engineering, University of Saskatchewan, 13- 20 (2003).

Bunch, A, Zhang, L, Karakas, G, Ozkan, S.U., "Reaction network of indole hydrodenitrogenation over NiMoS/γ-Al_2O_3 catalysts," Applied Catalysis: A. 190, 51-60 (2000).

Callant, M, Holder, K.A, Grange, P, Delmon, B, "Effect of the H_2S and H_2 partial pressure on the hydrodenitrogenation (HDN) of aniline and indole over a NiMoP/γ-Al_2O_3 catalyst". Bulletin des Sociétés Chimiques Belges. 104, 245-251 (1995).

Cronauer, D. C, Young, D. C, Solash, J, Seshadri, K.S, Danner, D.A, “Shale oil denitrogenation with ion exchange. 3. Characterization of hydrotreated and ion-exchange isolated products”. Industrial & Engineering Chemistry Process Design. 25, 756-762 (1986).

Daage, M. and R.R. Chianelli, "Structure-Function Relations in Molybdenum Sulfide Catalysts: The "Rim-Edge" Model," Journal of Catalysis. 149, 414-427 (1994).

David S.J.J. and Pujadó P. R, "Handbook of Petroleum Processing," Springer, Netherlands (2006).

Dong, D, Jeong, S, Massoth, F.E., “Effect of nitrogen compounds on deactivation of hydrotreating catalysts by coke”, Catalysis Today. 37, 267 (1997).

Duan, A, Xu, C, Gao, J, Lin, S, Chung H. K, “Molecular simulation for catalytic hydrotreatment of coker heavy gas oil derived from athabasca bitumen”, Journal of molecular structure 734, 89-97 (2005).

Energy Canada; http://www.energy.ca; (2000).

Ferdous D, “Surface morphology of NiMo catalyst supported on γ-Al_2O_3: Impact on hydroprocessing of heavy gas oil derived from Athabasca bitumen”, Department of chemical engineering, University of Saskatchewan, (2003a).

Ferdous, D, Dalai, A. K, Adjaye, J. “Comparison of Hydrodenitrogenation of Model Basic and Non-basic Nitrogen Species in a Trickle Bed Reactor Using Commercial NiMo/Al2O3 Catalyst”, Energy & Fuels. 17, 164-117 (2003b).

Ferdous D, Dalai, A.K, Adjaye, J, “A series of $NiMo/Al_2O_3$ catalysts containing boron and phosphorous part II. Hydrodenitrogenation and hydrodesulphurization using heavy gas oil derived from Athabasca bitumen”, Applied Catalysis: A. 260, 153-162 (2004).

Ferdous, D., A.K. Dalai and J. Adjaye, "Comparison of product selectivity during hydroprocessing of bitumen derived gas oil in the presence of NiMo/Al2O3 catalyst containing boron and phosphorus," Fuel. 85, 1286-1297 (2006a).

Ferdous, D., A.K. Dalai and J. Adjaye, "Hydrodenitrogenation and hydrodesulphurization of heavy gas oil using NiMo/Al2O3 catalyst containing boron: Experimental and kinetic studies," Industrial and Engineering Chemistry Research. 45, 544-552 (2006b).

Fogler, H.C, “Elements of Chemical Reaction Engineering – 4th Edition”, Pearson Education, Inc, 645-688 (2006).

Furimsky, E; Massoth, E.F, “Deactivation of Hydroprocessing Catalysts”, Catalysis Today. 52, 381-495 (1999).

Georgina, L.C., Efrain, A, Reyes Antonio De los, J, "Inhibition effects of nitrogen compounds on the hydrodesulphurization of dibenzothiophenes: part 2", Applied Catalysis: A. 243, 207-214 (2003).

Girgis, M.J, Gates, B.C, "Reactivities, reaction networks, and kinetics in high pressure catalytic hydroprocessing", Industrial and engineering chemistry research, 30, 2021-2058 (1991).

Gray, M.R, "Upgrading petroleum residues and heavy oils", Marcel Dekker, Inc, New york, (1994).

Gregg S.J., Sing K.S.W., "Adsorption, Surface Area and Porosity", London; New York Academic Press, (1967).

Gruia, A., David S.J., Pujado, P.R., "Handbook of Petroleum Processing", Springer Netherlands, Chapter 8 (2006).

Hong, Y, Jinwen, C, Craig, F, Yevgenia, B, Yu, Z.J., Zbigniew, R, "Inhibition of nitrogen compounds on the hydrodesulphurization of substituted dibenzothiophenes in light cycle oil", Fuel Process. Technol. 85, 1415-1429 (2004).

Janchig, N, Yoshikazu, S, "Removal of nitrogen compounds before deep hydrotreatment of synthetic crude oils", Journal of the Japan Petroleum Institution. 51, 165-173 (2008).

Jong, K.P de, "Synthesis of solid catalysts", WILEY-VCH Verlag GmBH & Co., Chapter 14 (2009).

Kanda, W, Siu, I, Adjaye, J, Nelson, E.A, Gray, R.M, "Inhibition and deactivation of hydrodenitrogenation (HDN) catalysts by narrow-boiling fractions of Athabasca coker gas oil", Energy & Fuels. 18, 539-546 (2004).

Kline, G.M, "Analytical Chemistry of Polymers. Part I", Interscience Publishing Inc, New York, 123-132 (1959).

Koltai, T, Macaud, M, Guevara, A, Schulz, E, Lemaire, M, Bacaud, R, Vrinat, M, "Comparative inhibiting effect of polycondensed aromatics and nitrogen compounds on the hydrodesulphurization of alkyldibenzothiophenes", Applied Catalysis: A. 231, 253-261 (2002).

Kwon, J, Moon, J, Bae, Y, Lee, D, Sohn, H, Lee, C, "Adsortive desulphurization and denitrogenation of refinery fuels using mesoporous silica adsorbents", ChemSuChem. 1, 307-309 (2008).

Laredo, C.G, Reyes, A.D.J, MCastillo, J.J, "Inhibition effects of nitrogen compounds on the hydrodesulphurization of dibenzothiophenes". Applied Catalysis A: General. 207, 103-112 (2001).

Laredo, C. G, Altamirano, E, Reyes, A.D.J, “Inhibition effects of nitrogen compounds on the hydrodesulphurization of dibenzothiophenes: part 2”, Applied Catalysis A: General. 243, 207-214 (2003).

Lauritsen, J.V., J. Kibsgaard, G.H. Olesen, P.G. Moses, B. Hinnemann, S. Helveg, J.K. Nørskov, B.S. Clausen, H. Topsøe, E. Lægsgaard and F. Besenbacher, "Location and coordination of promoter atoms in Co- and Ni-promoted MoS2-based hydrotreating catalysts," Journal of Catalysis. 249, 220-233 (2007).

LaVopa, V, Satterfield, C.N., “Poisoning of thiophene hydrodesulphurization by nitrogen compounds”, Journal of Catalysis. 110, 375 (1988).

Lee S., Speight J.G. and Loyalka S.K., "Handbook of Alternative Fuel Technologies," CRC Press, Taylor and Francis Group: Boca Raton, FL. (2007).

Lemaire, M, Schulz, E, Sevignon, M, Macaud, M, Favrereguillon, A, Thomas, M, Loutaty, R, “, Polymer-supported π-electron acceptors for charge-transfer-based denitrogenation-desulphurization of petroleum fractions”, PCT Int. Appl. 2002024836, (2002).

Lu, M, Wang, A, Li, X, Duan, X, Teng, Y, Wang, Y, Song, C, Hu, Y, “Hydrodenitrogenation of quinoline catalyzed by MCM-41 supported nickel phosphides”, Energy & Fuels. 21, 554-460 (2007).

Macaud, M, Sevignon, M, Favre-Reguillon, A, Lemaire, M, “Novel methodology toward deep desulphurization of diesel feed based on the selective elimination of nitrogen compounds”, Ind. Eng. Chem. Res. 43, 7843-7849 (2004).

Marroquín, G., J. Ancheyta and C. Esteban, "A batch reactor study to determine effectiveness factors of commercial HDS catalyst," Catalysis Today. 104, 70-75 (2005).

Masoud, A, Xiaoliag, M, Chunshan, S, “Selective Adsorption for removal of nitrogen compounds from liquid hydrocarbon streams over carbon and alumina based adsorbents”, Industrial & Engineering Chemistry Research. 48, 951-960 (2009a).

Masoud, A, Xiaoliang, M, Chunshan, S, “Role of surface oxygen-containing functional groups in liquid-phase adsorption of nitrogen compounds on carbon-based adsorbents”, Energy & Fuels. 23, 3940-3947 (2009b).

Milenkovic, A, Schulz, E, Meille, V, Loffreda, D, Forissier, M, Vrinat, M, Sautet, P, Lemaire, M, “Selective Elimination of Alkyldibenzothiophenes from Gas Oil by Formation of Insoluble Charge-Transfer Complexes”, Energy & Fuels. 13, 881 – 887 (1999).

Mochida, I, K, Choi, "An overview of hydrodesulphurization and hydrodenitrogenation," Journal of the Japan Petroleum Institute. 47, 145-163 (2004).

Muegge, B, Massoth, F.E., in: C.H. Bartholomew, J.B. Butt (Eds.), Catalyst Deactivation, Elsevier, Amsterdam, 297 (1991).

Nadine, M, Patrick, T, "Controlled synthesis of poly(acetone oxime acrylate) as a new reactive polymer: stimuli-responsive reactive copolymers", European Polymer Journal. 43, 1202-1209 (2007).

Nagai, M, Kabe, T, "Selectivity of molybdenum catalyst in hydrodesulphurization, hydrodenitrogenation, and hydrodeoxygenation: Effect of additives on dibenzothiophene hydrodesulphurization", Journal of Catalysis. 81, 440-449 (1983).

Newman, M.S, Lutz, W.B, "α-(2,4,5,7-Tetranitro-9-fluorenylideneaminoöxy)-propionic Acid, a New Reagent for Resolution by Complex Formation", Journal of American Chemical Society. 78, 2469 (1956).

Odebunmi, E.O., Ollis, D.F., "Catalytic hydrodeoxygenation: III. Interactions between catalytic hydrodeoxygenation of *m*-cresol and hydrodenitrogenation of indole", Journal of Catalysis. 80, 76 (1983).

Okubo, M, Okada, M, Miya, T, Takekoh, R, "Production of micron-sized, monodisperse composite polymer particles having epoxy groups by seeded dispersion polymerization", Colloid & Polymer Science. 279, 807-812 (2001).

Owusu-Boakye, A, Dalai K. A, Ferdous, D, Adjaye, J, "Experimental and Kinetic Studies of Aromatic Hydrogenation, Hydrodesulphurization, and Hydrodenitrogenation of Light Gas Oils Derived from Athabasca Bitumen", Industrial & Engineering Chemistry Research. 44, 7935-7944 (2005).

Prins, R, Jian, M, Flechsenhar, M, "Mechanism and kinetics of hydrodenitrogenation". Polyhedron. 16, 3235-3246 (1997).

Prudich, M.E, Cronauer, D.C, Vogel, R.F, Solash, J, "Shale oil denitrogenation with ion exchange. 1. Process concept and modeling". Ind. Eng. Chem. Process Des. 25, 742-746 (1986).

Qi, J, Yan, Y, Su, Y, Qu, F, Dai, Y, "Extraction of nitrogen compounds from catalytically cracked diesel oil with a volatile carboxylic acid based on reversible chemical complexation", Energy & Fuels. 12, 788-791 (1998a).

Qi, J, Yan, Y, Fei, W, Su, Y, Dai, Y, "Solvent extraction of nitrogen compounds from catalytically-cracked diesel oil by metal ion complexation", Fuel. 77, 255-258 (1998b).

Schuit, G.C.A. and B.C. Gates, "Chemistry and engineering of catalytic hydrodesulphurization", AICHE Journal. 19, 417-438 (1973).

Senkal, B.F, Bildik, F, Yavuz, E, Sarac, A, “Preparation of poly(glycidyl methacrylate) grafted sulfonamide based polystyrene resin with tertiary amine for the removal of dye from water”, Reactive and functional polymer. 67, 1471 – 1477 (2007).

Sigurdson, S.K., “Hydrotreating of light gas oil using carbon nanotube supported NiMoS catalysts: Influence of pore diameters”, Department of chemical engineering, University of Saskatchewan, (2009).

Speight J. G., "The Desulphurization of Heavy Oil and Residua ", Marcel Dekker Inc, (1999).

Speight, J.G, “The desulphurization of heavy oil and residue”, 2nd Edition, Marcel Dekker Inc, New York, (2000).

Speight J.G., Ozum, Baki, “Petroleum Refining Process”, Marcel Dekker Inc, 472-490 (2002).

Stern W. E., “Reaction Networks in Catalytic Hydrodenitrogenation”, Journal of Catalysis. 57, 390-396, (1979).

Sundaram, K.M, Katzer, J.R, Bischoff, K.B, “Modeling of Hydroprocessing Reactions”, Chemical Engineering Communications. 71, 53-71 (1988).

Svec, F, Hradil, J, Coupek, J, Kalal, J, “Reactive Polymers I. Macroporous Methacrylate Copolymers Containing Epoxy Groups”, Die Angewandte Makromolekulare Chemie. 48, 135 – 143 (1975).

Topsoe, H. and B.S. Clausen, "Importance of Co-Mo-S type structures in hydrodesulphurization", Catalysis Reviews. 26, 395-420 (1984).

Trytten, C.L, Gray, R.M, Sanford, C.E, “Hydroprocessing of narrow-boiling gas oil fractions: dependence of reaction kinetics on molecular weight”, Industrial & Engineering Chemistry Research. 29, 725-730 (1990).

Tuncer, C, Serife, A. S., “Preparation and characterization of novel poly(glycidyl methacrylate) beads carrying amidoxime groups”, Journal of Applied Polymer Science. 106, 2126-2131 (2007).

U.S. Energy Information Administration, “International Energy Outlook 2011” http://www.eia.gov/forecasts/ieo/pdf/0484%282011%29.pdf, (2011a).

U.S. Energy Information Administration, “International Energy Outlook 2011” http://www.eia.gov/forecasts/ieo/world.cfm, (2011b).

U.S. Energy Information Administration, “Canada”, http://www.eia.gov/countries/cab.cfm?fips=CA, (2011c).

Voorhoeve, R.J.H., "Electron spin resonance study of active centers in nickel-tungsten sulfide hydrogenation catalysts," Journal of Catalysis. 23, 236-242 (1971).

Vopa, L.V, Satterfield, N.C, “Poisoning of thiophene hydrodesulphurization by nitrogen compounds”, Journal of Catalysis.110, 375-387 (1988).

Wikipedia, “Simple aromatic ring”, http://en.wikipedia.org/wiki/Simple_aromatic_ring, (2011).

Wikipedia, “Gel Permeation Chromatography”, http://en.wikipedia.org/wiki/Gel_permeation_chromatography, (2012).

Woods J.R, Kung J, Pleizier G, Kotlyar L.S, Sparks B.D, Adjaye J, Chung K.H. “Characterization of a coker gas oil fraction from athabasca oilsands bitumen”, Fuel. 83, 1907-1914 (2004).

Xu, Y., H. Shang, R. Zhao and C. Liu, "The studies of hydrodesulfurization of 4,6-dimethyldibenzothiophene on sulfided Mo/γ-Al2O3: The effects of reactive temperature and pressure," ACS Division of Fuel Chemistry, Preprints 49 (2004).

Yang, S.H., Satterfield, C.N., “Catalytic hydrodenitrogenation of quinoline in a trickle-bed reactor. Effect of hydrogen sulfide”, Industrial & Engineering Chemistry Research. 23, 20 (1984).

Yosuke, S, Ki-Hyouk, C, Yozo, K, Isao, M, “Adsorptive removal of sulphur and nitrogen species from a straight run gas oil over activated carbons for its deep hydrodesulphurization”, Applied Catalysis: B. 49, 219-225 (2004a).

Yosuke, S, Ki-Hyouk, C, Yozo, K, Isao, M, “Effects of nitrogen and refractory sulphur species removal on the deep HDS of gas oil”, Applied Catalysis: B. 53, 169-174 (2004b).

Yui, S., "Producing quality synthetic crude oil from Canadian oil sands bitumen," Journal of the Japan Petroleum Institute. 51, 1-13 (2008).

APPENDICES

APPENDIX A

Calculation of Molar Product Concentrations of N/S and Reaction Rates of HDN/HDS

The sulphur and nitrogen concentrations in the feed and product gas oil were calculated by using the following equations:

$$C_s = \frac{(ppm_{wt}) \times \rho_L}{(10^6) \times M_s} = \frac{(ppm_{wt}) \times (0.98 \times 10^3 \frac{g}{L})}{(10^6) \times (32.0640 \frac{g}{mol})} \quad \textbf{[A.1]}$$

$$C_N = \frac{(ppm_{wt}) \times \rho_L}{(10^6) \times M_N} = \frac{(ppm_{wt}) \times (0.98 \times 10^3 \frac{g}{L})}{(10^6) \times (14.0067 \frac{g}{mol})} \quad \textbf{[A.2]}$$

ρ_L = Density of HGO feedstock and product (assumed equal)

$C_{S/N}$ = Sulphur/nitrogen heteroatom concentration, mol/L (M)

$M_{S/N}$ = Sulphur/nitrogen molecular weight, g/mol

The reaction rates of hydrodesulphurization and hydrodenitrogenation reactions were calculated based on the following equations:

$$\{R_{HDS}\} = \frac{([C_0]_S - [C_P]_S) \times LHSV}{(3600 \frac{s}{h}) \times \rho_{CAT}} \quad \textbf{[A.3]}$$

$$\{R_{HDN}\} = \frac{([C_0]_N - [C_P]_N) \times LHSV}{(3600 \frac{s}{h}) \times \rho_{CAT}} \quad \textbf{[A.4]}$$

$\{R_{HDS/HDN}\}$ = Global rate of the HDS/HDN reaction, mol/(s·kg-cat)

$[C_{O/P}]_{S/N}$ = Feedstock/product concentration of sulphur/nitrogen, mol/L

LHSV = Liquid hourly space velocity, hr^{-1}

ρ_{CAT} = Catalyst pellet density

APPENDIX B

Calculated Product Concentrations of Treated HGO for HDS and HDN Conversions Obtained For Kinetic Study.

Table B.1: Calculated product concentrations of treated HGO for HDS and HDN.

Treated HGO Feed					
Temperature (°C)	**Pressure (Mpa)**	**LHSV (hr^{-1})**	**H_2/GO Ratio (Nm^3/m^3)**	**$[C_p]_{sulphur}$ (mol/L)**	**$[C_p]_{nitrogen}$ (mol/L)**
375	8.6 - 8.8	1.0	600	0.0413	0.0697
375	8.6 - 8.8	1.0	600	0.1061	0.1542
375	8.6 - 8.8	1.0	600	0.1161	0.1705
385	8.6 - 8.8	1.0	600	0.0294	0.0493
385	8.6 - 8.8	1.0	600	0.0655	0.1227
385	8.6 - 8.8	1.0	600	0.0763	0.1441
395	8.6 - 8.8	1.0	600	0.0665	0.1292
395	8.6 - 8.8	1.0	600	0.0507	0.1181
395	8.6 - 8.8	1.0	600	0.0357	0.1057
395	8.6 - 8.8	0.5	600	0.0374	0.0473
395	8.6 - 8.8	0.5	600	0.0298	0.0413
395	8.6 - 8.8	0.5	600	0.0267	0.0342
395	8.6 - 8.8	2.0	600	0.1309	0.1542
395	8.6 - 8.8	2.0	600	0.1745	0.1988
395	8.6 - 8.8	2.0	600	0.1861	0.1987

Calculated Product Concentrations of Non-treated HGO for HDS and HDN Conversions Obtained For Kinetic Study.

Table B.2: Calculated product concentrations of non-treated HGO for HDS and HDN.

Non-Treated HGO Feed					
Temperature (°C)	**Pressure (Mpa)**	**LHSV (hr^{-1})**	**H_2/GO Ratio (Nm^3/m^3)**	**$[C_p]_{sulphur}$ (mol/L)**	**$[C_p]_{nitrogen}$ (mol/L)**
375	8.6 - 8.8	1.0	600	0.1331	0.1468
375	8.6 - 8.8	1.0	600	0.1755	0.1872
375	8.6 - 8.8	1.0	600	0.1893	0.1987
385	8.6 - 8.8	1.0	600	0.1288	0.1409
385	8.6 - 8.8	1.0	600	0.1361	0.1585
385	8.6 - 8.8	1.0	600	0.1426	0.1715
395	8.6 - 8.8	1.0	600	0.1121	0.1595
395	8.6 - 8.8	1.0	600	0.1071	0.1473
395	8.6 - 8.8	1.0	600	0.1023	0.1397
395	8.6 - 8.8	0.5	600	0.0989	0.1313
395	8.6 - 8.8	0.5	600	0.0774	0.1001
395	8.6 - 8.8	0.5	600	0.0555	0.0767
395	8.6 - 8.8	2.0	600	0.1216	0.1508
395	8.6 - 8.8	2.0	600	0.1640	0.1826
395	8.6 - 8.8	2.0	600	0.1873	0.1992

APPENDIX C

Permission to Use Figures from Literatures

1. Permission to use Figure 2.6

THE JAPAN PETROLEUM INSTITUTE

COSMO Hirakawa-cho Bldg., 1-3-14 Hirakawa-cho, Chiyoda-ku, Tokyo 102, JAPAN
TEL 03-3221-7301 FAX 03-3221-8175

Permission Form

To: The Japan Petroleum Institute

We are preparing a book/an article
Title: Selective Removal of Non-Basic Nitrogen Compounds from Heavy Gas Oil Using Functionalized Polymers
to be printed presumably in "a form of a thesis" published by "University of Saskatchewan" , and I am requesting permission to use the material described below from your publication as follows:

1. **Authors:** Isao Mochida, and Ki-Hyouk Choi
2. **Journal title:** Journal of the Japan Petroleum Institute **Volume:** 47 **No.:** 3
3. **Article title:** An overview of hydrodesulphurization and hydrodenitrogenation
4. **Material to be used:** Figure 4
5. **Page:** pp. 145-163
6. **Publisher:** The Japan Petroleum Institute
7. **Year of publication:** 2004

We, of course, make sure that full acknowledgment will be given to your publication. We will also give assurance that we will show an appropriate reference to "J. Jpn. Petrol. Inst." in the article(book).

We kindly should like to ask you to grant us the permission for our original publication and should like to ask you to sign below and return the form to the address given below:
Thanking you very much for your kind assistance.

Date: May 8th, 2012
Requested by: Danish Rizwan
Organization: University of Saskatchewan
Address: 57 Campus Drive, Saskatoon, SK, Canada, S7N 5A9

Permission granted: Michiharu Harakawa
(Authorized signature)
Michiharu HARAKAWA, Secretary General
The Japan Petroleum Institute

Date: May 10, 2012

2. Permission to use Figure 2.7

Copyright Clearance Center RightsLink®

Home | Account Info | Help

Title: Mechanism and kinetics of hydrodenitrogenation
Author: R. Prins,M. Jian,M. Flechsenhar
Publication: Polyhedron
Publisher: Elsevier
Date: 1997
Copyright © 1997, Elsevier

Logged in as:
Danish Rizwan
Account #:
3000531349
LOGOUT

Order Completed

Thank you very much for your order.

This is a License Agreement between Danish Rizwan ("You") and Elsevier ("Elsevier"). The license consists of your order details, the terms and conditions provided by Elsevier, and the payment terms and conditions.

Get the printable license.

License Number	2906031500812
License date	May 11, 2012
Licensed content publisher	Elsevier
Licensed content publication	Polyhedron
Licensed content title	Mechanism and kinetics of hydrodenitrogenation
Licensed content author	R. Prins,M. Jian,M. Flechsenhar
Licensed content date	1997
Licensed content volume number	16
Licensed content issue number	18
Number of pages	12
Type of Use	reuse in a thesis/dissertation
Portion	figures/tables/illustrations
Number of figures/tables /illustrations	1
Format	both print and electronic
Are you the author of this Elsevier article?	No
Will you be translating?	No
Order reference number	
Title of your thesis/dissertation	Selective Removal of Non-Basic Nitrogen Compounds from Heavy Gas Oil Using Functionalized Polymers
Expected completion date	May 2012
Estimated size (number of pages)	120
Elsevier VAT number	GB 494 6272 12
Permissions price	0.00 USD
VAT/Local Sales Tax	0.0 USD / 0.0 GBP
Total	0.00 USD

ORDER MORE... CLOSE WINDOW

3. Permission to use Figure 2.8

Copyright Clearance Center RightsLink®

Home | Account Info | Help

Title: Reaction network of indole hydrodenitrogenation over NiMoS/γ-Al2O3catalysts
Author: Abdu Bunch,Liping Zhang,Gurkan Karakas,Umit S Ozkan
Publication: Applied Catalysis A: General
Publisher: Elsevier
Date: 3 January 2000
Copyright © 2000, Elsevier

Logged in as:
Danish Rizwan
Account #:
3000531349
LOGOUT

Order Completed

Thank you very much for your order.

This is a License Agreement between Danish Rizwan ("You") and Elsevier ("Elsevier"). The license consists of your order details, the terms and conditions provided by Elsevier, and the payment terms and conditions.

Get the printable license.

License Number	2906040561300
License date	May 11, 2012
Licensed content publisher	Elsevier
Licensed content publication	Applied Catalysis A: General
Licensed content title	Reaction network of indole hydrodenitrogenation over NiMoS/γ-Al2O3catalysts
Licensed content author	Abdu Bunch,Liping Zhang,Gurkan Karakas,Umit S Ozkan
Licensed content date	3 January 2000
Licensed content volume number	190
Licensed content issue number	1-2
Number of pages	10
Type of Use	reuse in a thesis/dissertation
Portion	figures/tables/illustrations
Number of figures/tables /illustrations	1
Format	both print and electronic
Are you the author of this Elsevier article?	No
Will you be translating?	No
Order reference number	
Title of your thesis/dissertation	Selective Removal of Non-Basic Nitrogen Compounds from Heavy Gas Oil Using Functionalized Polymers
Expected completion date	May 2012
Estimated size (number of pages)	120
Elsevier VAT number	GB 494 6272 12
Permissions price	0.00 USD
VAT/Local Sales Tax	0.0 USD / 0.0 GBP
Total	0.00 USD

ORDER MORE... | CLOSE WINDOW

4. Permission to use Figure 2.11

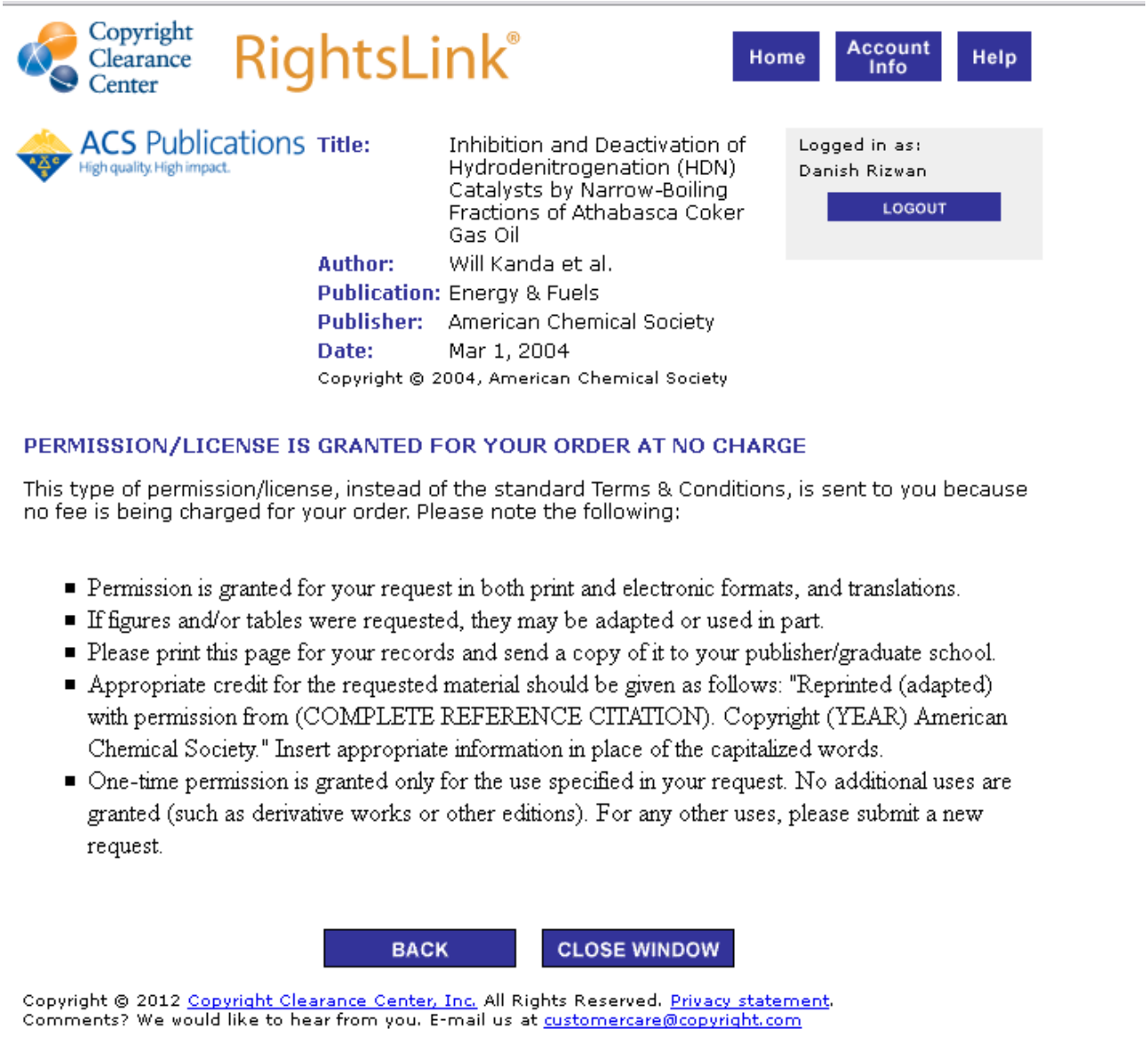

Copyright Clearance Center RightsLink®

Home | Account Info | Help

ACS Publications High quality. High impact.

Logged in as: Danish Rizwan

LOGOUT

Title: Inhibition and Deactivation of Hydrodenitrogenation (HDN) Catalysts by Narrow-Boiling Fractions of Athabasca Coker Gas Oil

Author: Will Kanda et al.

Publication: Energy & Fuels

Publisher: American Chemical Society

Date: Mar 1, 2004

Copyright © 2004, American Chemical Society

PERMISSION/LICENSE IS GRANTED FOR YOUR ORDER AT NO CHARGE

This type of permission/license, instead of the standard Terms & Conditions, is sent to you because no fee is being charged for your order. Please note the following:

- Permission is granted for your request in both print and electronic formats, and translations.
- If figures and/or tables were requested, they may be adapted or used in part.
- Please print this page for your records and send a copy of it to your publisher/graduate school.
- Appropriate credit for the requested material should be given as follows: "Reprinted (adapted) with permission from (COMPLETE REFERENCE CITATION). Copyright (YEAR) American Chemical Society." Insert appropriate information in place of the capitalized words.
- One-time permission is granted only for the use specified in your request. No additional uses are granted (such as derivative works or other editions). For any other uses, please submit a new request.

BACK | CLOSE WINDOW

Copyright © 2012 Copyright Clearance Center, Inc. All Rights Reserved. Privacy statement.
Comments? We would like to hear from you. E-mail us at customercare@copyright.com

5. Permission to use Figures 2.14, 2.15, 2.16

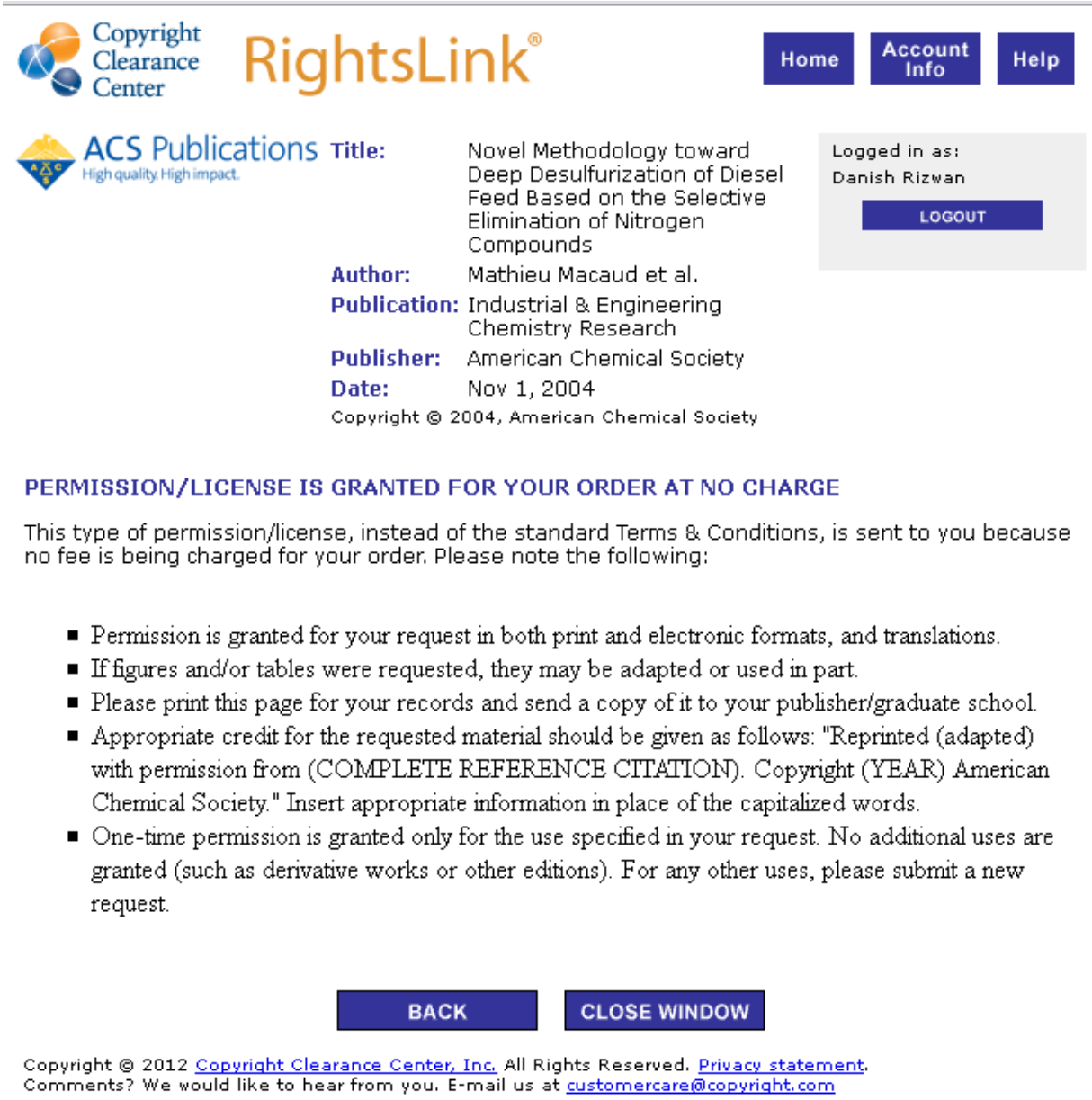

Copyright Clearance Center RightsLink®

Home | Account Info | Help

ACS Publications High quality. High impact.

Logged in as: Danish Rizwan

LOGOUT

Title: Novel Methodology toward Deep Desulfurization of Diesel Feed Based on the Selective Elimination of Nitrogen Compounds

Author: Mathieu Macaud et al.

Publication: Industrial & Engineering Chemistry Research

Publisher: American Chemical Society

Date: Nov 1, 2004

Copyright © 2004, American Chemical Society

PERMISSION/LICENSE IS GRANTED FOR YOUR ORDER AT NO CHARGE

This type of permission/license, instead of the standard Terms & Conditions, is sent to you because no fee is being charged for your order. Please note the following:

- Permission is granted for your request in both print and electronic formats, and translations.
- If figures and/or tables were requested, they may be adapted or used in part.
- Please print this page for your records and send a copy of it to your publisher/graduate school.
- Appropriate credit for the requested material should be given as follows: "Reprinted (adapted) with permission from (COMPLETE REFERENCE CITATION). Copyright (YEAR) American Chemical Society." Insert appropriate information in place of the capitalized words.
- One-time permission is granted only for the use specified in your request. No additional uses are granted (such as derivative works or other editions). For any other uses, please submit a new request.

BACK | CLOSE WINDOW

Copyright © 2012 Copyright Clearance Center, Inc. All Rights Reserved. Privacy statement.
Comments? We would like to hear from you. E-mail us at customercare@copyright.com